

# GPST Topic 9 – DER and Stability

## Stage 2 Final Report

**May 2022 - April 2023**

**Lead Organisation:** University of New South Wales (UNSW)

**Project Partners:** University of Wollongong (UoW),  
Commonwealth Scientific and Industrial Research Organisation (CSIRO),  
Australian Energy Market Operator (AEMO)

**Project Commencement Date:** May 2022

**Project Completion Date:** April 2023

**Contributors:** Georgios Konstantinou, Awais Ahmad, Obaidur Rahman, Sean Elphick,  
Duane Robinson, John Fletcher, Jenny Riesz, Pat Graham

**Contact Name:** Georgios Konstantinou

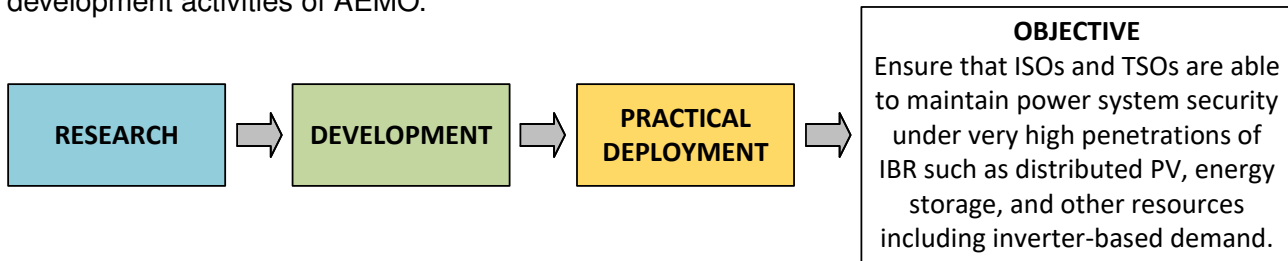
**Email:** [g.konstantinou@unsw.edu.au](mailto:g.konstantinou@unsw.edu.au)

**Date:** 2<sup>nd</sup> May, 2023

## Executive Summary

UNSW Sydney in collaboration with the University of Wollongong and support from the Commonwealth Scientific and Industrial Research Organisation (CSIRO), the Australian Energy Market Operator (AEMO) and GHD is undertaking Stage 2 of the Australian Research Program for the Global Power System Transformation (G-PST) Consortium.

Under **Topic 9 - DER and Stability**, we are focusing on modelling and analysis of distributed energy resources (DER), energy storage systems (ESS) both as standalone battery energy storage systems (BESS) as well as those integrated with PV systems (hybrid energy storage systems - HESS) and a broad variety of modern loads to ensure system operators can maintain power system security in the current challenging power system operation environment. The work that has been undertaken provides robust and accurate data for responses from a large number of devices which have been bench-tested using thorough experimental methods and directly informing the load model development activities of AEMO.



This report summarises UNSW's and UoW's findings to date on DER responses, ESS operation modes and testing resources and load testing during grid disturbances. The results collected also serve as inputs to ongoing load modelling activities. The main conclusions of Stage 2 work for Topic 9 are:

1. The behaviour of PV inverters when updated to the most recent AS4777.2:2020 standard is generally compliant and aligned with requirements. However, this observation does not extend to BESS and HESS systems where diverse responses to grid disturbances were observed in this round of testing.
2. The current RMS load models do not capture the diversity of load responses to grid disturbances. Distinct behaviours have been observed among devices within the same load category and the range of options further complicates testing for load modelling.
3. EV charging infrastructure should be tested and modelled depending on whether the EV chargers include active power electronics or not. When chargers do not have active power electronics, the response will depend on the connected EV.
4. The PV inverter testing experience emphasises the importance of evaluating multiple devices, with the results contributing to load models with greater confidence. Preliminary tests on BESS, HESS, EVs and loads have provided valuable insights into testing and general behaviour; however additional tests are required to validate observations.

## Key findings for PV Inverters

- Each tested single-phase grid-connected PV inverter configured to the AS/NZS 4777.2:2020 standard followed the defined fault-ride-through behaviour when subjected to voltage disturbances.
- Each single-phase grid-connected PV inverter presented expected ride-through and power curtailment behaviour when subjected to frequency disturbance.
- All the tested inverters rode through voltage phase-angle jump disturbance without significant output disruption.
- Extensive testing on the single-phase grid-connected PV inverters allowed AEMO to develop and tune the parameters of the composite load model, which further led to the update of AS4777.2:2020, yielding compliance from grid-connected PV inverters.

## Key findings for Battery Energy Storage Systems (BESS)

- The single BESS tested could only ride-through the voltage disturbance and provide Volt-Watt and Volt-Var responses. It was unable to meet expectations during the comprehensive voltage sag testing.
- While the performance during voltage swell testing was improved, compared to that observed during voltage sag events, it still did not meet all requirements and expectations.
- During frequency and phase jump disturbances, power oscillations were also observed leading to the eventual disconnection of the BESS inverter from the grid.
- When reconnecting after a disturbance, the BESS resumes operation from the same power level at which it got disconnected, causing high power injection or absorption from the grid.

## Key findings for Hybrid Energy Storage Systems (HESS)

- In Stage 2, only a small number of hybrid inverters were tested. While these tests provided useful insights, the limited scope cannot offer a comprehensive understanding of hybrid inverter behavior under grid disturbances, unlike the more extensive PV inverter testing.
- Drawing from our prior experience with single-phase inverter testing, hybrid inverters underwent extensive voltage sag and swell testing to identify any undesirable behaviour presented by hybrid inverters when subjected to grid disturbances of less than 1s. The results indicated that only one hybrid inverter managed to ride through all the sag disturbances, both at full and half power. Conversely, just two out of the four inverters successfully rode through at full power, while all four managed to ride through at half power.
- Testing at different power levels provides evidence that warrants reconsideration of the AS 4777.2 Standard and whether testing should be conducted at full power. To ensure credibility of the findings, additional hybrid inverters should be tested if a revision of the AS 4777.2:2020 is

proposed.

- Only one out of four hybrid inverters that were tested was able to provide ride-through behaviour under frequency disturbance tests under all modes of operation.
- Only one out of four hybrid inverters that were tested was able to ride-through all voltage disturbances. The remaining three inverters presented volt-watt response grid support functionality directed by AS 4777.2:2020
- Three out of the four inverters tested were unable to ride through all voltage phase-angle jump disturbances. This highlights a major issue with voltage phase-angle jump requirements that were introduced recently in AS 4777.2:2020.

## Insights into Load responses

- Load responses to grid disturbances verify certain characteristics of loads that are not modelled in the current rms composite load model. These characteristics include capacitor current overshoots and motor inrush currents. As EMT models of the composite load model are developed, results from Stage 2 can be used to incorporate these characteristics into EMT models.
- The current rms model of the composite load model fails to consider phase angle jumps often observed after grid faults. The results of this study provide preliminary results for incorporating phase angle jump behaviour into the EMT models.
- Most of the appliances tested exhibited only temporary power cessation during disturbances before resuming normal operation once the disturbances were cleared. However, inverter-based air conditioners disconnected after voltage sag events.
- Appliances with inverter-based interfaces, such as refrigerators and air conditioners, for disturbances which caused their traditional (DOL) counterparts to stall. This suggests that they should be included in the Electronic Load element of the load model instead of being represented separately.
- Electronic loads remained unaffected by frequency disturbance tests, except for the inverter-based microwave oven. Further tests are needed to determine if some of these loads are influenced by frequency variations.
- The operation of most tested loads remained unaffected by phase angle jump disturbances, except for the DOL motor-based refrigerator and air conditioner.
- Static loads responded as anticipated by the composite load model, behaving like constant load, power, or impedance loads.
- Similar to the DER inverter tests, testing multiple devices of the same type provides additional insights in their operation and modelling requirements. In Stage 3, attention should be given to other motor types (A, B, and C), including water pumps and commercial refrigerator systems.



## Insights into EV Charger responses

- The current complex load model lacks a component that represents EVs or EV Chargers.
- Many small residential EV chargers comprise electrical contactors, communication and control elements but lack active power electronics. The response of the EV charger to a grid disturbance will depend on the response of the EV onboard power electronics as well as any additional behaviour (e.g., internal tripping) of the EV charger itself.
- Given that the response depends on the EV fleet, a stochastic model for the behaviour of residential EV chargers could be more suitable.
- Since only one EV was available to the project during Stage 2, additional testing involving various EVs is required.
- Fast chargers (or Level 3 chargers) incorporate power electronics and mitigate the impact of individual EVs to grid disturbances. Stage 2 did not include testing on fast chargers.

## Engagement with Stakeholders and OEMs

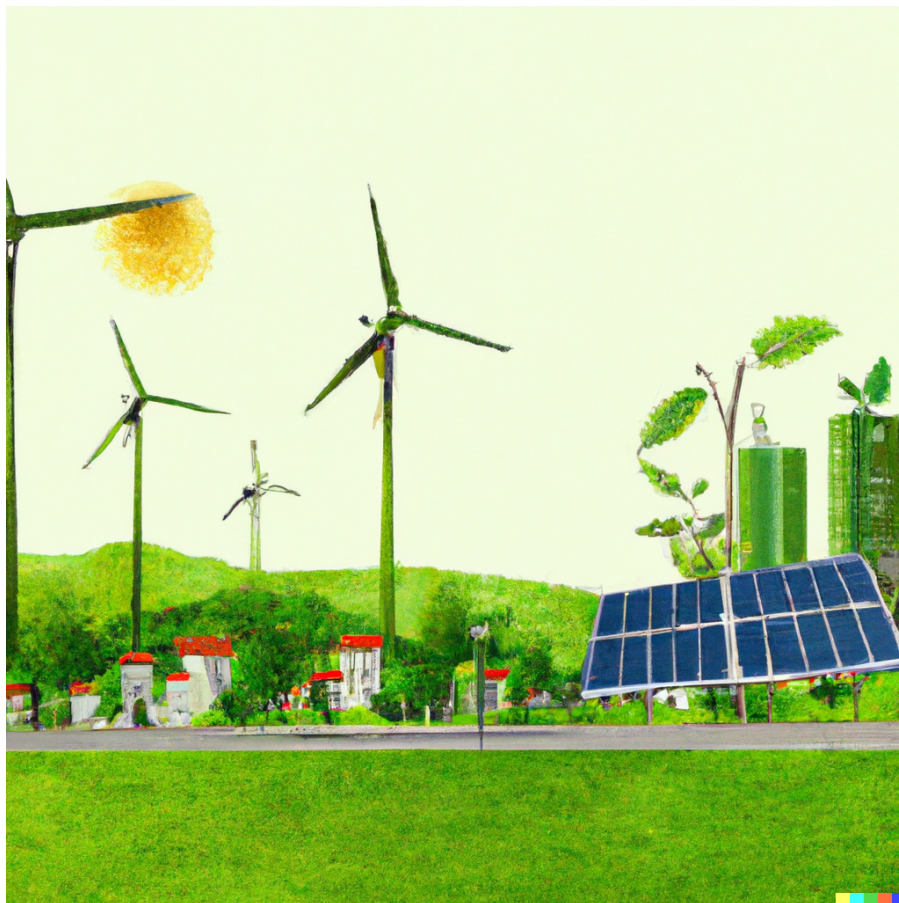
- BESS and HESS testing results were shared with stakeholders and OEMs to gather feedback on the methods and help us understand the captured behaviours.
- OEMs were provided with detailed results of unexplained or unexpected behaviours identifying recommended or necessary firmware updates.
- All tested systems were connected to OEM cloud services allowing interrogation of responses during faults from locally and remotely captured data.

## Project Resources and Results

Results from all tests can be found at <http://pvinverters.ee.unsw.edu.au/>

## Next Steps and Actions

- Development of time-domain aggregated models.
- Development of frequency-domain aggregated impedance models.
- Investigation of extended DER, BESS, and Hybrid PV/BESS inverter testing, focusing on BESS and HESS under grid disturbances.
- Identification of worse than expected effects and vulnerable DERs.
- Examination of the impact of external control devices on DER response.
- Extended testing of EVs and smart loads, emphasising power electronics converters, air-conditioners, and heat-pumps.
- Evaluation of interactions between smart loads and DER, and investigation differences between on-board EV chargers and converter-based charging infrastructure.
- Assessment of system restoration response of DER, ESS, and EVs in a low inertia environment with limited synchronous generation.
- Extended testing of motor types A, B, and C, including water pumps and commercial refrigerator systems.
- Continued engagement with OEMs to identify opportunities for improvement with available firmware, commissioning processes and remote capabilities.



## Contents

<b>1 Project Overview</b>	<b>14</b>
1.1 Project Scope . . . . .	15
<b>2 Project Alignment</b>	<b>17</b>
2.1 Alignment with GPST Consortium Research Program . . . . .	17
2.2 Alignment with Topic 9 Proposal . . . . .	19
2.3 Data Driven Aggregation . . . . .	19
2.4 Progress Against Topic 9 Key Research Questions . . . . .	21
<b>3 Testing Procedure</b>	<b>23</b>
3.1 DER and BESS Testing . . . . .	23
3.2 DER and BESS Testing Setup . . . . .	25
3.3 Load Testing Setup . . . . .	26
3.4 Load Tests . . . . .	27
3.5 Justification of Proposed Approach . . . . .	27
<b>4 DER Tests</b>	<b>29</b>
4.1 Inverter 41 (PV Inverter) . . . . .	30
4.1.1 Bench Testing Results . . . . .	30
4.1.2 Comprehensive Voltage Sag Results . . . . .	32
4.2 Inverter 42 (PV Inverter) . . . . .	33
4.2.1 Bench Testing Results . . . . .	33
4.2.2 Comprehensive Voltage Sag Results . . . . .	35
4.3 Observations . . . . .	36
<b>5 BESS &amp; HESS Testing</b>	<b>37</b>
5.1 Inverter 43 (Hybrid Inverter) . . . . .	37
5.1.1 Mode 1 . . . . .	37
5.1.2 Mode 2 . . . . .	42

5.1.3 Mode 3 . . . . .	44
5.2 Inverter 44 (Hybrid Inverter) . . . . .	48
5.2.1 Mode 2 . . . . .	48
5.3 Inverter 45 (BESS Inverter) . . . . .	53
5.4 Inverter 46 (Hybrid Inverter) . . . . .	59
5.4.1 Mode 2 . . . . .	59
5.5 Inverter 47 (Hybrid Inverter) . . . . .	62
5.5.1 Mode 2 . . . . .	62
<b>6 Load Tests</b>	<b>65</b>
6.1 Refrigerators . . . . .	65
6.2 Microwave Ovens . . . . .	67
6.3 Air Conditioners . . . . .	68
6.3.1 DOL Based Conventional Unit . . . . .	68
6.3.2 Inverter Based Units . . . . .	71
6.4 Motor Based Appliances . . . . .	74
6.4.1 Vacuum Cleaner . . . . .	74
6.4.2 Fans . . . . .	76
6.5 Static Loads . . . . .	77
6.5.1 Heaters . . . . .	77
6.5.2 LED Lighting . . . . .	79
<b>7 Residential Electric Vehicle Chargers</b>	<b>81</b>
7.1 Level 1 EV Charger . . . . .	81
7.2 Level 2 EV Charger . . . . .	83
<b>8 Load Modelling</b>	<b>87</b>
8.1 Comparison with PSSE Results . . . . .	88

## List of Figures

1	Links and alignments between GPST Topic 9 and other research topics. . . . .	17
2	Research Topics and alignment of Stage 2 research. . . . .	19
3	Complementary analysis techniques to assess DER behaviour during disturbance events [4] . . . . .	21
4	Schematic of the experimental setup at UNSW Sydney . . . . .	25
5	Inverter bench-testing setup at UNSW Sydney . . . . .	26
6	Load Testing Setup at UoW (a) Programmable Power Supply, and (b) Air Conditioner under Test . . . . .	26
7	Inverter 41 power curtailment behavior to step frequency change of 1.95Hz . . . . .	30
8	Inverter 41 ride-through behavior to voltage sag with amplitude of 0.8 p.u. and duration of 220 ms . . . . .	32
9	Inverter 42 ride-through behavior to voltage swell of 3x 230 to 270V for 0.1s . . . . .	33
10	Inverter 42 ride-through behavior to voltage sag with amplitude of 0.8 p.u. and duration of 800 ms. . . . .	35
11	Inverter 43 disconnection behavior to voltage sag to 50V for 0.9s. . . . .	38
12	Inverter 43 disconnection behavior at 100% power to voltage sag with amplitude of 0.8 p.u. and duration of 80 ms. . . . .	40
13	Inverter 43 disconnection behavior at 100% power to voltage swell with amplitude of 1.2 p.u. and duration of 220 ms. . . . .	41
14	Inverter 43 ride-through behavior at 50% power to voltage swell with amplitude of 1.2 p.u. and duration of 220 ms. . . . .	42
15	Inverter 43 disconnection behavior at 100% power to voltage sag with amplitude of 0.8 p.u. and duration of 800 ms. . . . .	43
16	Inverter 43 disconnection behavior at 50% power to voltage swell with amplitude of 1.2 p.u. and duration of 80 ms. . . . .	44
17	Inverter 43 disconnection behavior to voltage sag to 50V for 0.9s. . . . .	45
18	Inverter 44 power curtailment behavior to ramp voltage change to 265V in 0.5s. . . . .	50
19	Inverter 44 disconnection behavior to $\pm 30^\circ$ voltage phase-angle jump. . . . .	50
20	Inverter 44 disconnection behavior to voltage sag of 0.5 p.u for 80 ms. . . . .	51
21	Inverter 45 ride-through behavior to ramp frequency change of 0.4Hz/s to 51.95Hz. . . . .	54

22	Inverter 45 reconnection behavior to ramp frequency change of 0.1Hz/s to 47.05Hz. . . . .	55
23	Inverter 45 power curtailment behavior to ramp voltage change to 185V in 15s. . . . .	56
24	Inverter 45 disconnection behaviour to voltage sag of 0.7 p.u for 120 ms. . . . .	58
25	Impact of Voltage Sags on: (a) Refrigerator 1 (b) Refrigerator 2 . . . . .	66
26	Impact of Phase Angle Jumps on: (a) Refrigerator 1 (b) Refrigerator 2 . . . . .	67
27	Response of Microwave Load when subject to a Sag/Swell with duration of 220ms (a) Sag with magnitude 0.2pu (b) Swell with magnitude 1.2pu. . . . .	67
28	Frequency Change Response of the Microwave: (a) Step change from 50 Hz to 52 Hz, (b) 50 Hz to 47 Hz, (c) Ramp of +0.4 Hz/s (d) Ramp of -0.4 Hz/s. . . . .	68
29	Response of Air Conditioner when subject to Voltage Disturbances: (a) Voltage Sag, and (b) Voltage Swell . . . . .	69
30	Frequency Change Response for the Air Conditioner: (a) Step decrease to 47 Hz, and (b) Step increase to 52 Hz . . . . .	70
31	Impact of phase angle jump on the air conditioner operation: (a) P and Q response, and (b) Current drawn . . . . .	70
32	Response to a Swell of Voltage Magnitude 1.2 pu for 80ms (a) Air Conditioner 1 (b) Air Conditioner 2 (c) Air Conditioner 3 . . . . .	73
33	(a) Impact of Step Frequency Disturbance on Air Conditioner 1 (b) Impact of -90° Phase Angle Jump on Air Conditioner 1 . . . . .	74
34	Response of Vacuum Cleaner (a) Sag with retained Voltage of 0.2 pu for 220ms (b) Swell with Voltage of 1.2 pu for 220ms . . . . .	75
35	Frequency Response of the Vacuum Cleaner (a) Reduction in Frequency at 0.4 Hz/s (b) Step Increase in Frequency from 50 Hz to 52 Hz . . . . .	75
36	Response of Fan for Voltage Sag and Swell Disturbances (a) 0.2 pu Sag for 220ms (b) 1.2 pu Swell for 220ms . . . . .	76
37	Frequency Response of Fan (a) Step Decrease in Frequency from 50 Hz to 47 Hz (b) Step Frequency from 50 Hz to 52 Hz . . . . .	77
38	Heater Response to Sag of Retained Voltage Magnitude 0.2 pu for 220 ms (a) Heater 1 (b) Heater 2 . . . . .	78
39	Impact of Frequency Disturbance (a) Heater 1 (b) Heater 2. . . . .	78
40	Response of LED Light Bulb for Voltage Sag of duration 220ms with Retained Voltage Magnitude (a) 0.8 pu (b) 0.7 pu. . . . .	79

41	Response of LED Light Bulb (a) Voltage Swell of 1.2 pu for 220 ms (b) Step Frequency Increase from 50 Hz to 52 Hz . . . . .	80
42	Response of EV Charger to Sag of 0.6 pu for 220 ms (a) Voltage- Current Response (b) PQ Response . . . . .	82
43	Demonstration of different reconnection time depending on the retained voltage during a voltage sag (a) 0.4 pu (b) 0.3 pu . . . . .	82
44	Impact of Frequency and Phase Angle Jump for EV Charger (a) Step Frequency Change from 50 Hz to 52 Hz (b) Ramp Frequency at -4 Hz/s (c) Phase Angle Jump . . . . .	83
45	EV Charger Test Setup . . . . .	84
46	Response of EV Charger to a Voltage Sag of 0.2 pu Retained Voltage for 220 ms (a) Current response (b) P and Q response . . . . .	85
47	EV Charger Response to a Voltage Swell of Magnitude 1.2 pu for 220 ms (a) Current Response (b) P and Q Response . . . . .	85
48	EV Charger Response to Step Frequency Disturbances (a) 50 Hz to 47 Hz (b) 50 Hz to 52 Hz . . . . .	86
49	Diagram of the WECC Composite Load Model (WECC-CMLD). . . . .	87
50	Comparison of bench test and SMIB simulation for vacuum cleaner under voltage sag . . . . .	89

## List of Tables

1	Australian GPST Topics and Their Relevance to Topic 9 . . . . .	18
2	Modes of Inverter Testing . . . . .	23
3	Steady-state Performance validation . . . . .	23
4	Voltage Disturbances – Steps and Ramps . . . . .	24
5	Voltage Disturbances - Sags . . . . .	24
6	Voltage Disturbances - Swell . . . . .	24
7	Frequency Disturbances . . . . .	25
8	Phase-angle Jump . . . . .	25
9	Modern Loads Selected for Tests . . . . .	27
10	Detailed ac voltage sag testing schedule . . . . .	29
11	Summary of bench testing results of inverter 41. . . . .	31
12	Inverter 41 voltage sag test results . . . . .	31
13	Summary of bench testing results of inverter 42. . . . .	34
14	Inverter 42 voltage sag test results . . . . .	34
15	Summary of bench testing results of inverter 43 in mode 1. . . . .	39
16	Inverter 43 voltage sag test results at 100% Power . . . . .	39
17	Inverter 43 voltage swell test results at 100% Power . . . . .	40
18	Inverter 43 voltage swell test results at 50% Power . . . . .	41
19	Inverter 43 voltage sag test results at 100% Power . . . . .	43
20	Inverter 43 voltage swell test results at 100% Power . . . . .	44
21	Summary of bench testing results of inverter 43 in mode 3. . . . .	46
22	Inverter 43 voltage sag test results at 100% Power . . . . .	46
23	Inverter 43 voltage swell test results at 100% Power . . . . .	47
24	Summary of bench testing results of inverter 44 in mode 2. . . . .	49
25	Inverter 44 voltage sag test results at 100% Power . . . . .	49
26	Inverter 44 voltage swell test results at 100% Power . . . . .	52
27	Summary of bench testing results of inverter 45 (Battery ESS only). . . . .	57

28	Inverter 45 voltage sag test results at 100% Power . . . . .	57
29	Inverter 45 voltage swell test results . . . . .	58
30	Inverter 46 voltage sag test results at 50% Power . . . . .	59
31	Summary of bench testing results of inverter 46 in mode 2. . . . .	60
32	Inverter 44 voltage swell test results at 100% Power . . . . .	61
33	Inverter 44 voltage swell test results at 100% Power . . . . .	61
34	Summary of bench testing results of inverter 47 in mode 2. . . . .	63
35	Inverter 46 voltage sag test results at 50% Power . . . . .	63
36	Inverter 44 voltage swell test results at 100% Power . . . . .	64
37	Inverter 44 voltage swell test results at 100% Power . . . . .	64
38	Summary of Voltage Sag Tests for Air Conditioner 1 . . . . .	71
39	Summary of Voltage Sag Tests for Air Conditioner 2 . . . . .	72
40	Summary of Voltage Sag Tests for Air Conditioner 3 . . . . .	72
41	Response of EV Charger for Voltage Sags of Different Magnitude and Duration . . . . .	83

## 1 Project Overview

The continuous growth of distributed energy resources (DER), predominantly in the form of solar PV systems, combined with hybrid and standalone battery energy storage systems (HESS and BESS), electric vehicle chargers, and power-electronics based loads into distribution networks complicates network management and necessitates development of new tools and methods. To this extent, AEMO in Australia, TNSPs and DNSPs as well as all other organisations that are tasked with operating networks and associated markets need to have access to up-to-date, precise, efficient, and future-proof tool-sets that accurately reflect and represent the state of a system at any location and point in time.

AEMO recognises that the “ZIP” load models that have been in use for the past 20 years no longer capture i) the current composition of the loads commonly connected to distribution networks or ii) the response of power electronics converters [5]. This requires the development of sophisticated aggregate load models capable of replicating the dynamic responses observed in the networks.

In the short term, it is critical to include the response of the large amounts of DER that is connected to distribution systems in load models maintaining system security under very high penetrations of DER [6]. One such example is the use of composite load models (See Figure 1) which account for the additional elements in distribution networks. In the longer term, it is important to account for the impact of modern, flexibly controlled loads, including domestic loads, industrial loads, electrolyzers, BESS and Electric Vehicle Chargers.

All these new devices demonstrate rapid and complex behaviours during power system disturbances and, even in steady state; their detailed modelling is a requirement for System Operators to make operational and planning decisions, and eventually satisfy their key responsibilities towards maintaining a stable and resilient power system. Understanding and modelling DERs and future flexible loads for the purposes of supporting ISOs requires understanding a broad range of behaviours that can be generally classified into two distinct categories:

- **Their extrinsic behaviour**, which relates to the provision of ancillary services to the network from DER, assisting with load management, voltage regulation strategies from flexible loads, generation variability and uncertainty, operation and planning etc. Current approaches for such issues consider high-level control of DER, integrated communication (to central or distributed controllers), use of setpoints etc, and
- **Their intrinsic behaviour**, which relates to how DER are programmed to respond to external events and also includes load – DER interactions. These include fault-ride through (FRT and LVRT) capabilities, over/under frequency response, phase angle jumps, faults to the HV network that propagate to the LV, reactive power requirements, etc.

As these load models are used for multiple power system studies, additional requirements for

evaluating DER and load responses as well as load models include detailed modelling suitable for Root Mean Square [RMS] studies, EMT-type as well as real-time studies.

Identifying the causes and impact of disturbances on the behaviour of DER and loads alike requires detailed understanding of both intrinsic and extrinsic behaviours which in turn lead to a variety of responses, such as a temporary cessation or slow recovery to nominal set-points or inaccurate following of predefined set-points. These are often observed combined with inverter protection functionalities enabled by the same event, for instance DC overvoltage / overcurrent, AC overvoltage / overcurrent and frequency related protections. In fact, all of these behaviours are commonly seen across the fleet of DPV inverters and are expected to be seen in all future DER.

Furthermore, the transient behaviour of loads has not been considered important as the power system could always be relied on to have sufficient inertia and ensure that load continued to operate through short-term transient events or to enable restarting of loads. The dynamic interaction between loads and DER was also not a consideration. Better understanding of load performance has been identified by AEMO as a key component of developing models that better reflect the electricity supply network as it transitions to a clean energy paradigm and are sufficiently accurate to predict the dynamic operation of the power system.

Whilst there is substantial activity in various specialised research areas related to inverter control and controller design it is clear that many of these do not focus on the practical implementation and associated limitations that are imposed by standards and regulations, nor does the work make serious attempts at considering the economics of inverter design and control.

The intrinsic behaviour of DER should also account for their role in an environment where greater amount of DER is connected to weaker grids, “– how is distributed PV affected by system strength? If system strength is low, would distributed PV be less likely to ride-through? Is there a threshold of system strength we need to maintain in the transmission network, to allow distributed PV to remain connected in disturbances?”

## 1.1 Project Scope

The scope of Stage 2 work for Topic 9 includes the following:

- 1. A future-proof pathway for load modelling** – Power system loads are consistently evolving and a prompt response to developments and changes is of paramount importance [7]. Futureproofing load models to account for changes in load compositions and new responses will allow operators to identify and predict future causes of power reduction and system instability. It also allows studies to further validate the interaction between DER and flexible loads, supports research on improvements that can be made to the system to allow it to remain operational during fault events, and contributes to information sharing with the industry regarding systemic risks.

2. **A research team that can readily adapt to the testing needs of AEMO** – The skills and resources generated by the project can be readily used by AEMO to test specific events or specific inverters / loads and support ongoing development work, including in-field data driven analysis to support model validation.
3. **Open data sharing of inverter and load responses** – An extensive dataset from the bench-testing of DER, BESS, EVs and loads will be made openly available. Expanding the availability of open datasets allows for further work and more solutions to be developed both from the PIs of the project as well as other research organisations.
4. **New bench-testing capabilities at UNSW and UoW**. The extension of the ongoing PV inverter bench-testing at UNSW [6], and complementing it with the capabilities at UoW, the project will enable development of a comprehensive platform for experimental testing of multiple devices. This outcome is important as the true response of all devices can only be observed through experimental testing which facilitates accurate measurements across multiple tests.
5. **Updated Load Models** – By extending experimental testing and measurements, the project will support the development of a new AEMO tool set for load modelling including revisions required to include higher penetrations of IBR throughout DNSPs networks. This objective can only be met through an integrated examination of inverter benchmark responses as well as network measurements and correlation of responses with real-world measurements.

## 2 Project Alignment

### 2.1 Alignment with GPST Consortium Research Program

The initial Report of Topic 9 "Ensuring System Security and Modelling Fast Load DER Responses with high penetrations of IBR" highlighted the broader alignment of the research with the broader GPST research program, mapping onto related GPST questions and synergies between Topic 9 and the rest of the work conducted in Australia.

The priority research questions addressed through Stage 1 and Stage 2 research are:

- The behaviour of the DER installed fleet will continue to change (GPST Q6, Q10, Q12)
- Evidence of DER behaviours are inputs to operational decisions around management of system security (GPST Q12, Q44, Q45, Q46)
- Targeted modification to power system operating processes are necessary to maintain security (GPST Q45, Q46)
- Better evidence for less conservative assumptions is critical (GPST Q21, Q45, Q46)
- Meeting obligations to ensure modelling data used for planning, design and operational purposes. (GPST Q46)

while Fig. 2 and Table 1 [1] identify the relations and links between Topic 9 and the rest of the GPST research topics.

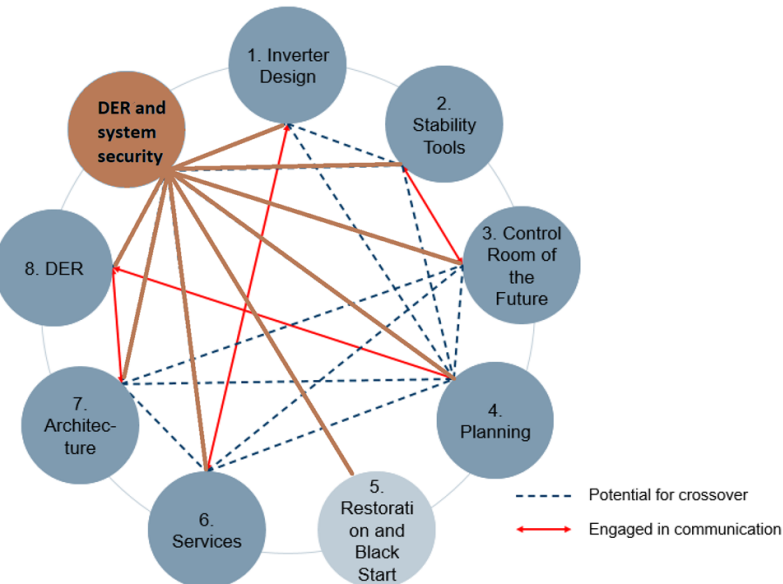


Figure 1: Links and alignments between GPST Topic 9 and other research topics.

Table 1: Australian GPST Topics and Their Relevance to Topic 9

#	Identified Topic	Relevant Inputs	Relevant Outputs
1	Inverter Design	Performance metrics: A/us, large- and small-signal current bandwidth	Response requirements
2	Stability Tools	Performance requirements of models including physical range, time granularity, small-signal response	Large-signal response of DER/IBR
3	Control Room of the Future	Definition of HMI and underpinning modelling toolset requirements	Load-IBR composite models
4	Planning	Planning tools and developments	Load-IBR composite models, security issues related to large-signal responses
5	Black start	Blackstart procedures based on Topics 4 and 7 affect the frequency and severity of disturbances seen by IBRs	Large-signal response of DER/IBR, start-up behaviour, standards
6	Services	Service requirements and specifications	Verification of IBR performance
7	Architecture	Proposed suite of architectures and their reliance on DER/IBR response	Load-IBR composite models, security issues related to large-signal responses of DER/IBR, start-up behaviour, standards
8	DER	Desired DER responses	Load-IBR composite models, security issues related to large-signal responses of DER/IBR, start-up behaviour, standards

## 2.2 Alignment with Topic 9 Proposal

The broad objective of Topic 9 within the GPST Research program is to "ensure that ISOs and TSOs are able to maintain power system security under very high penetrations of IBR such as distributed PV, energy storage, and other resources including inverter-based demand."

Australia is uniquely placed to deliver valuable knowledge to international ISOs and TSOs, owing to its longitudinal, weak and weakly interconnected power system [3], coupled with an extensive, and perhaps unparalleled, implementation of distributed solar PV systems and the growth in distributed energy storage systems.

Fig. 2 shows an overview of the Topic 9 research program and how the proposed research and development schedule and topics offers can support practical deployment. The figure also highlights the key areas that are covered as part of Stage 2, with a particular focus on:

- Inverter Responses and sensitivities
- Dynamics of Power Quality Modes,
- Fault and disturbance propagation,
- Extension of the AEMO tool-set,
- Input to development and validation of the Load-DER composite model,
- Roll-out of the revised AEMO tool-set, and
- Engagement with stakeholders.

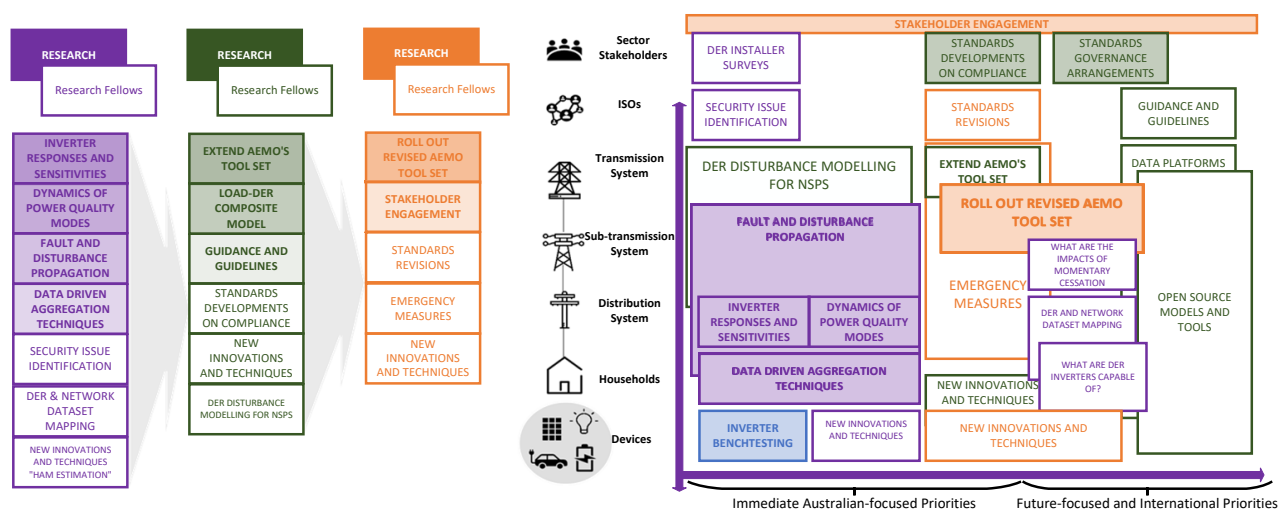


Figure 2: Research Topics and alignment of Stage 2 research.

## 2.3 Data Driven Aggregation

Data-driven analysis and aggregation techniques play a crucial role in comprehending the real-world performance of DER. Despite certain limitations, these techniques serve as complementary tools to in-lab bench-testing and power system modelling for understanding DER behaviour. Data-driven

aggregation and analysis techniques are particularly valuable for [1]:

- Validating the accuracy of power system models,
- Capture diverse DER behaviours in response to complex conditions, and
- Identify ‘unknown unknowns’.

Examination of in-field DER behaviour is essential to understand the variety of responses that may arise. This is particularly critical given the variety and complexity of disturbances across the transmission and distribution networks. For instance, under-voltage disturbance events can cause load ‘shake off,’ leading to localised over-voltage conditions. As a consequence, DER might react to either the original under-voltage disturbance or the emerging over-voltage situation in the surrounding network.

The limitations of data-driven methods include sample size, the suitability of specific measurement approaches, as well as sampling frequency and interval. Combining data-driven methods with other ways to examine the behaviour of DER as well as loads, such as bench-testing and analysis of power system disturbances and their propagation, can enhance their effectiveness. Fig. 3 [1] shows how a relevant, comprehensive research program can develop thorough understanding of DER risks to power system stability, security by integrating multiple research techniques. The focus of Stage 2 has been on extending the original PV inverter testing (bottom right corner of Fig. 3) to accommodate the broader variety of distributed generation, storage, loads and their combinations of a future power system. Fig. 3) also provides an illustrative example of how the proposed program of research could build a more complete picture of DER risks to power system security through combining a number of research techniques.

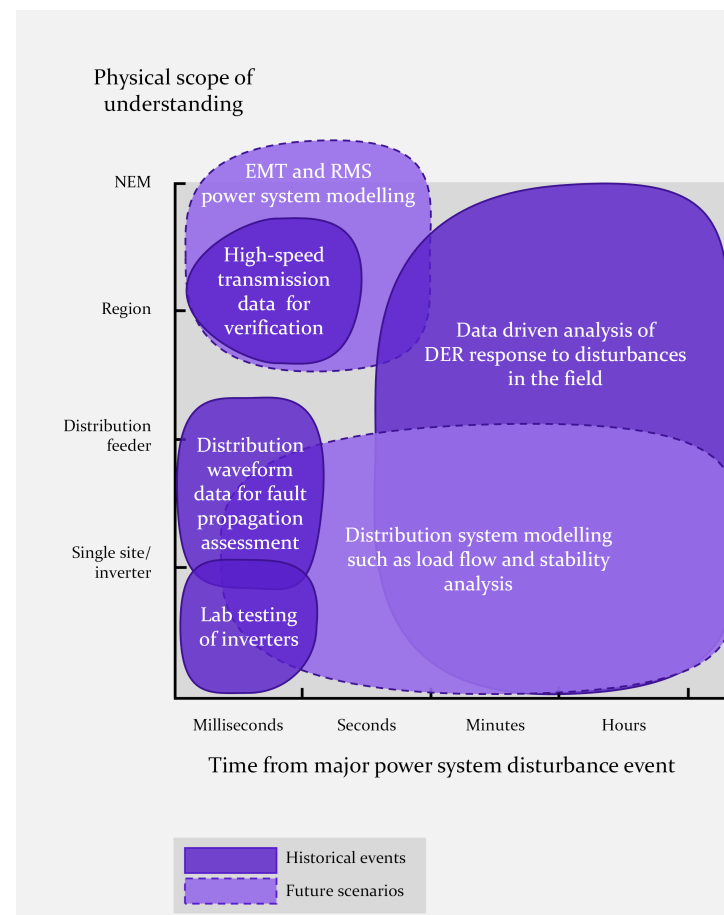


Figure 3: Complementary analysis techniques to assess DER behaviour during disturbance events [4]

## 2.4 Progress Against Topic 9 Key Research Questions

Topic 9 [1] introduced key research questions related to DER, their integration and their impact on grid stability and relation to the GPST research plan [2]. The following section summarises the progress against each question completed as part of Stage 2.

1. *What pilot studies must be performed on the network to better understand the behaviour of DER to grid disturbances?*
  - **Continuous testing of DPV inverters (100%).** With the extensive tests completed at UNSW over the past 4 years and the open release of the testing procedure, we consider this aspect complete. However, continuous testing is required to ensure that newer DPV inverters meet requirements.
  - **Testing of BESS and HESS (50%).** Testing of 5 devices demonstrated issues with responses when exposed to grid disturbances. The testing procedure is released but additional tests are required to provide adequate input to load modelling in RMS and EMT models.
  - **Testing of EVs (10%).** The complexities introduced by EV charging infrastructure and

EVs requires further testing, especially as EVs are expected to drive major load growth in distribution networks. Testing of 2 EV chargers and 1 EV do not provide sufficient results for load modelling.

- **Testing of loads (40%).** Additional testing is required for loads that correspond to Motor types A, B and C of the CMPLDW load models. Load coincidence or diversity factor also needs to be accounted for.
  - **Validation against observations in the networks (20%).** Preliminary work has been undertaken, but additional model development is required.
2. *What international activity is underway and the extent of this activity, and what opportunities are there for our research in DER in Australia to be of practical use in other regions? What are those regions and how do we engage and with whom?*
    - Not within the scope of Stage 2.
  3. *How do we future-proof the technical interventions being made in the LV network to solve other technical or regulatory challenges given the likely impacts of increased penetrations of DER within the areas of influence of those interventions?*
    - Not within the scope of Stage 2.
  4. *How have standards for inverters evolved internationally around disturbance ride-through, response time definitions and power quality modes? Where do we see the technical requirements evolving to?*
    - No major revisions to Australian and relevant international standards during Stage 2 work.  
See Appendix in [1] for a list of relevant standards and the current requirements for grid connection of DER.
  5. *What are the possible interactions between inverter responses to network dynamic operating envelopes and major power system disturbances. What have we seen happen? What can we predict will happen in the future following various scenarios in AEMO plans?*
    - The work that has been undertaken in Stage 2 has informed the development of EMT models for appropriate validation that can be used to evaluate the dynamic performance of networks during major power system disturbances. As noted above, additional testing is required for a number of devices before a comprehensive understanding of the interactions between modern generation and loads and networks behaviour during power system disturbance can be achieved..
    - Fault propagation within power systems, especially from transmission to distribution networks were considered but the work was considered not to be within the scope of Stage 2.

### 3 Testing Procedure

The first task of the project was a review (with extensive input from AEMO) of the testing procedure that was developed by UNSW as part of the previous ARENA project. The key reasons for the review and the subsequent revision of the testing procedure were:

- To reduce and rationalise the number of tests that are performed for each device under test,
- To identify the key tests that provide useful information for the load modelling process, and
- To align the previous DPV testing with the extended DER and load tests undertaken as part of this project.

#### 3.1 DER and BESS Testing

As the new DER tests cover both inverters used in standalone BESS as well as hybrid inverters which include a BESS together with a PV system, the inverter testing modes were separated into two as shown in the following table.

Table 2: Modes of Inverter Testing

Mode	Hybrid Inverters	Battery Inverters
1	PV + Battery	Battery
2	PV	
3	Battery	

All devices are validated for their steady state performance, specifically looking at their steady-state performance of the inverter at its lowest possible setting (Min%) and at 100% of its rated power (Max%).

Table 3: Steady-state Performance validation

Sr.	Test
1.	Steady State performance of inverter at Min%
2.	Steady State performance of inverter at 100%

The system disturbance tests are classified into three categories:

- Voltage Disturbances,
- Frequency Disturbances, and
- Phase Angle Jumps.

These tests are summarised in the following tables and further details will be provided in the detailed testing procedure document that will be released as part of the first deliverable of the project.

The testing procedure will be made openly available so that the test can be repeated and replicated from any other interested party.

Table 4: Voltage Disturbances – Steps and Ramps

Sr.	Step Voltage Change
1.	230 to 260V
2.	230 to 50V sag for 0.9s
3.	230 to 160V sag for 9s
4.	230 to 270V Swell for 0.9s
Ramp Voltage Change	
5.	230 to 185V for 15s
6.	230 to 265V for 15s

Table 5: Voltage Disturbances - Sags

Voltage Sag Magnitude (pu)	Duration of Sag (ms)		
0.8	80	120	220
0.7	80	120	220
0.6	80	120	220
0.5	80	120	220
0.4	80	120	220
0.3	80	120	220
0.2	80	120	220

Table 6: Voltage Disturbances - Swell

Voltage Swell Magnitude (pu)	Duration of Sag (ms)		
1.05	80	120	220
1.1	80	120	220
1.125	80	120	220
1.15	80	120	220
1.175	80	120	220
1.2	80	120	220

Table 7: Frequency Disturbances

Frequency Disturbance Type	Frequency Change ( $\Delta F$ )
Step Frequency	+1.95 Hz
	-2.95 Hz
	+2 Hz
	-3 Hz
	$\pm 5$ Hz
Ramp Frequency Variation (RoCoF)	$\pm 0.4$ Hz/s
	$\pm 1$ Hz/s
	$\pm 4$ Hz/s

Table 8: Phase-angle Jump

	Phase angle change ( $\Delta \theta$ )
Phase Jump	$\pm 15^\circ$
	$\pm 30^\circ$
	$\pm 45^\circ$
	$\pm 60^\circ$
	$\pm 90^\circ$

### 3.2 DER and BESS Testing Setup

The test setup at UNSW' Power Electronics Research Laboratory used for the experiments are shown in Fig. 4 and Fig. 5 [8].

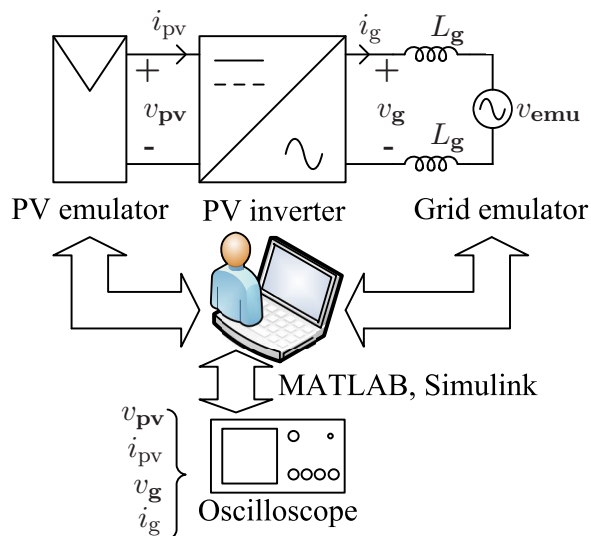


Figure 4: Schematic of the experimental setup at UNSW Sydney

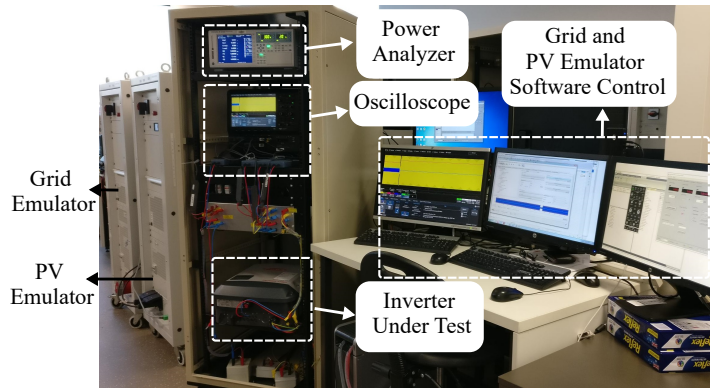


Figure 5: inverter bench-testing setup at UNSW Sydney

### 3.3 Load Testing Setup

To apply the mentioned disturbances, a California Instruments (MX45-3PI 45) arbitrary programmable power supply was employed as the power source. The load under examination was connected at the output of the power supply, and the voltage and current waveforms were measured and processed using MATLAB to assess the required active and reactive power responses of the devices. The utilized MATLAB program had the capability to calculate the root mean square (rms) variations in active power ( $P$ ) and reactive power ( $Q$ ) when subjected to changes in magnitude, frequency and phase angle of the supply voltage.

Figure 6 shows the laboratory setup employed for the load testing. In Figure 6(a), the programmable power supply (waveform generator) utilized to apply the disturbances is displayed, while Figure 6(b) presents an example of an air conditioner load connected to the bench testing setup.



Figure 6: Load Testing Setup at UoW (a) Programmable Power Supply, and (b) Air Conditioner under Test

### 3.4 Load Tests

During 2022, most of the time was assigned to the development of the load testing plan and undertaking the tests for the loads available in UOW's laboratory. At this stage all the different equipment listed in Table 8 have been completed, except for the EV charger. Due to the complexity of moving the power supply to the EV charging station (available in UOW), this task is planned to be completed early next year. The completed bench testing results have already been sent to AEMO. For each of the individual loads there are 21 voltage sag tests, 17 voltage swell tests, 8 frequency disturbance tests and 5 phase angle jump tests.

Table 9: Modern Loads Selected for Tests

Load Types
Heaters (e.g., electric fan, radiant heater)
Kettles
Fluorescent lights
Refrigerators (e.g., inverter based)
Fans (e.g., exhaust and pedestal)
Equipment with switching mode power supplies: <ul style="list-style-type: none"> <li>* Computers</li> <li>* Televisions</li> <li>* Other small electric devices</li> </ul>
Microwave
Equipment with DOL motors (e.g., bench grinder, vacuum cleaner)
Air Conditioners (e.g., inverter based)
Electric Vehicle chargers (e.g., residential)

### 3.5 Justification of Proposed Approach

The project and its outcomes have been designed to build on collaboration between UNSW and UoW, leverage the expertise of each organisation, optimise the available resources at both institutions and minimise the risks for the successful completion of the project. Specifically,

1. The proposed approach is laboratory and experimentally based, with complementary data-driven opportunities for model validation. By probing DER and flexible load responses and potential interactions between DER and loads, the proposed project will capture multiple characteristic responses which are commonly ignored in high-level models for instance, staged frequency tripping, rate of change of frequency (RoCoF) triggered tripping, asymmetric voltage - reactive power (volt-VAR) response, unexpected load behaviours, etc
2. Builds on UNSW's experience on inverter bench-testing and load modelling and the capabilities

and resources of UoW for flexible load testing.

3. Leverages existing infrastructure at both universities. This minimises the time and cost for the development of new experimental facilities in order to meet the ambitious outcomes proposed for the project while minimising resource duplication.
4. Proven compatibility and value to AEMO's current load modelling update methodology. Building on experience in testing and sharing of experimental results already used in the DER specific RMS load modelling, WP1a and WP1b can provide results directly usable by WP2 as well as AEMO with minimal friction.
5. By leveraging the bench-testing results of DER, BESS/HESS, EV chargers and flexible loads as part of WP1a and WP1b, the project enables holistic evaluation of load responses at different DER penetrations and under weaker grid conditions.
6. Testing of flexible loads allows for investigation of reactive power issues, especially recent observations across multiple system operators that power factor is no longer lagging and in some cases is becoming leading. The exact reason for this change in power factor behaviour and the implication for voltage regulation strategies such as volt/var response remains unknown.

## 4 DER Tests

Power electronics inverters have enabled the growth of renewable energy installations connecting to the grid at low voltage. Installed capacity from DER of less than 10 kW (mostly residential rooftop PV systems) makes up about the 60% off all PV capacity installed in the National Electricity Market (NEM). Grid and energy market operators have scarce visibility and no control of these small-scale systems, yet their aggregate electricity production is comparable to those of large power plants, which on the other hand are well visible and controlled in real-time by grid operators. These aspects become critical in the event of grid disturbances, where thousands of rooftop PV inverters may unexpectedly disconnect, removing significant amount of power generation from the system, challenging frequency management and contingency planning, therefore posing a risk to the secure operation of the bulk power system.

Technical product standards (such as AS 4777.2 [10]) are the only mechanism to ensure the correct operation of inverters during normal and abnormal grid conditions, as each inverter needs to pass a rigorous set of tests before being certified and allowed to be installed in Australia. Nevertheless, standards are continuously evolving and findings from the previous reporting periods identified potential shortcomings in the current standards which result in degraded inverter performance and vulnerability to grid events. It was identified that fast voltage sags, phase-angle jumps and rate of change of frequency can cause undesired inverter disconnection or unwanted power curtailments, lasting up to several minutes, and threatening the bulk power system stability when these behaviours affect large number of units during a grid event. In the case of South Australia, which is the state with the highest PV penetration and largest contribution from small-scale PV systems, AEMO identified voltage sags as a major threat to system security, exacerbated by disconnection of up to 53% of inverter connected DER [9]. The estimate given by AEMO, relies on analysis of field measurements and observation of results from inverter voltage sag tests conducted at UNSW under this project. After the update of the current Australian standard AS 4777.2:2020 [10], it is imperative to check that the new standard is appropriately implemented on the inverters. For this purpose, several tests were carried out to identify potential shortcomings of the current standard [11]. The test setup used for the experiments is represented in Fig 5. A set of comprehensive voltage sag tests has been carried out as specified in Table 10.

Table 10: Detailed ac voltage sag testing schedule

sag duration	sag magnitude							
	10%	20%	30%	40%	50%	60%	70%	80%
80 ms								
120 ms								
220 ms								

Additional tests:

- 800ms, 230 - 50 V sag

## 4.1 Inverter 41 (PV Inverter)

The bench testing process is used to understand the response of DER inverters to different grid disturbances. The tests which have been performed did not necessarily reflect those prescribed by the standard AS 4777.2:2020 [10]. The objective is to see the adaptation of the Australian standard and see the performance against it by new inverters to see any gaps in the new standard that need further investigation.

### 4.1.1 Bench Testing Results

This inverter showed desired response to different disturbances following the AS 4777.2:2020. An example of the step frequency change test is shown in Fig 7, where the frequency is increased near the trip limit and output power is curtailed by the inverter to zero. Inverter took several minutes to return to the pre-fault power level after the frequency was restored to a nominal level following the frequency ramp rate. A summary of bench testing test results of inverter 41 is shown in Table 11.

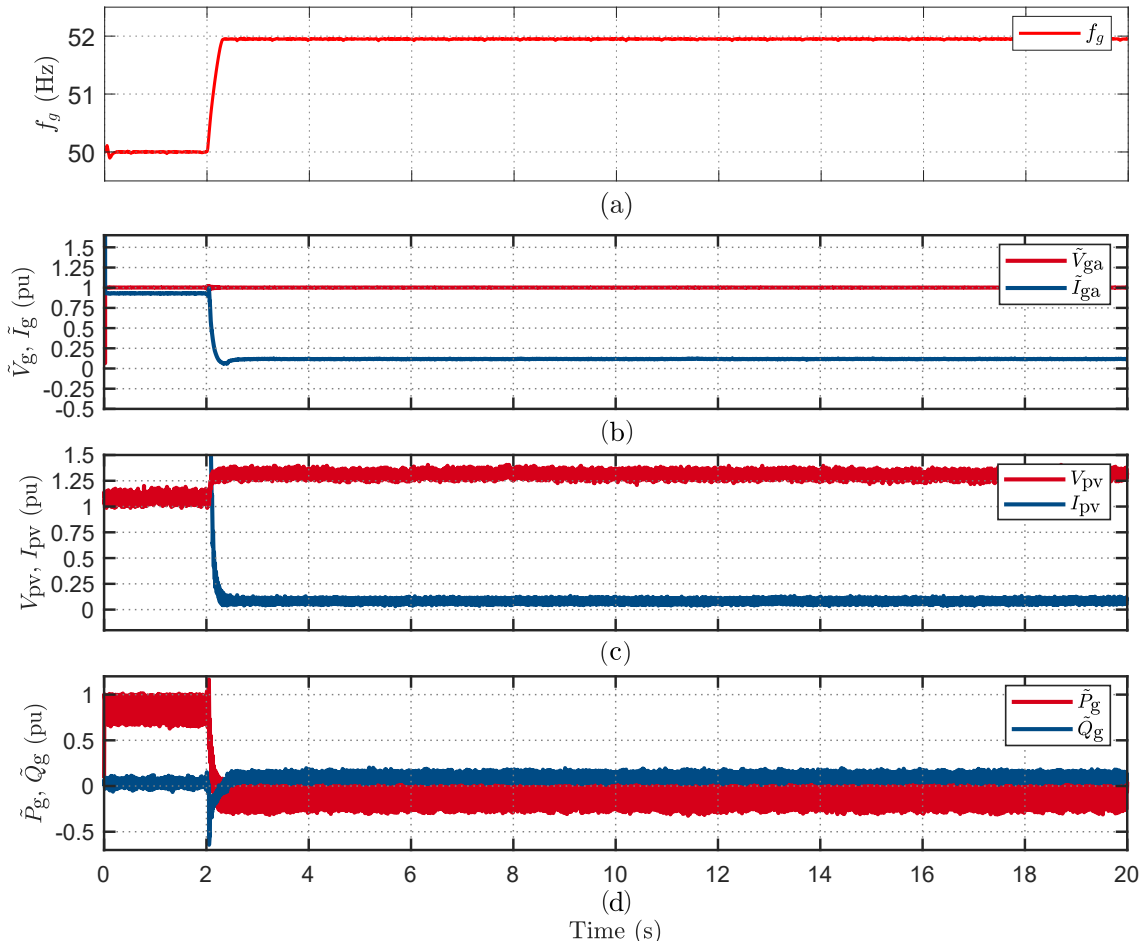


Figure 7: Inverter 41 power curtailment behavior to step frequency change of 1.95Hz

Table 11: Summary of bench testing results of inverter 41.

Response type	Steady state	Power dynamic	Test		
			Step frequency	Ramp frequency	Voltage disturbance
Ride-through	<b>0%, 50%, 100%</b>	<b>Step: 50% - 100% Ramp: 50% - 100%</b>	<b>-2.95Hz,</b> <b>230 to 50 for 0.1s</b> <b>230 to 160 for 0.9s</b> <b>3x 230 to 50 for 0.1s</b> <b>3x 230 to 270 for 0.1s</b>	-	<b>+/-15, +/-30, +/-45, +/-90</b>
Disconnect	-	-	<b>+5Hz, -5Hz</b>	-	230 to 270 for 7s, 230 to 160 for 4s 230 to 160 for 10s 230 to 280 for 10s
Power reduction	-	-	<b>+1.95Hz, +2Hz, -3Hz</b> <b>+1Hz/s to 51Hz, +1Hz/s to 52Hz, +4Hz/s, -1Hz/s, -4Hz/s</b>	-	-

Table 12: Inverter 41 voltage sag test results

sag duration	Voltage amplitude during the sag (p.u.)					
	0.8	0.7	0.6	0.5	0.4	0.3
80 ms	✓	✓	✓	✓	✓	✓
120 ms	✓	✓	✓	✓	✓	✓
220 ms	✓	✓	✓	✓	✓	✓

Additional tests:  
 • 800ms, 230 - 50 V sag: ✓  
 Legend:  
 ✓ : ride-through

#### 4.1.2 Comprehensive Voltage Sag Results

This inverter rides through all voltage sag tests. An example of ride-through behaviour performed by Inverter 41 on a voltage sag with an amplitude of 0.8 p.u and duration of 220 ms is displayed in Fig 8. Note that the injected current to the grid during the disturbance,  $I_{ga}$  is reduced to zero. After the disturbance, when the voltage is recovered,  $I_{ga}$  recovers with an overshoot close to 1.2 p.u. Then inverter resumes the injection of current to the pre-disturbance level. After the sag, the inverter power remains the same as the pre-sag condition.

The authors understand that momentary cessation is a desirable feature because if the voltage disturbance is cleared quickly (e.g. within one second), then, during the fault clearance time, PV inverters will not inject current into the fault, hence avoiding causing undesired trip of protection relays in the grid. This is important, especially under the assumption that protection relays in distribution networks were designed and rated without considering the eventual fault-current contribution from DER. The behaviours displayed by this inverter under the new voltage sag testing schedule are summarized in Table 12.

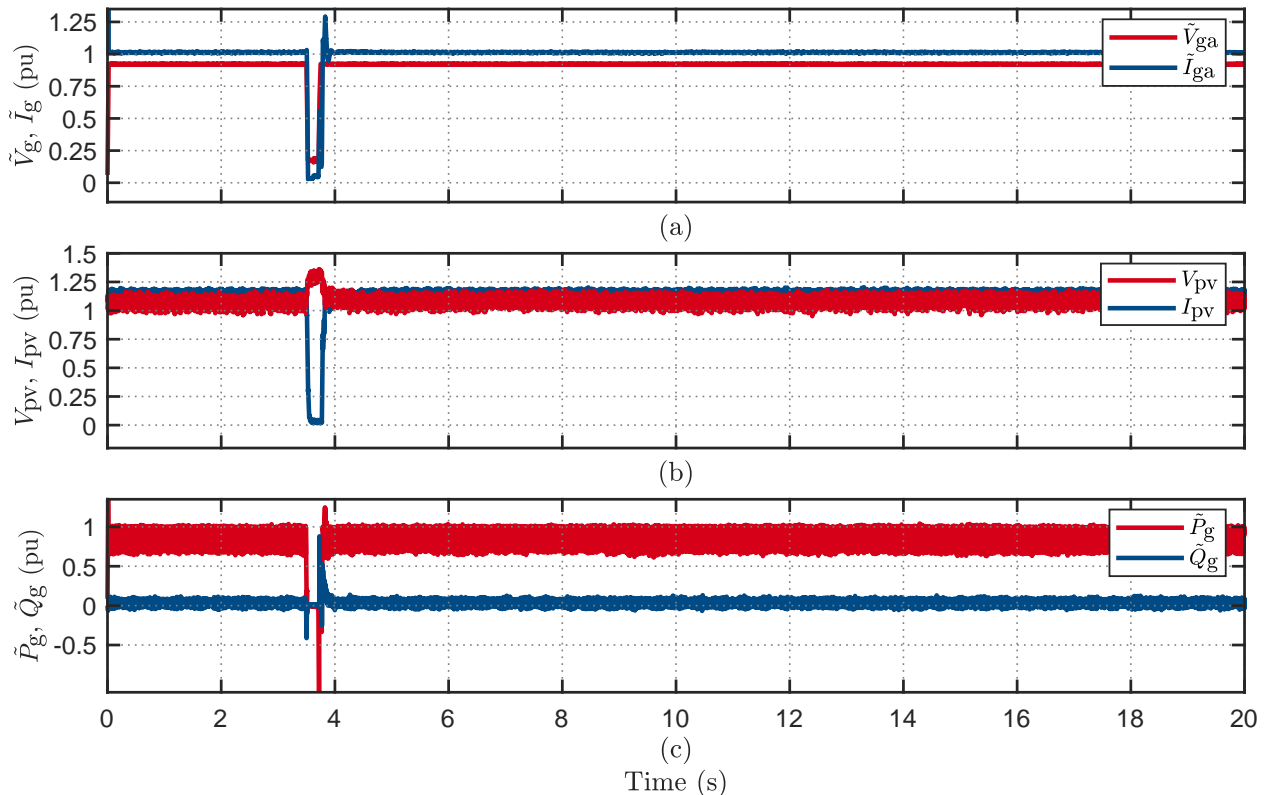


Figure 8: Inverter 41 ride-through behavior to voltage sag with amplitude of 0.8 p.u. and duration of 220 ms

## 4.2 Inverter 42 (PV Inverter)

The bench testing process is performed on inverter 42 to analyse the performance against those prescribed by the standard AS 4777.2:2020. The objective is to see the adaptation of the Australian standard and see the performance against it by new inverters to see any gaps in the new standard that need further investigation.

### 4.2.1 Bench Testing Results

This inverter showed desired responses to different disturbances following AS 4777.2:2020. An example of the step voltage change test is shown in Fig 9, where the voltage is increased three times to 270V for 0.1s. This change in voltage is above (overvoltage 1) specified disconnection limit, and the duration is less than the trip delay time the inverter rode through the disturbance without significant distortion in the output. A summary of bench testing test results of inverter 42 is shown in Table 13.

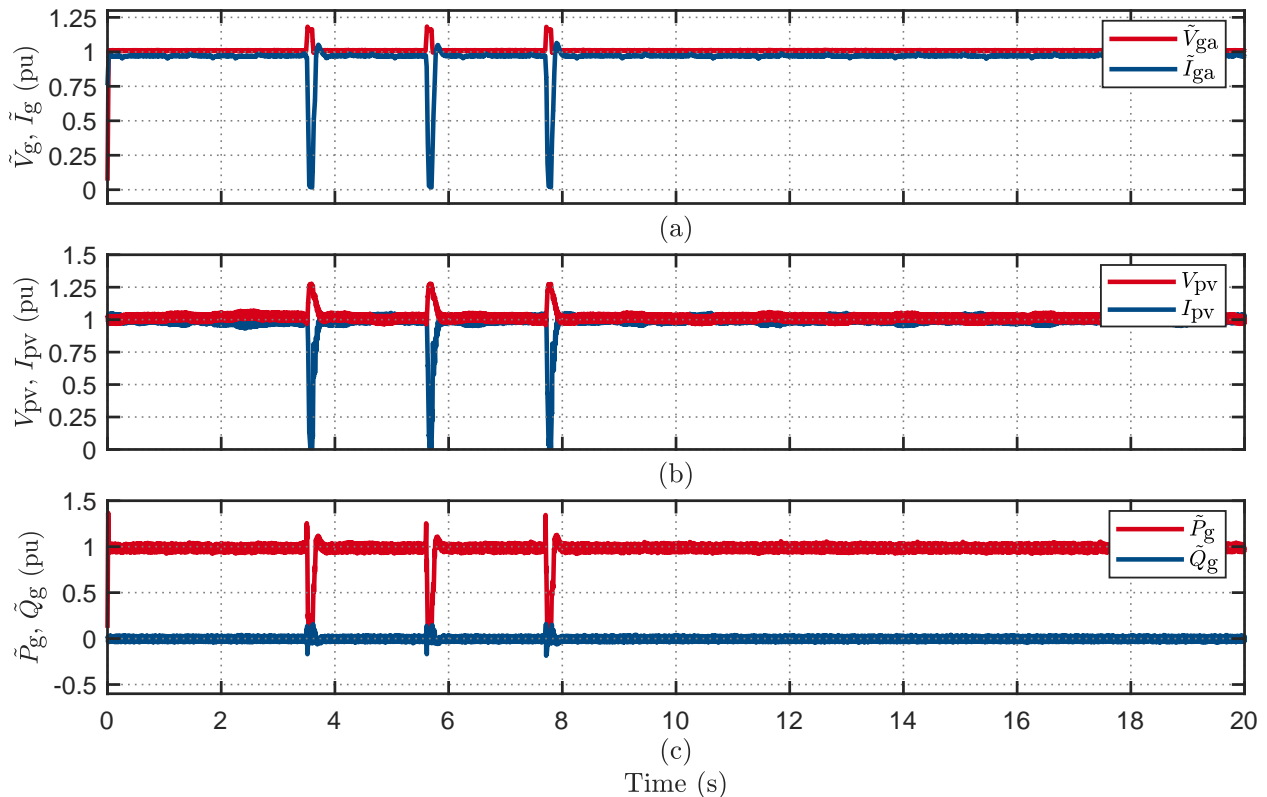


Figure 9: Inverter 42 ride-through behavior to voltage swell of 3x 230 to 270V for 0.1s

Table 13: Summary of bench testing results of inverter 42.

Response type	Steady state	Power dynamic	Test				Phase jump (deg)
			Step frequency	Ramp frequency	Voltage disturbance	Phase jump (deg)	
Ride-through	0%, 50%, 100%	<b>Step: 50% - 100%</b> <b>Ramp: 50% - 100%</b>	-2.95Hz, -3Hz	-1Hz/s, -4Hz/s	<b>230 to 50 for 0.1s</b>	+/-15, +/-30, +/-45, +/-60, +/-90	
Disconnect	-	-	+2Hz, +5Hz, -5Hz	-	230 to 270 for 7s, 230 to 160 for 0.9s, 230 to 160 for 4s 230 to 160 for 10s 230 to 280 for 10s		
Power reduction	-	-	+1.95Hz, +4Hz/s, +10Hz/s, -10Hz/s	+1Hz/s to 51Hz, +1Hz/s to 52Hz, 3x 230 to 50 for 0.1s, 3x 230 to 270 for 0.1s			

Table 14: Inverter 42 voltage sag test results

sag duration	0.8	0.7	0.6	0.5	0.4	0.3	0.2
80 ms	✓	✓	✓	✓	✓	✓	✓
120 ms	✓	✓	✓	✓	✓	✓	✓
220 ms	✓	✓	✓	✓	✓	✓	✓

Additional tests:

- 800ms, 230 - 50 V sag: ✓

Legend:

✓ : ride-through

#### 4.2.2 Comprehensive Voltage Sag Results

This inverter rides through all voltage sag tests, which are done at full and half power. An example of ride-through behaviour performed by Inverter 42 on a voltage sag with an amplitude of 0.8 p.u. and duration of 800 ms is displayed in Fig 10. Note that the injected current to the grid during the disturbance,  $I_{ga}$  is reduced to zero. After the disturbance, when the voltage is recovered,  $I_{ga}$  recovers with an overshoot close to 1.2 p.u. Then inverter resumes the injection of current to the pre-disturbance level. After the sag, the inverter power remains the same as the pre-sag condition. The behaviours displayed by this inverter under the new voltage sag testing schedule are summarized in Table 14.

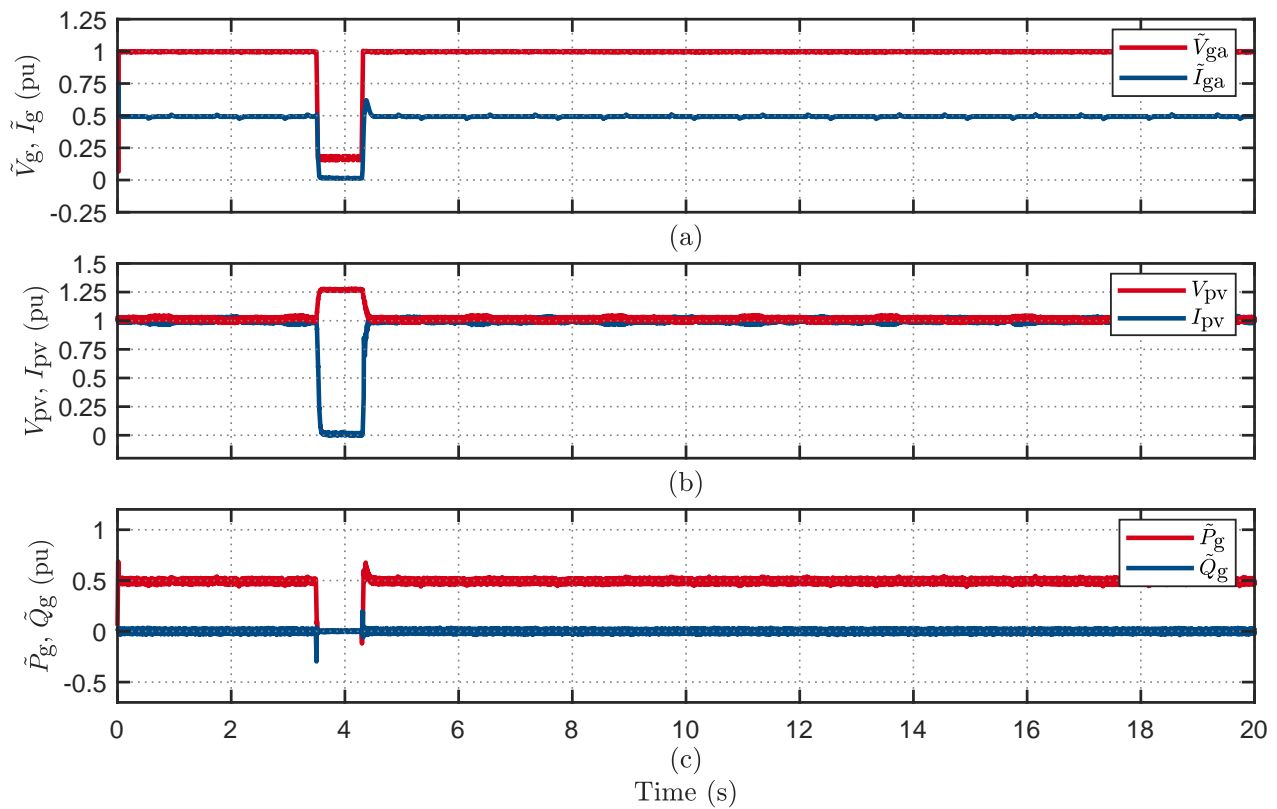


Figure 10: Inverter 42 ride-through behavior to voltage sag with amplitude of 0.8 p.u. and duration of 800 ms.

### 4.3 Observations

All inverters exhibited the desired response to under-frequency disturbances, riding through a frequency reduction of -2.95 Hz. They maintained continuous operation at the pre-disturbance power level after the disturbance. Similarly, the inverters showed the desired response for over-frequency disturbances of +1.95 Hz, with an expected power reduction close to 0 W observed in the recorded results. These results are in compliance with the Australian AS 4777.2:2020 standard. Detailed short-duration voltage sag tests were also conducted on selected AS 4777.2:2020 compliant inverters. They all displayed the desired response to voltage sags, riding through voltage sags with a duration of 220 ms or less, resuming operation at the pre-disturbance power level immediately after the voltage sag. Overall, all tested inverters demonstrated compliance with the AS 4777.2:2020 standard under voltage sag tests.

## 5 BESS & HESS Testing

The connection of distributed energy resources (DER) to distribution networks will only continue to grow, with AEMO predicting annual growth of 2GW for new rooftop solar PV in the short term and over 5GW of EV charging infrastructure from 2030 onwards. The introduction of battery and hybrid energy storage systems (BESS/HESS) necessitates the development of new tools and methods. An experimental bench-testing of inverters compliant with the newest AS4777.2020 standard extends testing to BESS and HESS that have the capacity to respond to grid disturbances. In addition, supporting evidence from real-world DER data offers a complementary understanding in-field diversity of behaviours. It also addresses the dynamic interaction between loads and small-scale generation during network disturbances, providing critical inputs to developing a holistic load model that accurately reflects the dynamic operation of the modern power system.

### 5.1 Inverter 43 (Hybrid Inverter)

Hybrid inverters can operate in three modes as described in Table 2. Each mode went through same testing procedure to identify the differences of behaviours under different modes of operation. The testing procedure illustrated in Sec 3 is used to conduct bench testing of BESS & HESS. The behaviour of the inverter under different modes of operation is discussed in the following sections:

#### 5.1.1 Mode 1

Bench testing, voltage sag and voltage swell summaries are presented in tables below:

**Bench Testing Summary:** This inverter showed undesired behaviour to voltage disturbance following AS 4777.2:2020. Fig 11 represents inverter behaviour for a voltage sag to 50V for 0.9s, where the inverter disconnected instantly after the sag. However, the standard suggests that the inverter should remain connected for 1s which is the trip delay time and then disconnect. One factor of disconnection is that these voltage disturbance tests were conducted at full power, but the standard suggests conducting these tests at half power. A summary of the bench testing is shown in Table 15.

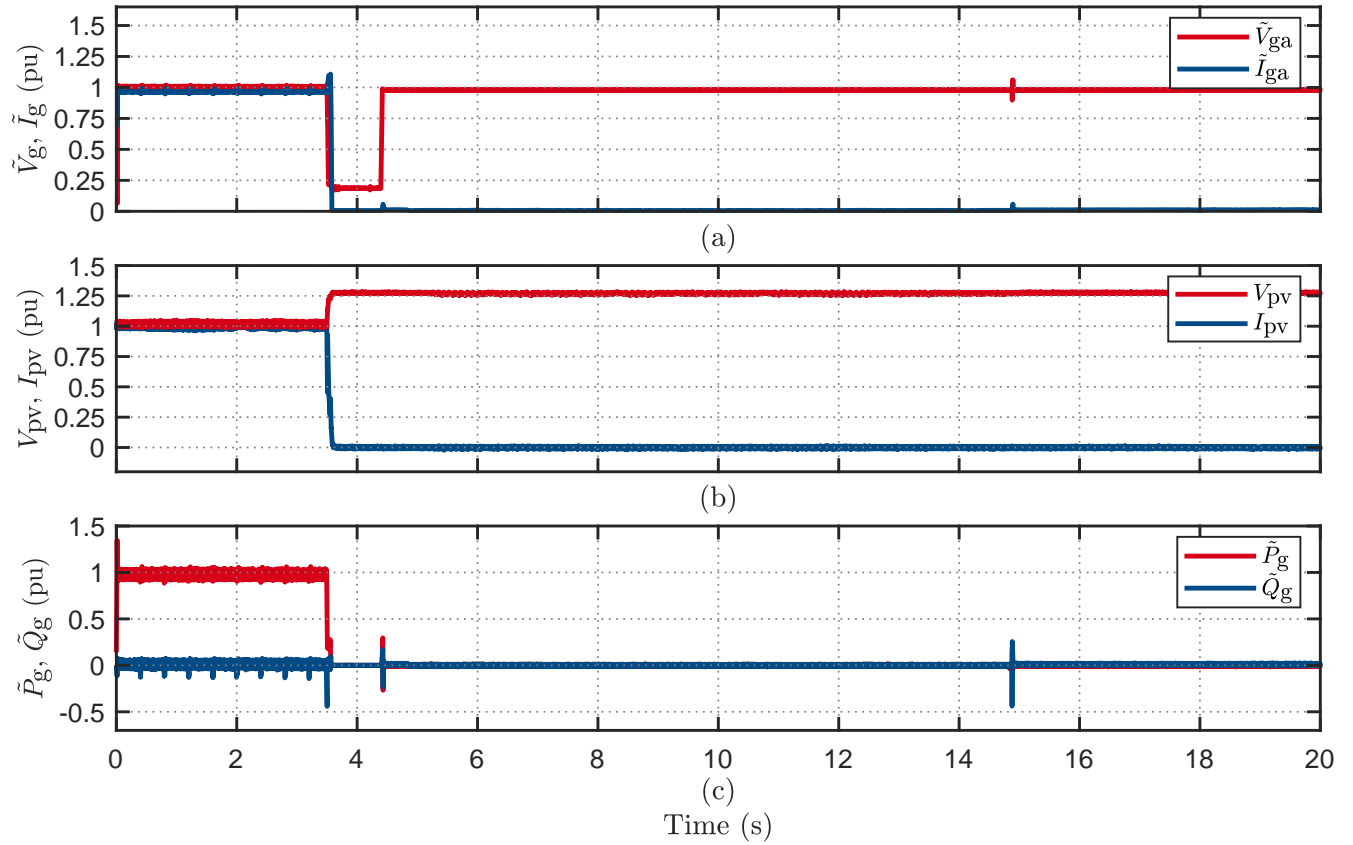


Figure 11: Inverter 43 disconnection behavior to voltage sag to 50V for 0.9s.

**Voltage Sag Test Summary:** Comprehensive voltage sag tests were conducted on the inverter at full and half power, and both presented the same behaviour shown in Table 16 to identify any difference in the behaviour of the inverter at full and half power as standard suggested to conduct the voltage sag tests at half power. Fig 12 shows the response of the inverter to voltage sag of 0.8 p.u for 80ms.

Table 15: Summary of bench testing results of inverter 43 in mode 1.

Response type	Test			Phase jump (deg)
	Steady state	Step frequency	Ramp frequency	
Ride-through	<b>0%</b>	-	-	+/-15, +/-30, +/-45, +/-60, +/-90
Disconnect	-	+2Hz +5Hz -5Hz	-	<b>230 to 50 for 0.9s</b> -
Power reduction	-	1.95Hz -2.95Hz -3Hz	+1Hz/s to 51.95Hz +4Hz/s to 47.05Hz -4Hz/s to 47.05Hz +0.4Hz/s to 51.95Hz -0.4Hz/s to 47.05Hz	230 to 260 230 to 270 for 0.9s 230 to 160 for 9s 230 to 185 in 15s 230 to 265 in 15s

Table 16: Inverter 43 voltage sag test results at 100% Power

sag duration	0.8	0.7	0.6	0.5	0.4	0.3	0.2
80 ms	✓	✓	✓	✓	✓	✓	X
120 ms	✓	✓	✓	✓	✓	✓	X
220 ms	✓	✓	✓	✓	✓	✓	X

Additional tests:

- 800ms, 230 - 50 V sag: X

Legend:

✓ : ride-through, X: disconnects

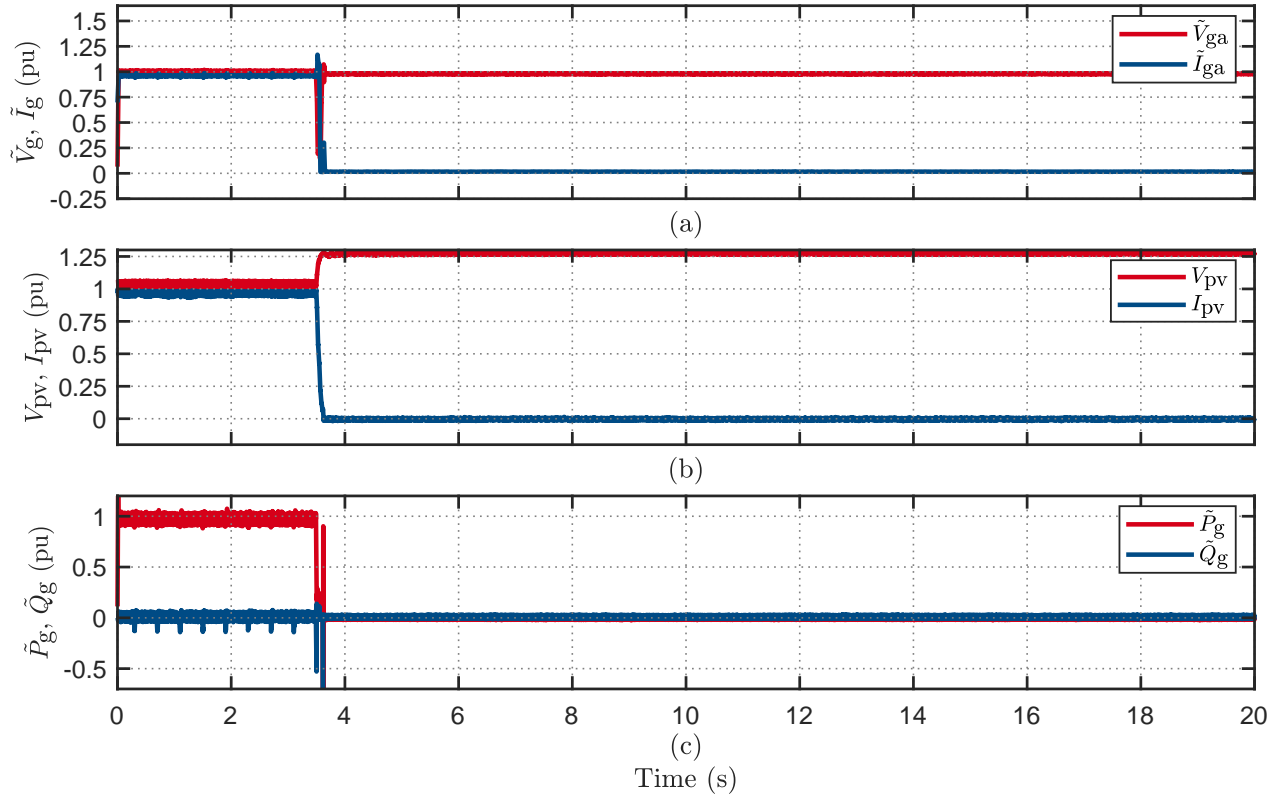


Figure 12: Inverter 43 disconnection behavior at 100% power to voltage sag with amplitude of 0.8 p.u. and duration of 80 ms.

**Voltage Swell Test Summary:** Voltage swell tests were performed on the inverter at full and half power, and the results were recorded in Table 17 and Table 18 respectively. The aim was to see if the behaviour of the inverter changed when operated at full power compared to half power. The results indicate that the inverter's behaviour can vary based on operating power and does not depend upon the swell's duration but rather the swell's amplitude. Fig 13 and Fig 14 compare inverter behaviour at full and half power to a voltage swell of 1.175 p.u for 220ms. Inverter remained connected for the swell when operating at half power. Although the standard requires conducting the test at half power, it raises the question of whether these tests should be conducted at full power or half.

Table 17: Inverter 43 voltage swell test results at 100% Power

sag duration	Voltage amplitude during the swell (p.u.)					
	1.05	1.1	1.125	1.15	1.175	1.2
80 ms	✓	✓	✓	✓	✓	X
120 ms	✓	✓	✓	✓	✓	X
220 ms	✓	✓	✓	✓	✓	X

Additional tests:

- 800ms, 230 - 275 V swell: X

Legend:

✓: ride-through, X: disconnects

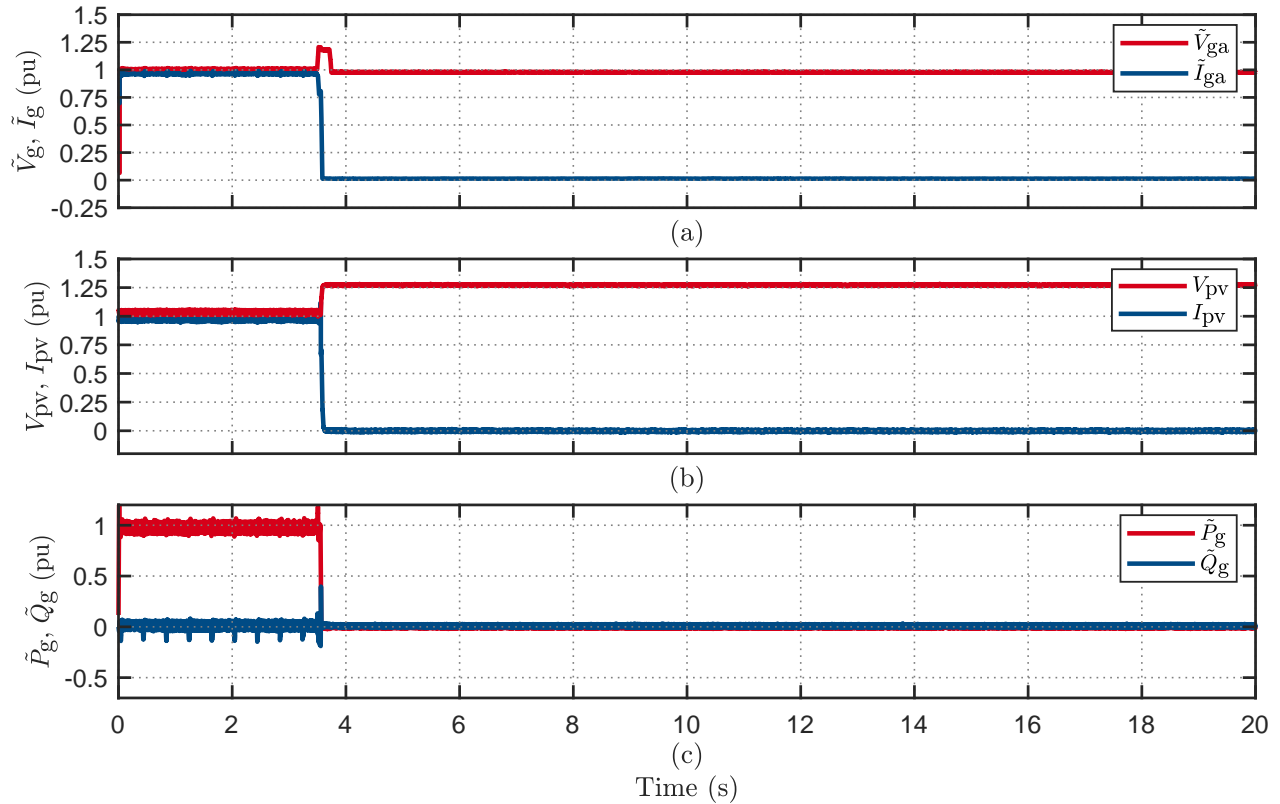


Figure 13: Inverter 43 disconnection behavior at 100% power to voltage swell with amplitude of 1.2 p.u. and duration of 220 ms.

Table 18: Inverter 43 voltage swell test results at 50% Power

sag duration	Voltage amplitude during the swell (p.u.)					
	1.05	1.1	1.125	1.15	1.175	1.2
80 ms	✓	✓	✓	✓	✓	✓
120 ms	✓	✓	✓	✓	✓	✓
220 ms	✓	✓	✓	✓	✓	✓

Additional tests:

- 800ms, 230 - 50 V sag: ✓

Legend:

✓: ride-through

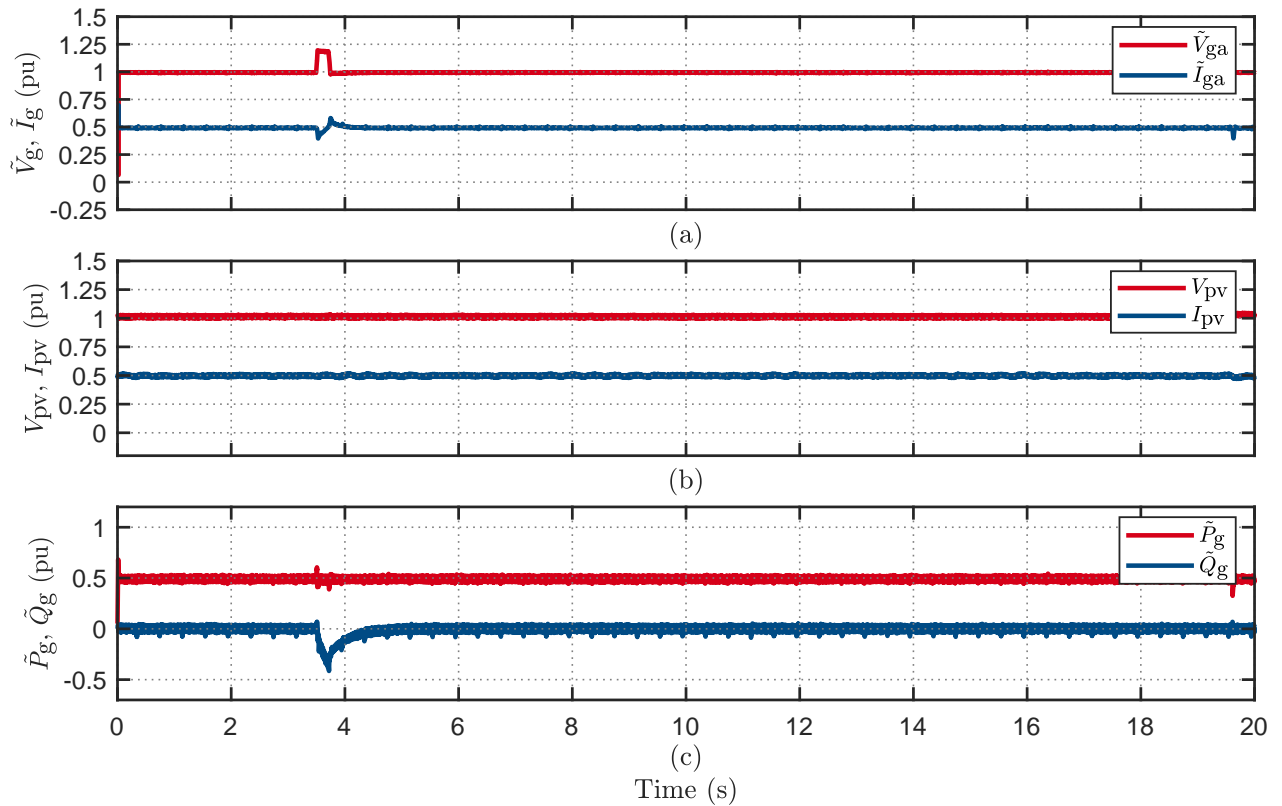


Figure 14: Inverter 43 ride-through behavior at 50% power to voltage swell with amplitude of 1.2 p.u. and duration of 220 ms.

### 5.1.2 Mode 2

In this mode inverter is working as on-grid system, PV is directly feeding power to the grid. Bench testing, voltage sag and voltage swell summaries are presented in tables below:

**Bench Testing Summary:** In this mode, the inverter presented a similar behaviour to mode 1. A summary of the bench testing is shown in Table15.

**Voltage Sag Test Summary:** Comprehensive voltage sag tests were conducted on the inverter at full and half power, and both presented the same behaviour shown in Table19 to identify any difference in the behaviour of the inverter at full and half power as standard suggested to conduct the voltage sag tests at half power. Fig 15 shows the response of the inverter to voltage sag of 0.8 p.u for 800ms.

Table 19: Inverter 43 voltage sag test results at 100% Power

sag duration	Voltage amplitude during the sag (p.u.)						
	0.8	0.7	0.6	0.5	0.4	0.3	0.2
80 ms	✓	✓	✓	✓	✓	✓	X
120 ms	✓	✓	✓	✓	✓	✓	X
220 ms	✓	✓	✓	✓	✓	✓	X

Additional tests:

- 800ms, 230 - 50 V sag: X

Legend:

✓: ride-through, X: disconnects

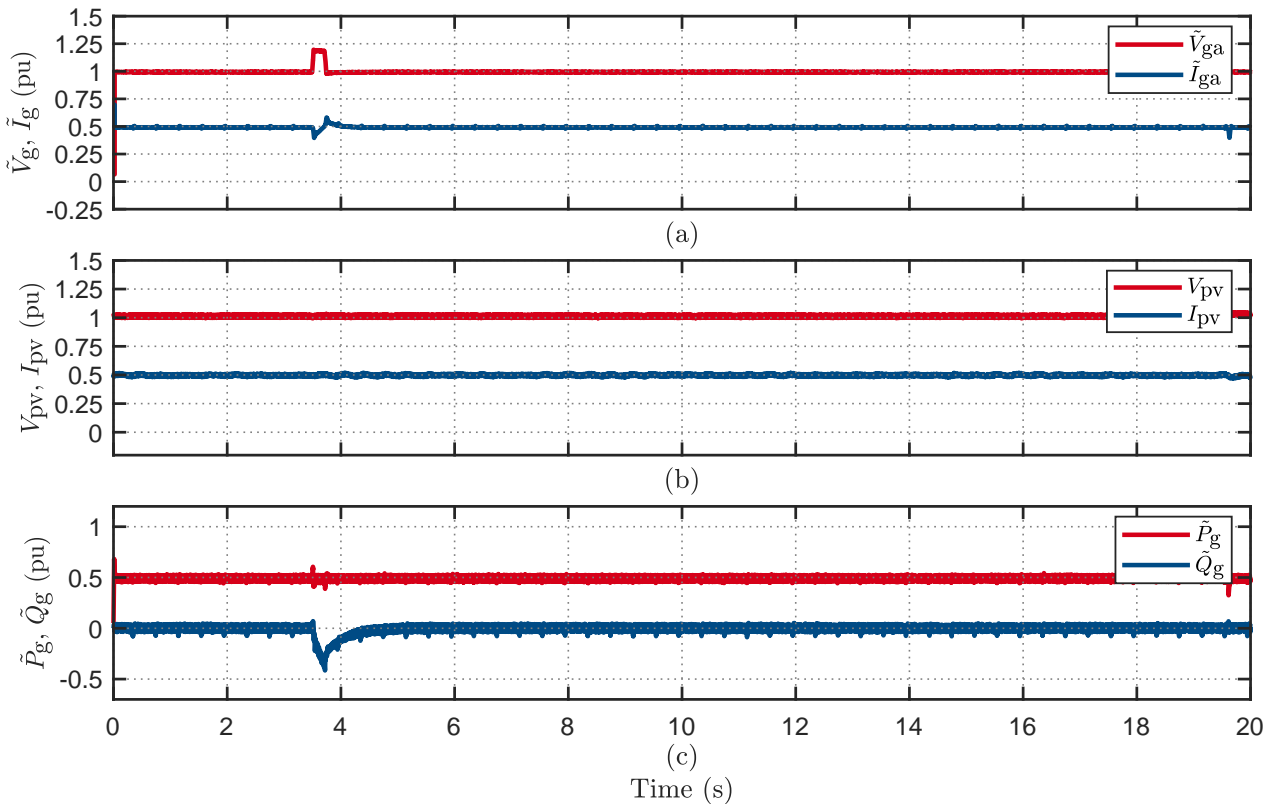


Figure 15: Inverter 43 disconnection behavior at 100% power to voltage sag with amplitude of 0.8 p.u. and duration of 800 ms.

**Voltage Swell Test Summary:** Voltage swell tests were performed on the inverter at full and half power, and both presented similar behaviour under full and half power recorded in Table 20. Fig 16 shows the response of the inverter to a voltage swell of 1.2 p.u for a duration of 80ms at 50% power.

Table 20: Inverter 43 voltage swell test results at 100% Power

sag duration	Voltage amplitude during the swell (p.u.)					
	1.05	1.1	1.125	1.15	1.175	1.2
80 ms	✓	✓	✓	✓	✓	X
120 ms	✓	✓	✓	✓	✓	X
220 ms	✓	✓	✓	✓	✓	X

Additional tests:

- 800ms, 230 - 275 V swell: X

Legend:

✓ : ride-through, X: disconnects

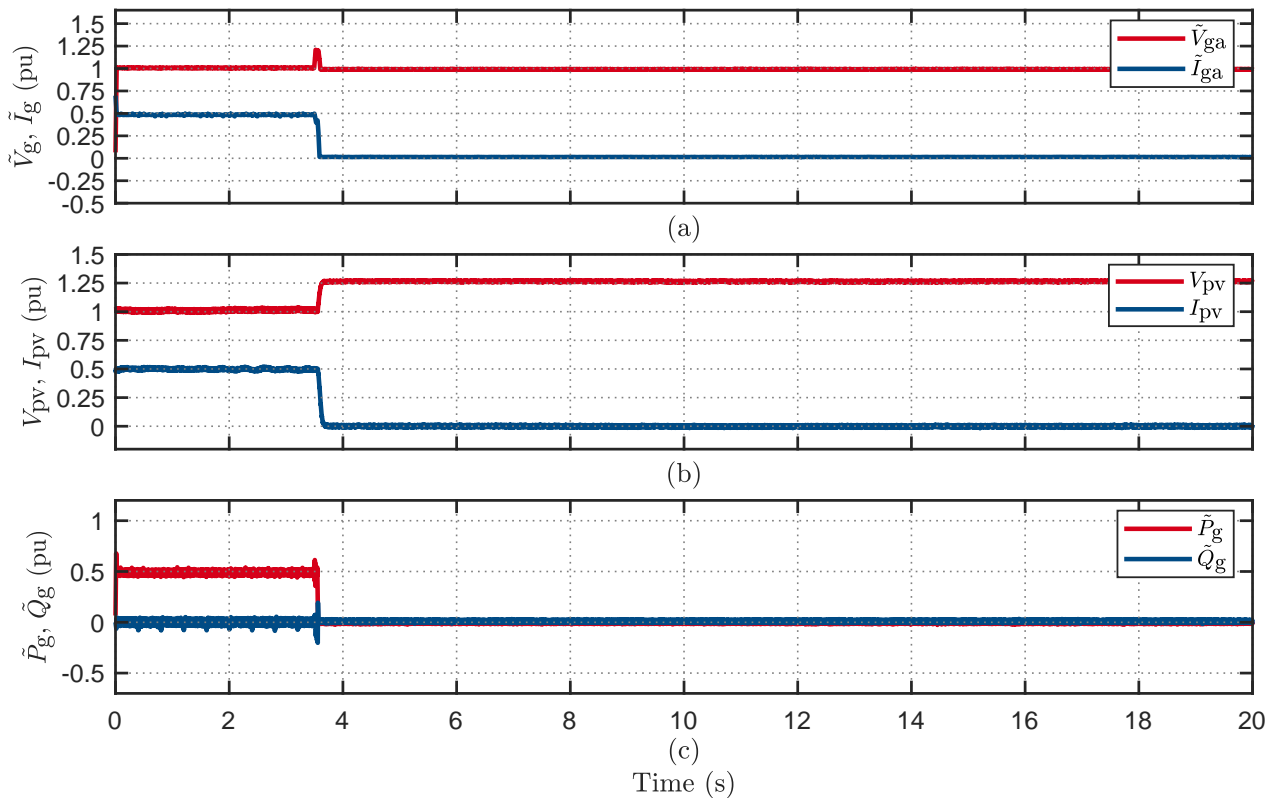


Figure 16: Inverter 43 disconnection behavior at 50% power to voltage swell with amplitude of 1.2 p.u. and duration of 80 ms.

### 5.1.3 Mode 3

In this mode, the inverter is working as an on-grid system without PV, and the load is either consuming power from the battery or the grid. Bench testing, voltage sag and voltage swell summaries are presented in the tables below:

**Bench Testing Summary:** Fig 17 represents inverter behaviour for a voltage sag to 50V for 0.9s, where the inverter disconnected from the grid instantly after the sag. This inverter showed undesired

behaviour to voltage disturbance following AS 4777.2:2020. However, when the sag was cleared, it again started drawing reactive power from the grid and, after a minute, suddenly disconnected for 4 minutes. A summary of the bench testing is shown in Table 21.

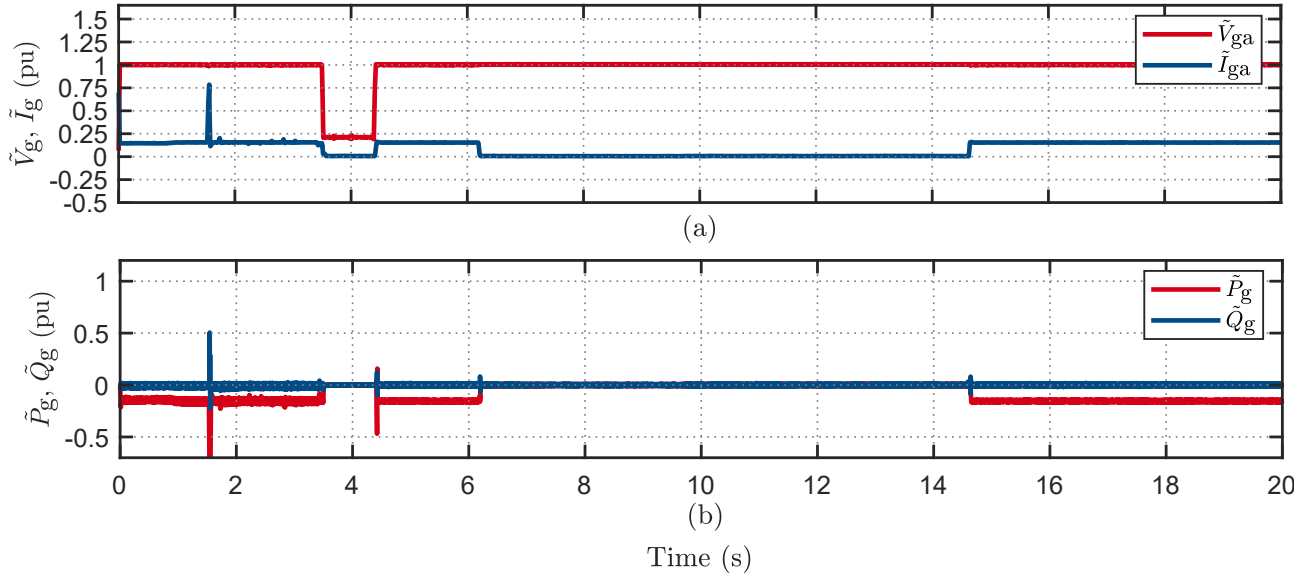


Figure 17: Inverter 43 disconnection behavior to voltage sag to 50V for 0.9s.

**Voltage Sag Test Summary:** Comprehensive voltage sag tests were conducted on the inverter at full and half power, shown in Table 22 to identify any difference in the behaviour of the inverter at full and half power as standard suggested to conduct the voltage sag tests at half power. Inverter presented similar behaviour on both power levels.

Table 21: Summary of bench testing results of inverter 43 in mode 3.

Response type	Steady state		Step frequency	Ramp frequency	Test	Voltage disturbance	Phase jump (deg)
Ride-through	0%	100%	1.95Hz -2.95Hz -3Hz	+1Hz/s to 51.95Hz -1Hz/s to 47.05Hz -0.44Hz/s to 47.05Hz	230 to 260 230 to 160 for 9s 230 to 270 for 9s 230 to 185 in 15s 230 to 265 in 15s	230 to 160 for 9s 230 to 270 for 9s 230 to 185 in 15s 230 to 265 in 15s	+/-15 +/-30 +/-45 +/-60 +/-90
	-	-	+2Hz +5Hz -5Hz	-	+2Hz +5Hz -5Hz	+2Hz +5Hz -5Hz	-
	-	-	-	+4Hz/s to 51.95Hz -4Hz/s to 47.05Hz +0.4Hz/s to 51.95Hz	-	-	-
	-	-	-	-	-	-	-
Disconnect	-	-	-	-	-	-	-
Power reduction	-	-	-	-	-	-	-

Table 22: Inverter 43 voltage sag test results at 100% Power

sag duration	0.8	0.7	0.6	0.5	0.4	0.3	0.2
80 ms	✓	✓	✓	✓	✓	✓	✓
120 ms	✓	✓	✓	✓	✓	✓	✓
220 ms	✓	✓	✓	✓	✓	✓	✓

Additional tests:

- 800ms, 230 - 50 V sag: ✓

Legend:

✓ : ride-through

**Voltage Swell Test Summary:** Voltage swell tests were performed on the inverter at full and half power, and both presented similar behaviour under full and half power recorded in Table 23.

Table 23: Inverter 43 voltage swell test results at 100% Power

sag duration	Voltage amplitude during the swell (p.u.)					
	1.05	1.1	1.125	1.15	1.175	1.2
80 ms	✓	✓	✓	✓	✓	✓
120 ms	✓	✓	✓	✓	✓	✓
220 ms	✓	✓	✓	✓	✓	✓

Additional tests:

- 800ms, 230 - 275 V swell: ✓

Legend:

✓: ride-through

## 5.2 Inverter 44 (Hybrid Inverter)

Hybrid inverters can operate in three modes as described in Table 2. Each mode went through same testing procedure to identify the differences of behaviours under different modes of operation. The testing procedure illustrated in Sec 3 is used to conduct bench testing of BESS & HESS. The behaviour of the inverter under for only mode 2 is discussed in the following sections:

### 5.2.1 Mode 2

In this mode inverter is working as on-grid system, PV is directly feeding power to the grid. Bench testing, voltage sag and voltage swell summaries are presented in tables below:

**Bench Testing Summary:** This inverter showed undesired behaviour to different grid disturbances following AS 4777.2:2020. Fig. 18 represents inverter behaviour for a ramp voltage change to 265V in 15s, where the inverter curtailed output active and reactive power. Inverter injects reactive power into the grid around 7.5s, and active power starts to reduce around 13.5s to 0.5 p.u. A grid disturbance of voltage phase-angle jump of  $\pm 30^\circ$  is shown in Fig. 19, where the inverter got disconnected right after the phase jump. A summary of the bench testing is shown in Table 24.

Table 24: Summary of bench testing results of inverter 44 in mode 2.

Response type	Test			Voltage disturbance	Phase jump (deg)
	Steady state	Step frequency	Ramp frequency		
Ride-through	<b>0%</b> <b>100%</b>	-	<b>-1Hz/s to 47.05Hz</b> <b>-4Hz/s to 47.05Hz</b> <b>-0.4Hz/s to 47.05Hz</b>	-	<b>+/-15</b>
Disconnect	-	<b>-3Hz, -2.95Hz, +5Hz, -5Hz</b>	-	<b>230 to 50 for 0.9s 230 to 270 for 0.9s 230 to 185 in 15s</b>	<b>+/-30 +/-45 +/-60 +/-90</b>
Power reduction	-	<b>1.95Hz 2Hz</b>	<b>+1Hz/s to 51.95Hz +4Hz/s to 51.95Hz +0.4Hz/s to 51.95Hz</b>	<b>230 to 260 230 to 160 for 9s 230 to 265 in 15s</b>	-

Table 25: Inverter 44 voltage sag test results at 100% Power

sag duration	0.8	0.7	0.6	0.5	0.4	0.3	0.2
80 ms	✓	✓	X	X	X	X	X
120 ms	✓	✓	X	X	X	X	X
220 ms	✓	✓	X	X	X	X	X

Additional tests:

- 800ms, 230 - 50 V sag: **X**

Legend:

✓: ride-through, X: disconnects



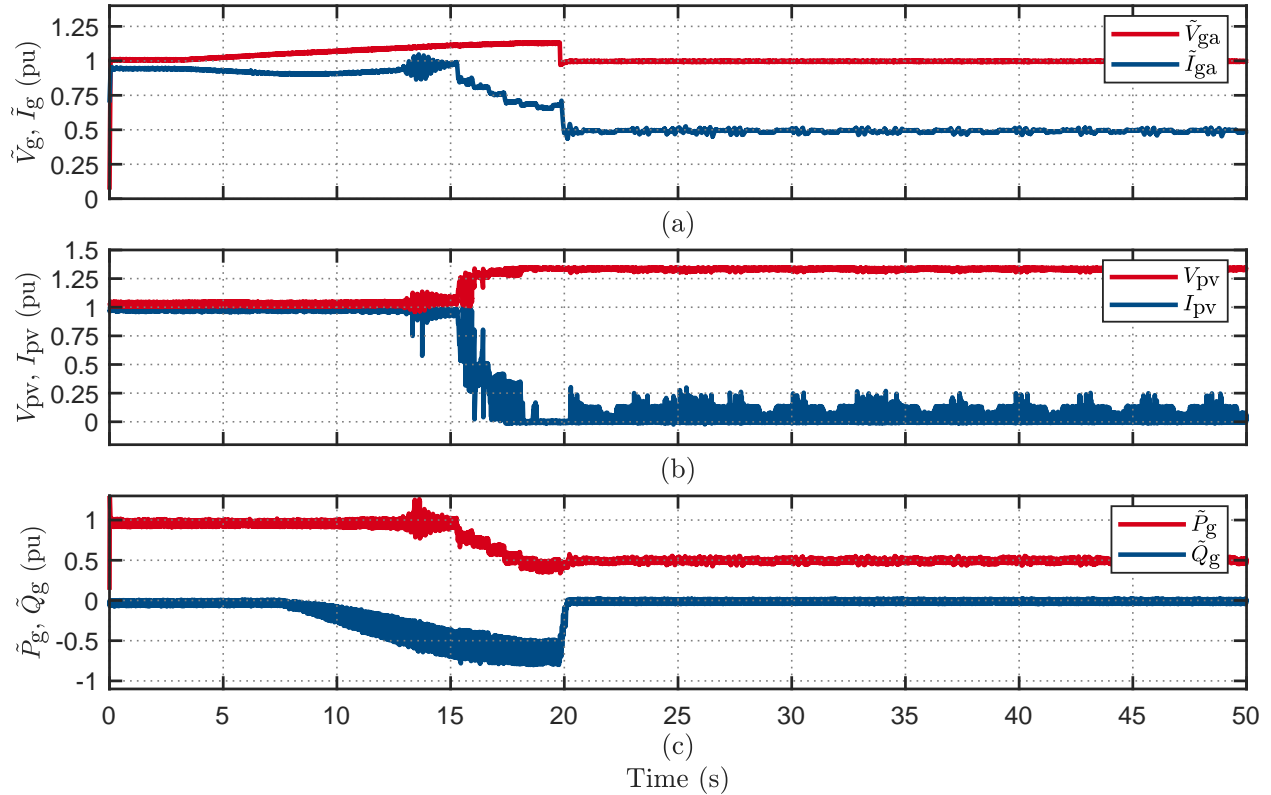


Figure 18: Inverter 44 power curtailment behavior to ramp voltage change to 265V in 0.5s.

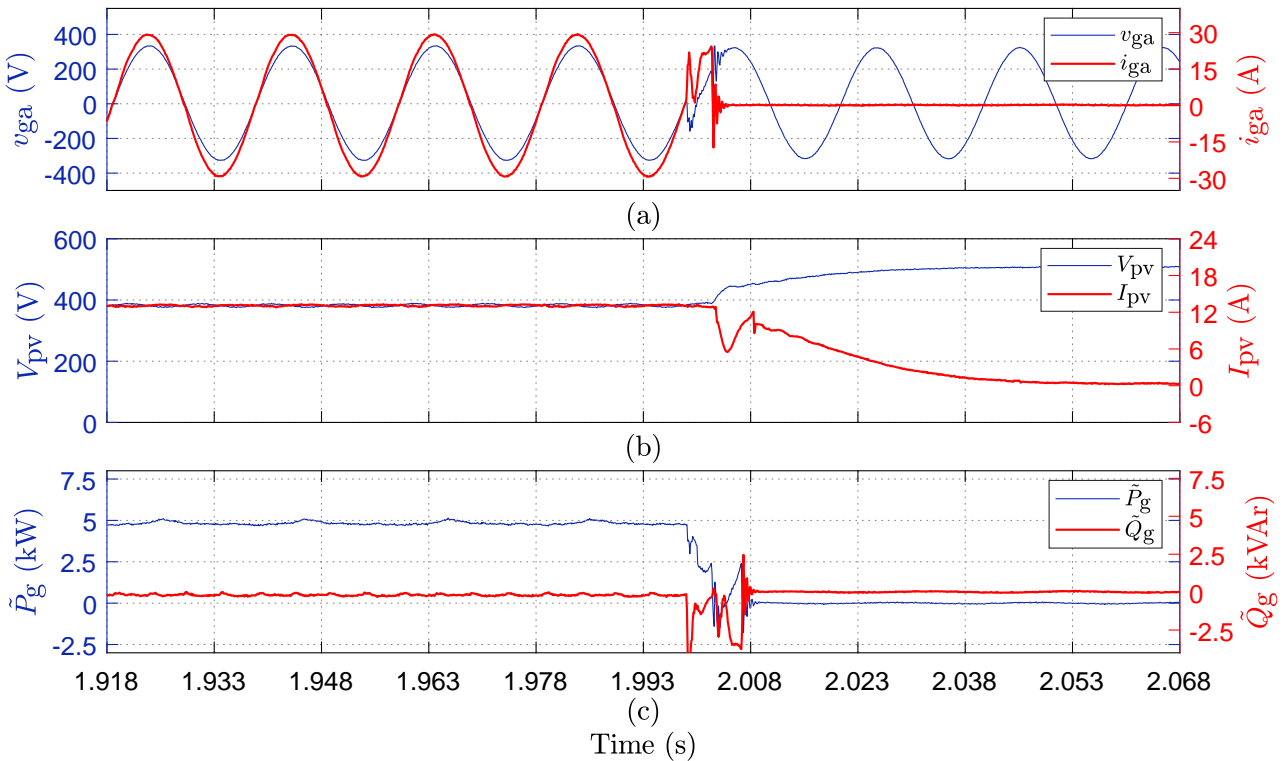


Figure 19: Inverter 44 disconnection behavior to  $\pm 30^\circ$  voltage phase-angle jump.

**Voltage Sag Test Summary:** Comprehensive voltage sag tests were conducted on the inverter at full and half power, shown in Table 25 to identify any difference in the behaviour of the inverter at full and half power as standard suggested to conduct the voltage sag tests at half power. Inverter presented similar behaviour on both power levels, but the results were not as expected from the inverter; it should ride through all the disturbances as time is less than the trip delay time. An example of voltage sag of 0.5 p.u for 80 ms is presented in Fig. 20.

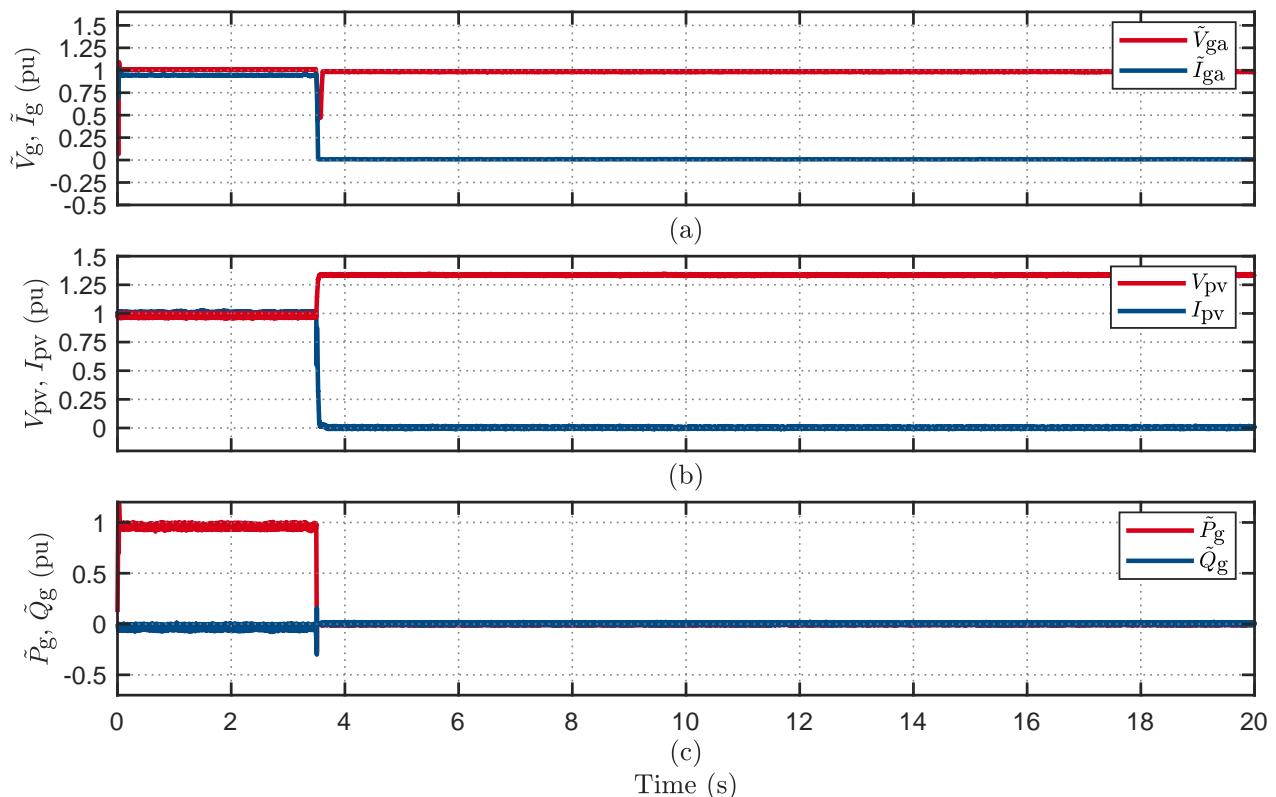


Figure 20: Inverter 44 disconnection behavior to voltage sag of 0.5 p.u for 80 ms.

**Voltage Swell Test Summary:** Voltage swell tests were performed on the inverter at full and half power, and both presented similar behaviour by riding through all disturbances under full and half power recorded in Table 26.

Table 26: Inverter 44 voltage swell test results at 100% Power

sag duration	Voltage amplitude during the swell (p.u.)					
	1.05	1.1	1.125	1.15	1.175	1.2
80 ms	✓	✓	✓	✓	✓	✓
120 ms	✓	✓	✓	✓	✓	✓
220 ms	✓	✓	✓	✓	✓	✓

Additional tests:

- 800ms, 230 - 275 V swell: ✓

Legend:

✓ : ride-through

### 5.3 Inverter 45 (BESS Inverter)

Energy storage systems can charge from the grid or from PV but cannot inject power to the grid. This BESS went under similar testing procedure to understand the different behaviours of the system. The testing procedure illustrated in Sec 3 is used to conduct bench testing of BESS. The behaviour of the BESS is discussed in the following sections:

**Bench Testing Summary:** This inverter showed undesired behaviour to different grid disturbances following AS 4777.2:2020. Fig. 21 represents inverter behaviour for a ramp frequency of 0.4Hz/s to 51.95Hz, where the inverter started charging the battery at double the power it was charging before, this is started after the frequency went above 51.1Hz. A RoCoF of 0.1Hz/s to 47.05Hz is generated from the grid emulator see Fig. 22, and the reconnection behaviour of the inverter is analysed. It is observed that the inverter starts to inject power into the grid from the battery to support the grid, and after the grid frequency jumps back to the pre-fault level, the inverter disconnects. When the inverter reconnected, it remembered the faulted condition power level, started injecting power into the grid, and slowly ramped down from injection to charging. Fig. 23 presents a volt-watt and volt-var response from the inverter in response to ramp voltage disturbance to 185V in 15 seconds. As the inverter reduces the voltage output, the inverter stops charging from the grid and injects reactive power to provide grid support. A summary of the bench testing is shown in Table 27.

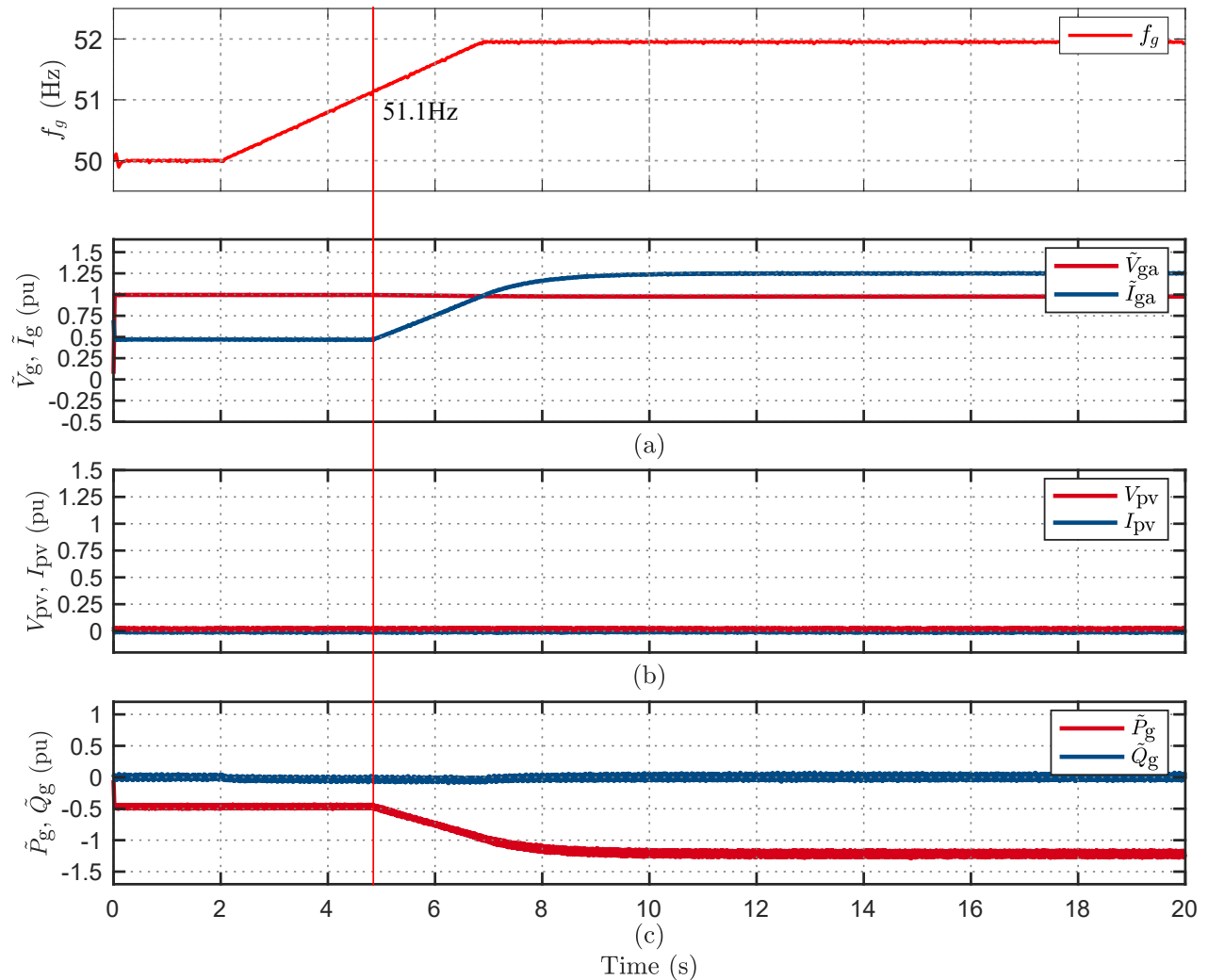


Figure 21: Inverter 45 ride-through behavior to ramp frequency change of 0.4Hz/s to 51.95Hz.

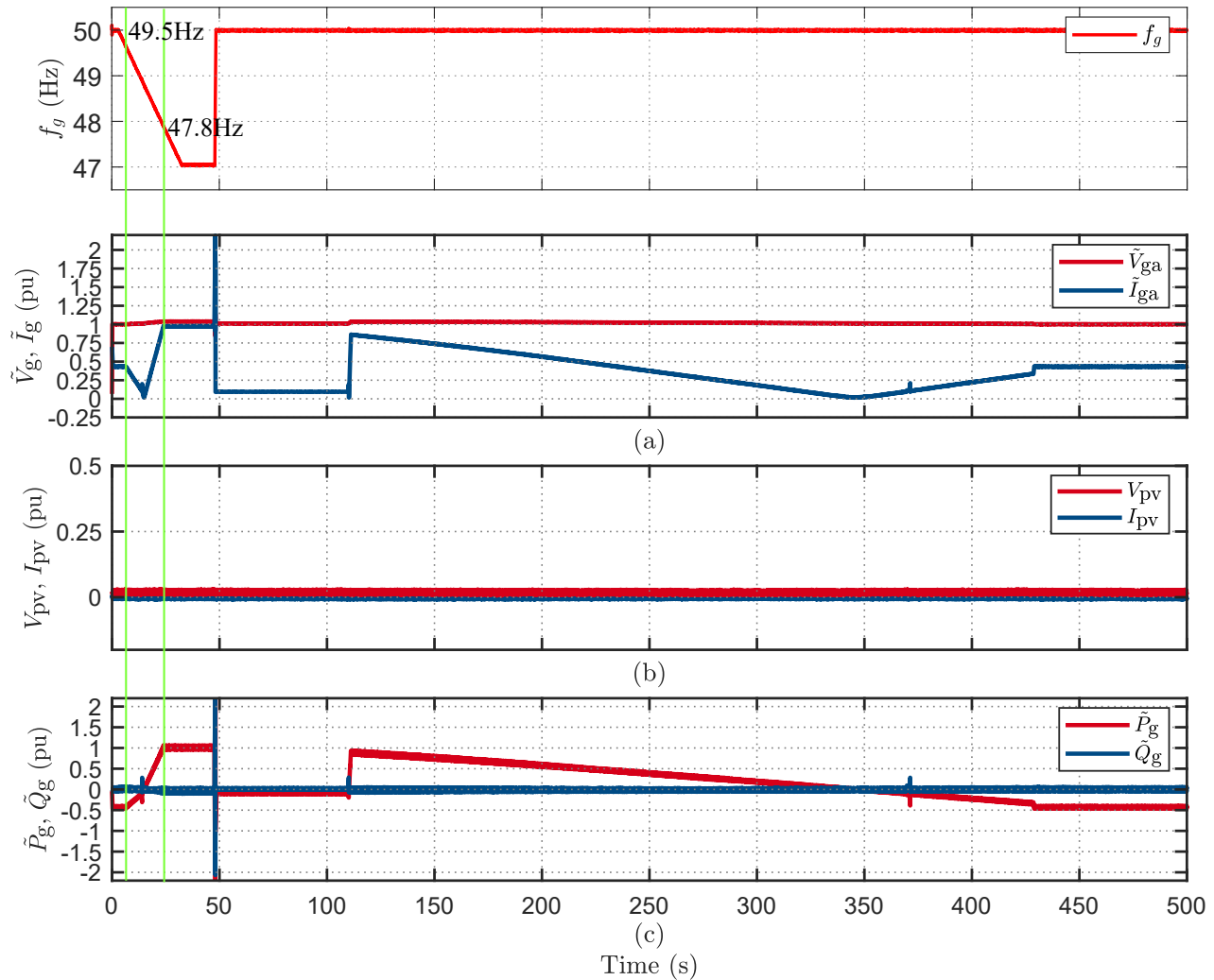


Figure 22: Inverter 45 reconnection behavior to ramp frequency change of 0.1Hz/s to 47.05Hz.

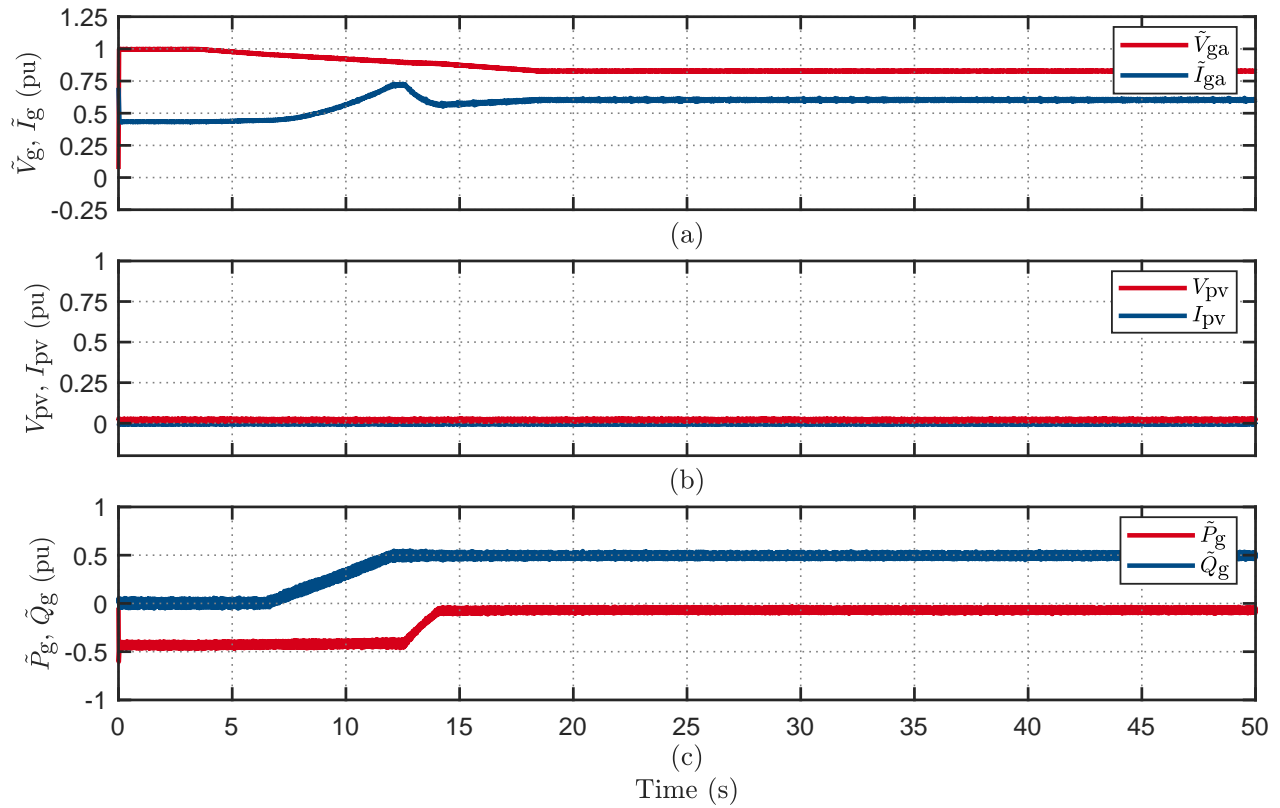


Figure 23: Inverter 45 power curtailment behavior to ramp voltage change to 185V in 15s.

Table 27: Summary of bench testing results of inverter 45 (Battery ESS only).

Response type	Test					
	Steady state	Step frequency	Ramp frequency	Voltage disturbance	Phase jump (deg)	
Ride-through	<b>0%</b> <b>100%</b>	-	-	<b>230 to 260</b> <b>230 to 270 for 0.9s</b>	<b>+/-15</b>	
Disconnect	-	<b>+5Hz, -5Hz</b> <b>2Hz-3Hz, 1.95Hz</b> <b>2.95Hz</b>	<b>+1Hz/s to 51.95Hz</b> <b>-1Hz/s to 47.05Hz</b> <b>+4Hz/s to 51.95Hz</b> <b>-4Hz/s to 47.05Hz</b>	<b>230 to 50 for 0.9s</b> <b>230 to 160 for 9s</b>	<b>+/-30</b> <b>+/-45</b> <b>+/-60</b> <b>+/-90</b>	
Power reduction	-	-	<b>+0.4Hz/s to 51.95Hz</b> <b>-0.4Hz/s to 47.05Hz</b>	<b>230 to 265 in 15s</b> <b>230 to 185 in 15s</b>	-	

Table 28: Inverter 45 voltage sag test results at 100% Power

sag duration	0.8	0.7	0.6	0.5	0.4	0.3	0.2
80 ms	✓	✓	X	X	X	X	X
120 ms	✓	X	X	X	X	X	X
220 ms	✓	X	X	X	X	X	X

Additional tests:

- 800ms, 230 - 50 V sag: X

Legend:

✓ : ride-through, X: disconnects



**Voltage Sag Test Summary:** Comprehensive voltage sag tests were conducted on the inverter presenting undesirable behaviour shown in Table 28. Inverter started disconnection at 0.7 p.u sag for 120ms before disconnection inverter wobbles the frequency to maintain connection but eventually disconnects as shown in Fig. 24; this shows the inverter is sensitive to depth and the duration of sag as well.

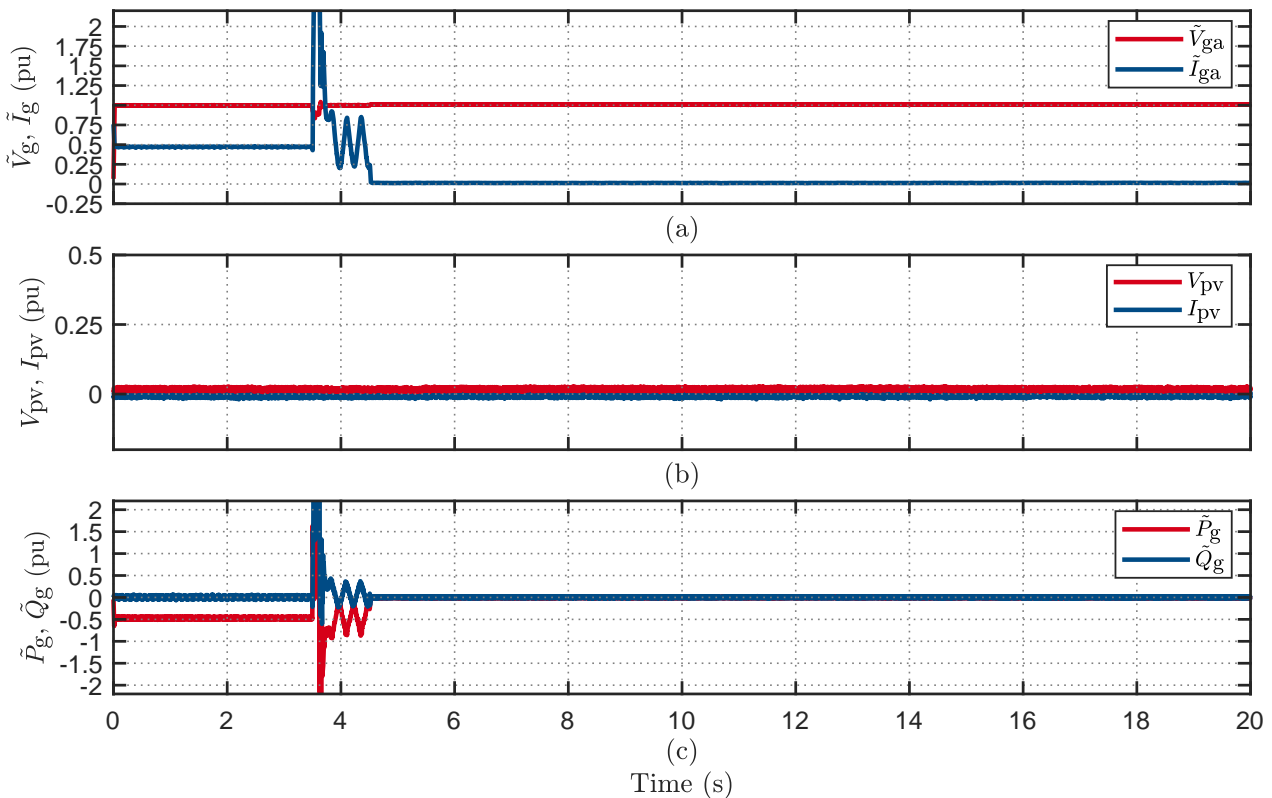


Figure 24: Inverter 45 disconnection behaviour to voltage sag of 0.7 p.u for 120 ms.

**Voltage Swell Test Summary:** Voltage swell tests were performed on the inverter presenting undesirable behaviours shown in Table 29.

Table 29: Inverter 45 voltage swell test results

sag duration	Voltage amplitude during the sag (p.u.)					
	1.05	1.1	1.125	1.15	1.175	1.2
80 ms	✓	✓	✓	✓	✓	X
120 ms	✓	✓	✓	✓	✓	X
220 ms	✓	✓	✓	✓	✓	X

Additional tests:

- 800ms, 230 - 50 V sag: X

Legend:

✓ : ride-through, X: disconnects

## 5.4 Inverter 46 (Hybrid Inverter)

Hybrid inverters can operate in three modes as described in Table 2. Each mode went through same testing procedure to identify the differences of behaviours under different modes of operation. The testing procedure illustrated in Section 3 is used to conduct bench testing of BESS & HESS. The behaviour of the inverter under for only mode 2 is discussed in the following sections:

### 5.4.1 Mode 2

In this mode inverter is working as on-grid system, PV is directly feeding power to the grid. Bench testing, voltage sag and voltage swell summaries are presented in tables below:

**Bench Testing Summary:** This inverter showed undesired behaviour to different grid disturbances following AS 4777.2:2020. A summary of the bench testing is shown in Table 31.

**Voltage Sag Test Summary:** Comprehensive voltage sag tests were conducted on the inverter at full and half power, shown in Table 30 to identify any difference in the behaviour of the inverter at full and half power as standard suggested to conduct the voltage sag tests at half power. Inverter presented similar behaviour on both power levels, but the results were not as expected from the inverter; it should ride through all the disturbances as time is less than the trip delay time.

Table 30: Inverter 46 voltage sag test results at 50% Power

sag duration	Voltage amplitude during the sag (p.u.)						
	0.8	0.7	0.6	0.5	0.4	0.3	0.2
80 ms	✓	X	X	X	X	X	X
120 ms	✓	X	X	X	X	X	X
220 ms	✓	X	X	X	X	X	X

Additional tests:

- 800ms, 230 - 50 V sag: X

Legend:

✓: ride-through, X: disconnects

Table 31: Summary of bench testing results of inverter 46 in mode 2.

Response type	Steady state	Test			Phase jump (deg)
		Step frequency	Ramp frequency	Voltage disturbance	
Ride-through	<b>0%</b> <b>100%</b>	<b>2Hz</b>	-	-	+/-15
Disconnect	-	+5Hz, -5Hz- 3Hz, 2.95Hz	-	230 to 50 for 0.9s 230 to 160 for 9s 230 to 270 for 0.9s 230 to 260	+/-30 +/-45 +/-60 +/-90
Power reduction	<b>1.95Hz</b>	-	+1Hz/s to 51.95Hz -1Hz/s to 47.05Hz +4Hz/s to 51.95Hz -4Hz/s to 47.05Hz	230 to 265 in 15s 230 to 185 in 15s	
			+0.4Hz/s to 51.95Hz -0.4Hz/s to 47.05Hz		

**Voltage Swell Test Summary:** Voltage swell tests were performed on the inverter at full and half power, and both presented different behaviours under full and half power recorded in Table 32 and Table 33 respectively.

Table 32: Inverter 44 voltage swell test results at 100% Power

sag duration	Voltage amplitude during the sag (p.u.)					
	1.05	1.1	1.125	1.15	1.175	1.2
80 ms	✓	✓	✓	✓	✓	✓
120 ms	✓	✓	✓	✓	✓	X
220 ms	✓	✓	✓	✓	✓	X

Additional tests:

- 800ms, 230 - 50 V swell: X

Legend:

✓: ride-through, X: disconnects

Table 33: Inverter 44 voltage swell test results at 100% Power

sag duration	Voltage amplitude during the swell (p.u.)					
	1.05	1.1	1.125	1.15	1.175	1.2
80 ms	✓	✓	✓	✓	✓	✓
120 ms	✓	✓	✓	✓	✓	✓
220 ms	✓	✓	✓	✓	✓	✓

Additional tests:

- 800ms, 230 - 275 V swell: ✓

Legend:

✓: ride-through



## 5.5 Inverter 47 (Hybrid Inverter)

Hybrid inverters can operate in three modes as described in Table 2. Each mode went through same testing procedure to identify the differences of behaviours under different modes of operation. The testing procedure illustrated in Sec 3 is used to conduct bench testing of BESS & HESS. The behaviour of the inverter under for only mode 2 is discussed in the following sections:

### 5.5.1 Mode 2

In this mode inverter is working as on-grid system, PV is directly feeding power to the grid. Bench testing, voltage sag and voltage swell summaries are presented in tables below:

**Bench Testing Summary:** This inverter showed undesired behaviour to different grid disturbances following AS 4777.2:2020. A summary of the bench testing is shown in Table 34.



Table 34: Summary of bench testing results of inverter 47 in mode 2.

	Response	Steady state	Step frequency	Ramp frequency	Voltage disturbance	Phase jump (deg)
Ride-thru type	0%	100%	2Hz	-	-	+/-15
Disconnect	-	+5Hz, -5Hz- 3Hz, 2.95Hz	-	-	230 to 50 for 0.9s 230 to 160 for 9s 230 to 270 for 0.9s 230 to 260	+/-30 +/-45 +/-60 +/-90
Power reduction	1.95Hz	-	+1Hz/s to 51.95Hz -1Hz/s to 47.05Hz +4Hz/s to 51.95Hz -4Hz/s to 47.05Hz +0.4Hz/s to 51.95Hz -0.4Hz/s to 47.05Hz	-	230 to 265 in 15s 230 to 185 in 15s	-

Table 35: Inverter 46 voltage sag test results at 50% Power

sag duration	Voltage amplitude during the sag (p.u.)					
	0.8	0.7	0.6	0.5	0.4	0.3
80 ms	✓	✗	✗	✗	✗	✗
120 ms	✓	✗	✗	✗	✗	✗
220 ms	✓	✗	✗	✗	✗	✗

### Additional tests:

- 800ms, 230 - 50 V sag: X

Legend:  
✓: ride-through, X: disconnects

**Voltage Sag Test Summary:** Comprehensive voltage sag tests were conducted on the inverter at full and half power, shown in Table 35 to identify any difference in the behaviour of the inverter at full and half power as standard suggested to conduct the voltage sag tests at half power. Inverter presented similar behaviour on both power levels, but the results were not as expected from the inverter; it should ride through all the disturbances as time is less than the trip delay time.

**Voltage Swell Test Summary:** Voltage swell tests were performed on the inverter at full and half power, and both presented different behaviours under full and half power recorded in Table 36 and Table 37 respectively.

Table 36: Inverter 44 voltage swell test results at 100% Power

sag duration	Voltage amplitude during the sag (p.u.)					
	1.05	1.1	1.125	1.15	1.175	1.2
80 ms	✓	✓	✓	✓	✓	✓
120 ms	✓	✓	✓	✓	✓	X
220 ms	✓	✓	✓	✓	✓	X

Additional tests:

- 800ms, 230 - 50 V sag: X

Legend:

✓ : ride-through, X: disconnects

Table 37: Inverter 44 voltage swell test results at 100% Power

sag duration	Voltage amplitude during the swell (p.u.)					
	1.05	1.1	1.125	1.15	1.175	1.2
80 ms	✓	✓	✓	✓	✓	✓
120 ms	✓	✓	✓	✓	✓	✓
220 ms	✓	✓	✓	✓	✓	✓

Additional tests:

- 800ms, 230 - 275 V swell: ✓

Legend:

✓ : ride-through

## 6 Load Tests

Precise load modelling is essential for Network Service Providers (NSPs) to evaluate power system performance under various operating conditions, assess network stability issues, and devise effective control solutions [12, 13]. In recent years, power systems across the world have undergone major transformation with the introduction of distributed energy resources (DERs) and modern flexible loads. When subjected to faults and disturbances power systems that incorporate these devices exhibit dynamic behaviours [14, 15] which traditional static load models used by NSPs are incapable of capturing. The present load models used by the Australian Energy Market Regulator (AEMO), known as ZIP (impedance, current, power-based) models, were last calibrated and validated in 1999, and they are unable to accurately model the complex dynamic behaviour of modern loads [16].

Sophisticated composite load models are now available that can capture both the dynamic and static response of loads [5]. Composite load models consider the diverse aspects of load behaviour, such as dynamic response, sensitivity to voltage changes, and response to frequency fluctuations. In order to better model the response of modern power systems, the Western Electricity Coordinating Council (WECC) has developed an advanced composite load (termed CMPLDW) model with various components, including different types of motor loads, electronic/static loads as well as the inclusion of DERs [17]. The addition of electrical distance between the transmission network and end load also allows this model to capture delayed voltage recovery events from transmission faults [18, 19]. The North American Electricity Reliability Corporation (NERC) recommends the use of the CMPLDW model for dynamic studies in power systems [20]. The model however incorporates complex load characteristics which requires input of as many 133 parameters into the model. The model is constantly updated using inputs from NSPs, through utilisation of data measured during power system faults and laboratory testing of appliances.

Specifically, the work aims to undertake extensive experimental testing of modern loads when subject to various voltage, frequency and phase disturbances which were designed to replicate real life network disturbances. The objective was to obtain information on the response of typical loads connected to distribution networks, enabling a better comprehension of their behaviour, and facilitating the update of the parameters of the CMPLDW load models.

### 6.1 Refrigerators

To analyse the behaviour of refrigerators, two devices were evaluated. Refrigerator 1 is an inverter-based unit, while Refrigerator 2 is a conventional compressor unit. The inclusion of both refrigerator types in the study allowed a preliminary comparison of their responses to power system transients. According to the CMPLDW classifications, Refrigerator 1 is categorised as a motor D type load, which is known to be susceptible to stalling due to sags or undervoltages. On the other hand, Refrigerator

2 would be classified as an Electronic Load.

During the tests, both refrigerators were subjected to voltage sags, and they each demonstrated the ability to ride through all of the administered disturbances. The only notable change during the transient period was a momentary variation in power consumption. Figs. 25(a) and (b) depict the current waveform of the two refrigerators when exposed to a voltage sag of magnitude 0.2 pu for a duration of 80 ms. The waveforms show that there is different dynamic response between the two refrigerators. After the sag was cleared, both devices experienced an overshoot in current. For Refrigerator 1, the overshoot was due to the dc side capacitor charging to its nominal value (characterised by a very short-term high magnitude current value), while for Refrigerator 2, it was due to motor inrush current (characterised by a longer term decaying current magnitudes). The duration of the sags applied had no notable change on the response of the devices.

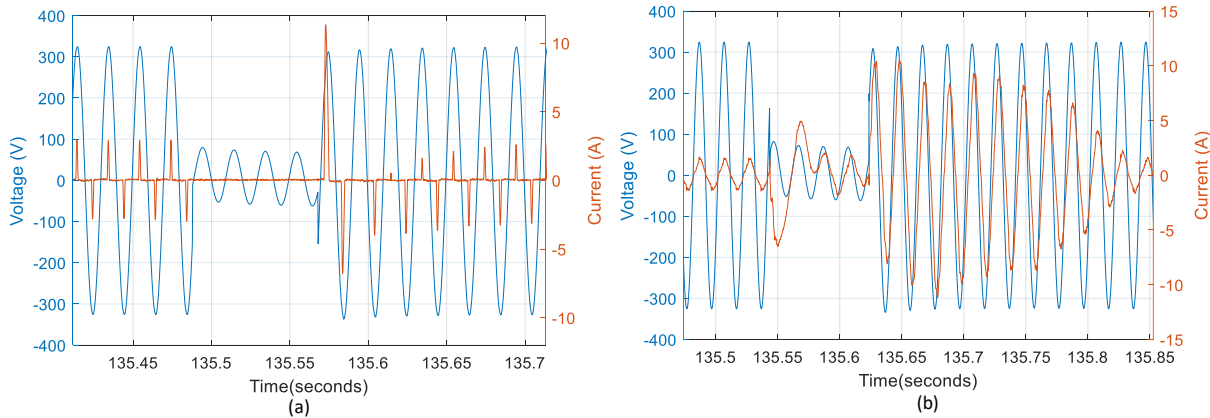


Figure 25: Impact of Voltage Sags on: (a) Refrigerator 1 (b) Refrigerator 2

During voltage swell tests, both refrigerators were able to withstand the voltage swells without any disconnection. The only change observed during the transient period was a temporary variation in the current drawn by the devices. A total of 18 voltage swell disturbances were applied, with the maximum applied voltage reaching 1.2 pu. Nevertheless, neither device encountered disruptions to their normal operation after the swells were cleared.

During the phase angle jump tests, the conventional compressor system in Refrigerator 2 stalled when the phase angle magnitude was  $-90^\circ$ , causing an increase in active power consumption from 100 W to approximately 1200 W while reactive power absorption increased from 45 VAr to 1000 VAr. The device remained in the stalled state for several minutes before returning to normal. There was no impact on Refrigerator 2 under all other phase angle jumps with an angle less than  $90^\circ$ . The performance of the inverter-based Refrigerator was not impacted by any of the applied phase angle jumps. The currents drawn by Refrigerator 1 and Refrigerator 2 during a phase angle jump of  $-90^\circ$  are shown in Fig. 26(a) and Fig. 26(b), respectively.

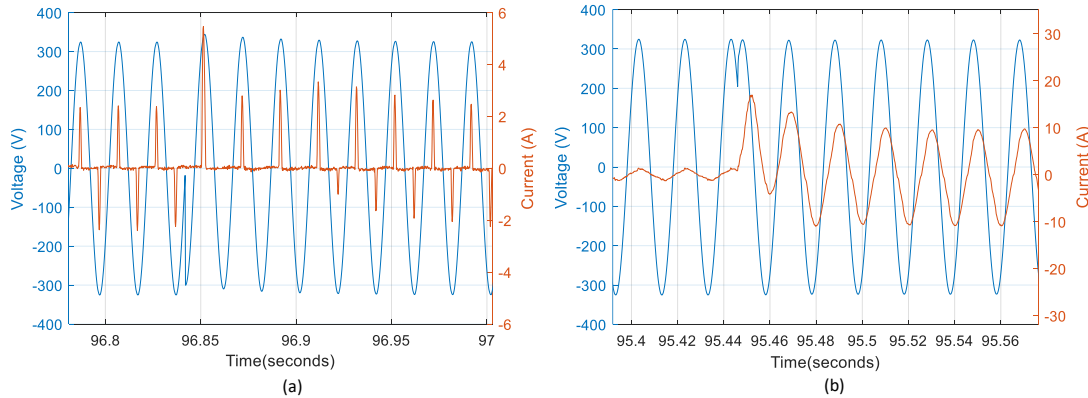


Figure 26: Impact of Phase Angle Jumps on: (a) Refrigerator 1 (b) Refrigerator 2

## 6.2 Microwave Ovens

This section presents the response of an inverter-based microwave oven to different grid disturbances. This device, which has a steady-state active power consumption of 1050 W and a capacitive reactive power generation injection of 180 VAr is classified as an electronic load according to the definition in the CMPLDW.

Fig. 27 shows the variation of active and reactive power during a voltage sag with retained voltage of 0.2 pu and a swell event where the voltage was increased to 1.2 pu. During the sag, the device experiences momentary cessation, while during the swell, the active power consumption increased to 1250 W and the reactive power changed from -180 VAr to +900 VAr. After the fault transient was cleared, the device returned to its steady-state conditions operation without any significant transient peaks in either the real or reactive power. Similar responses were recorded for all the other sag and swell tests of different magnitude and duration.

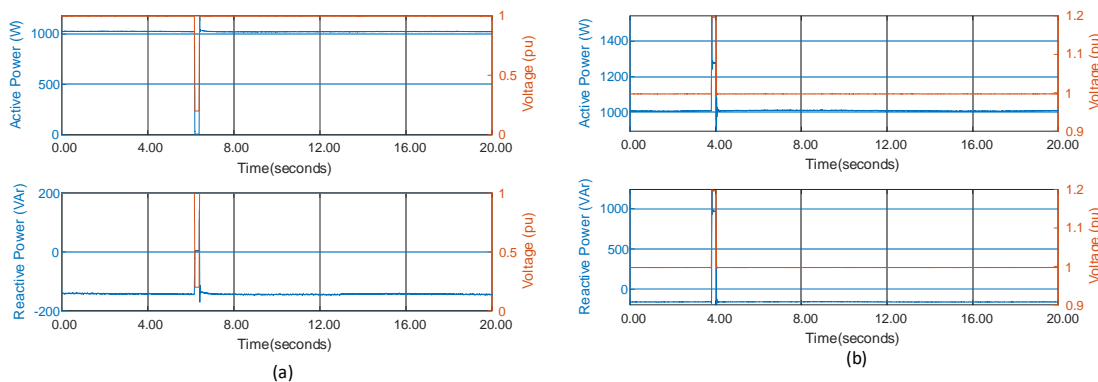


Figure 27: Response of Microwave Load when subject to a Sag/Swell with duration of 220ms (a) Sag with magnitude 0.2pu (b) Swell with magnitude 1.2pu.

The response of the microwave during frequency disturbance tests exhibited some interesting characteristics, despite not being expected to exhibit any changes in active and reactive power according to the CMPLDW definition for an Electronic Load. Fig. 28 shows that a change in frequency caused the active power consumption of the device to vary in a linear manner for both step and ramp frequency changes. The same behaviour was observed for reactive power. Figs. 28 (a) to (d) depict the changes in active power consumption of the device during step changes in the supplied voltage frequency from 50 to 52 Hz, 50 Hz to 47 Hz, and ramp frequency changes of +0.4 Hz/s and -0.4 Hz/s, respectively. The device operated without any significant variation in its power characteristics for all phase angle jump tests. Such behaviour requires further investigation across different load types to allow for appropriate modelling and classification of different devices.

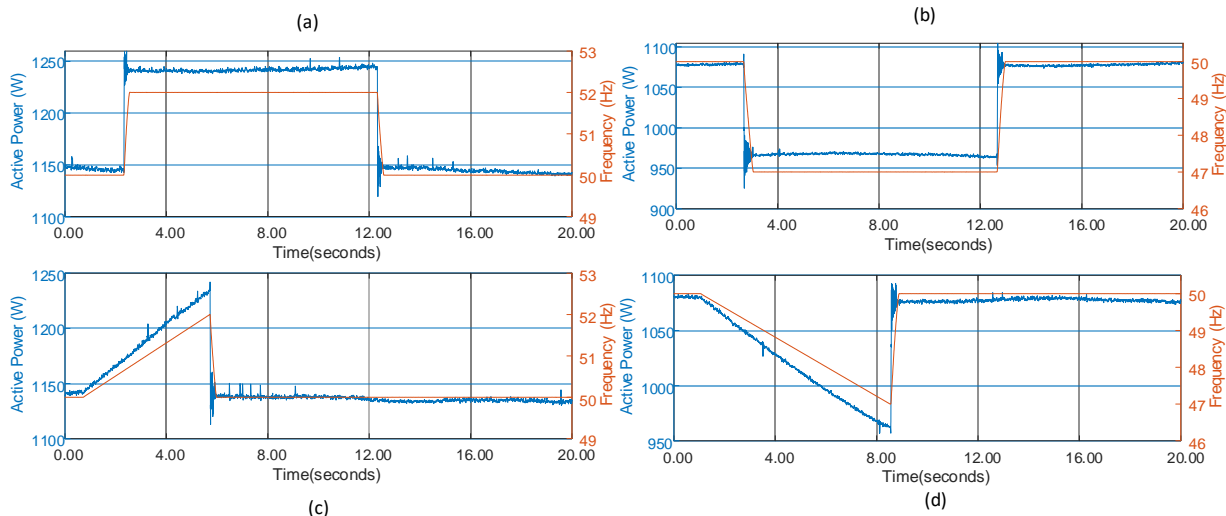


Figure 28: Frequency Change Response of the Microwave: (a) Step change from 50 Hz to 52 Hz, (b) 50 Hz to 47 Hz, (c) Ramp of +0.4 Hz/s (d) Ramp of -0.4 Hz/s.

## 6.3 Air Conditioners

### 6.3.1 DOL Based Conventional Unit

This section of the paper summarizes the outcomes of the test results for a portable air conditioner. The device has a power consumption of approximately 1 kW and draws 100 VAr during steady state conditions. The Air Conditioner was set to maximum cooling setting during the tests. It is worth noting that this device is categorized as a Motor D type in CMPLDW and as such may be susceptible to stalling in the event of power system faults.

For all sag and swell tests, except for the sag with a retained voltage of 0.2 pu (the lowest) the air conditioning unit returned to its normal operating condition when voltage returned to nominal. However, in the case of the sag with a retained voltage of 0.2 pu, the compressor motor stalled for

a brief period and the cooling system turned off. The motor then resumed operation after about 30 s. Fig. 29(a) demonstrates the stall characteristics of the air conditioner during a sag with a voltage reduction to 0.2 pu for 220 ms. This behaviour was also observed for sags of different durations at the same magnitude. Fig. 29(b) shows the response of the device when subjected to a voltage swell for 220 ms. Here the voltage was increased to 1.2 pu. It can be seen that the impact of the swell was a momentary change in both active and reactive power.

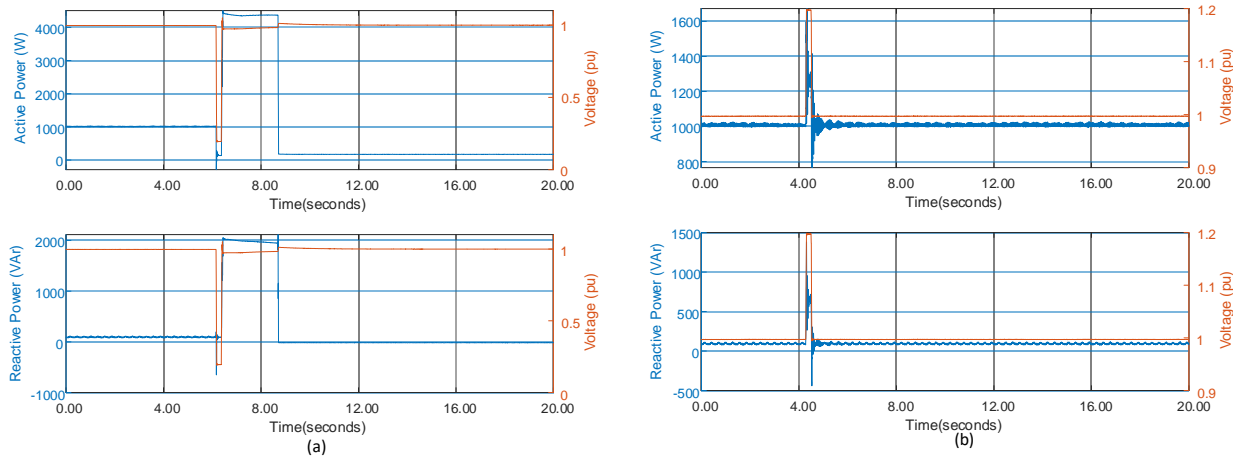


Figure 29: Response of Air Conditioner when subject to Voltage Disturbances: (a) Voltage Sag, and (b) Voltage Swell

The air conditioner experienced brief fluctuations in active power in response to both step and ramp changes in frequency. However, the reactive power consumption varied inversely with the frequency change. Fig. 30 presents the active and reactive power response of the device to step changes in frequency. The graph indicates that the reactive power consumption increased from 100 VAr to 300 VAr when the frequency was reduced from 50 Hz to 47 Hz, and the reactive power consumption dropped to zero when the frequency was increased from 50 Hz to 52 Hz. Similar behaviour was observed in the reactive power characteristics for ramp changes in frequency.

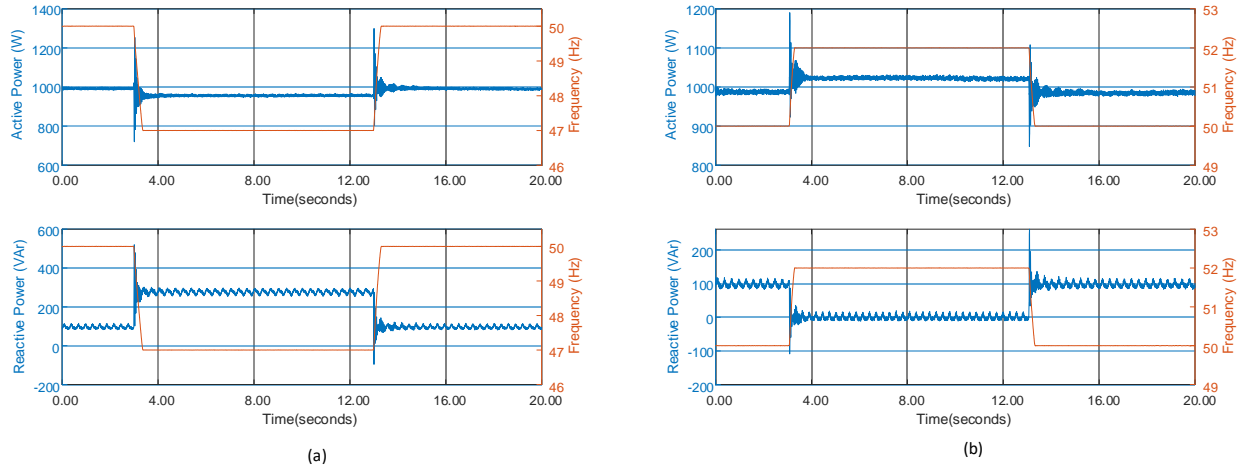


Figure 30: Frequency Change Response for the Air Conditioner: (a) Step decrease to 47 Hz, and (b) Step increase to 52 Hz

Regarding phase angle jumps, the air conditioner only experienced brief changes in both active and reactive power for phase angle magnitudes below  $90^\circ$ . However, for a voltage phase shift of  $90^\circ$ , the device was not impacted by the  $+90^\circ$  shift but appeared to stall when subjected to a phase shift of  $-90^\circ$ . The active and reactive power variations when the device was subjected to the  $90^\circ$  phase shift disturbance are shown in Fig. 31(a). The graph depicts an increase in both the active power increased to 4500 W and the reactive power drawn increased to over 2000 VAr. Fig. 31(b) illustrates how the current drawn by the unit varies, and it is evident that the current drawn during the period where it appeared to be stalled is significantly higher than during steady-state operations.

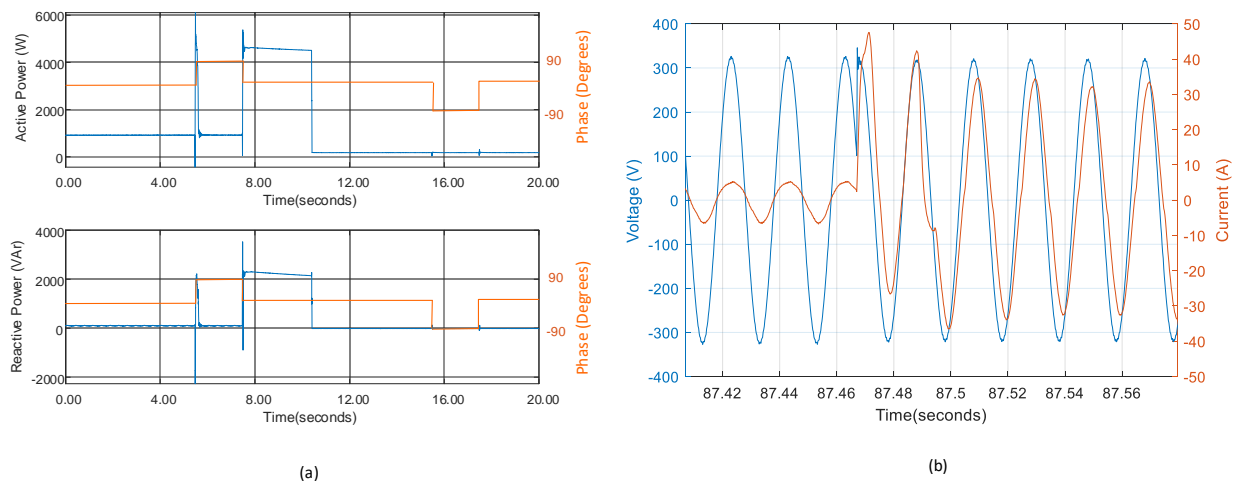


Figure 31: Impact of phase angle jump on the air conditioner operation: (a) P and Q response, and (b) Current drawn

### 6.3.2 Inverter Based Units

This section presents the results obtained from testing three inverter-based air conditioner units, specifically split air conditioning systems commonly found in residential homes and offices. It is important to note that these units differ from the conventional Direct-On-Line (DOL) based unit studied in Section 4.3.1, as they are classified as Electronic Load devices. Unlike DOL units, inverter-based units employ advanced power electronic based control algorithms to modulate the power output based on the requirements. The three units tested have been labelled as Air Conditioner 1, Air Conditioner 2 and Air Conditioner 3.

For voltage sag tests, in contrast to the DOL air conditioner, which exhibited stalling behaviour during voltage sag tests, the Inverter-based units did not experience any stalling issues across the range of voltage sag scenarios evaluated. Table VII, Table VIII, and Table IX, representing Air Conditioner 1, Air Conditioner 2, and Air Conditioner 3, respectively provide indication of the voltage sag magnitudes that caused the devices to either continue operating normally or cease operation.

From the tables, it is evident that Air Conditioner 1 was able to continue operating without as long as the voltage magnitude remained at 0.4 pu or higher. In the case of Air Conditioner 2, the unit ceased operation for sags with a duration of 220ms and when the voltage magnitude dropped to 0.5 pu or lower. For Air Conditioner 3 the unit ceased operation for sags of any duration as soon as the retained voltage was 0.4 pu or lower.

These results indicate that each unit has its own distinct control and protection mechanism, which leads to variations in their behaviour. Another interesting observation from these results was the fact that Air Conditioner 3 had a delay after the voltage sag before it ceased operation. In comparison, Air Conditioner 1 and Air Conditioner 2 ceased operation as soon as the sag disturbance was applied.

Table 38: Summary of Voltage Sag Tests for Air Conditioner 1

sag duration	Voltage amplitude during the sag (p.u.)							
	0.9	0.8	0.7	0.6	0.5	0.4	0.3	0.2
80 ms	✓	✓	✓	✓	✓	✓	X	X
120 ms	✓	✓	✓	✓	✓	✓	X	X
220 ms	✓	✓	✓	✓	✓	✓	X	X

Legend:

✓: ride-through, X: disconnects

Table 39: Summary of Voltage Sag Tests for Air Conditioner 2

sag duration	Voltage amplitude during the sag (p.u.)							
	0.9	0.8	0.7	0.6	0.5	0.4	0.3	0.2
80 ms	✓	✓	✓	✓	✓	✓	✓	✓
120 ms	✓	✓	✓	✓	✓	✓	✓	✓
220 ms	✓	✓	✓	✓	X	X	X	X

Legend:

✓ : ride-through, X: disconnects

Table 40: Summary of Voltage Sag Tests for Air Conditioner 3

sag duration	Voltage amplitude during the sag (p.u.)							
	0.9	0.8	0.7	0.6	0.5	0.4	0.3	0.2
80 ms	✓	✓	✓	✓	✓	X	X	X
120 ms	✓	✓	✓	✓	✓	X	X	X
220 ms	✓	✓	✓	✓	✓	X	X	X

Legend:

✓ : ride-through, X: disconnects

With respect to voltage swell tests, all the inverter-based air conditioners included in this project did not appear to be impacted by the applied voltage swells. The response of Air Conditioner 1, Air Conditioner 2, and Air Conditioner 3 during a voltage swell test, where the voltage was increased to 1.2 pu for 80ms, is shown in Figs. 32(a), (b) and (c), respectively. The plots clearly illustrate that during the swell event, there is a brief spike in current, which can be attributed to the charging of the capacitors within the units. However, once the voltage returned to normal, the devices resumed their normal operation, as indicated by the subsequent plots. Similar responses were observed for the other voltage swell tests conducted, indicating the ability of these inverter-based air conditioners to effectively ride through such disturbances without any adverse effects.

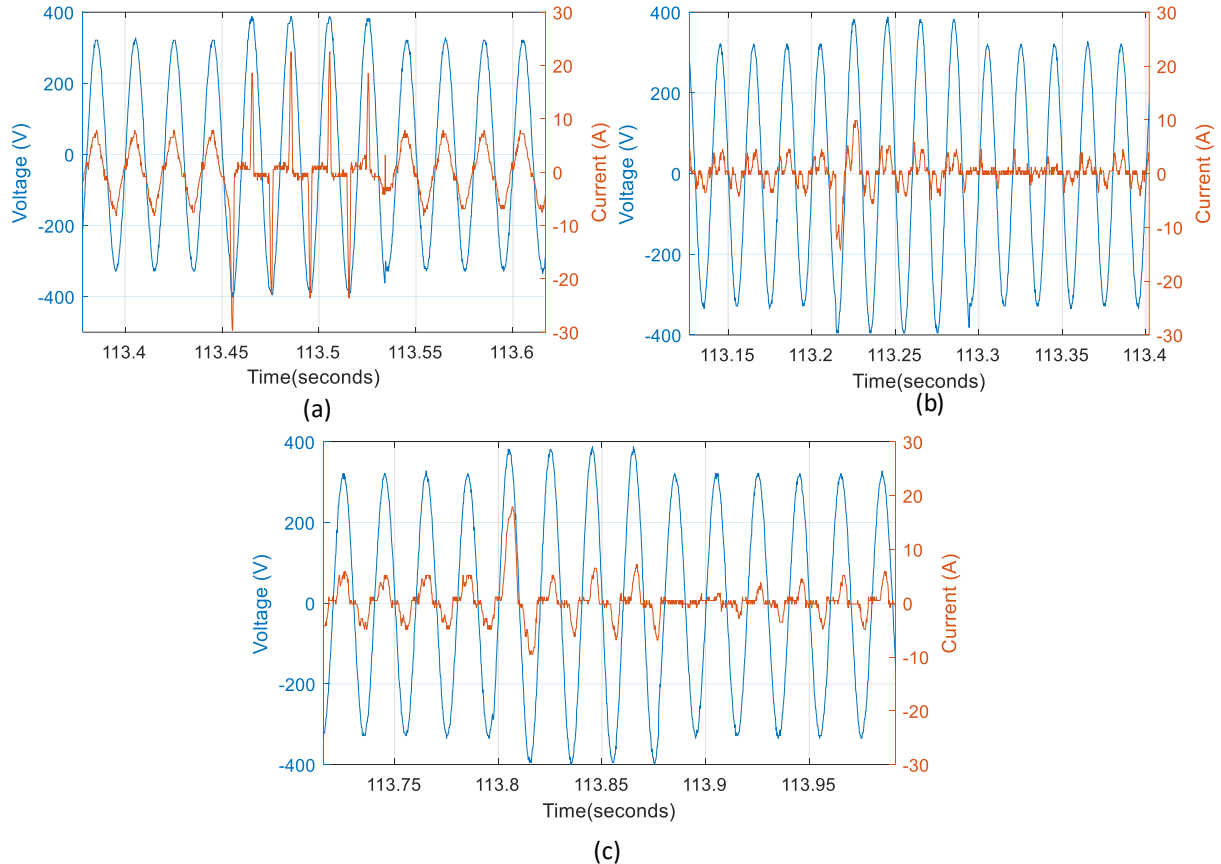


Figure 32: Response to a Swell of Voltage Magnitude 1.2 pu for 80ms (a) Air Conditioner 1 (b) Air Conditioner 2 (c) Air Conditioner 3

In relation to frequency and phase angle jump disturbances, the inverter-driven air conditioners maintained normal operation throughout all the conducted tests in this project. An example of this can be seen in Fig. 33(a), which shows the response of Air Conditioner 1 to a frequency step change from 50 Hz to 47 Hz. This consistent behaviour was observed across all frequency tests conducted on the three air conditioners. Additionally, Fig. 32(b) displays the current waveform of Air Conditioner 1 during a  $-90^\circ$  phase angle jump, where no significant impact is evident as the current continues its regular operation following the phase jump in the voltage waveform. Once again, all three devices exhibited similar responses.

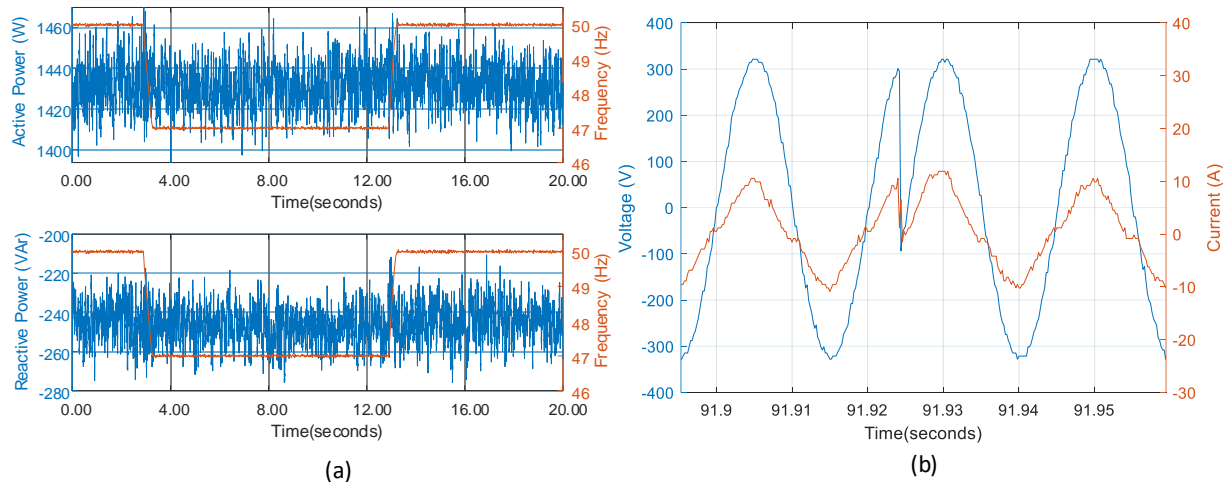


Figure 33: (a) Impact of Step Frequency Disturbance on Air Conditioner 1 (b) Impact of  $-90^\circ$  Phase Angle Jump on Air Conditioner 1

## 6.4 Motor Based Appliances

### 6.4.1 Vacuum Cleaner

This section presents the test results for a vacuum cleaner. The appliance has a power rating of 2 kW, and during the tests conducted at maximum power, it consumed 1.6 kW of active power and 100 VAr of reactive power. This resulted in a lagging power factor of 0.998.

Fig. 34 (a) illustrates the response of the device during the maximum voltage sag test, where the retained voltage was at 0.2 pu. Fig. 34(b) depicts the response for both active power (P) and reactive power (Q) when the voltage was increased to 1.2 pu, representing the maximum voltage swell test. It is evident from the results that the device was able to resume normal operation once the disturbances were complete.

As the vacuum cleaner is a motor-based device, the transient overshoot in the real and reactive power responses indicates the inrush currents associated with the motor's operation.

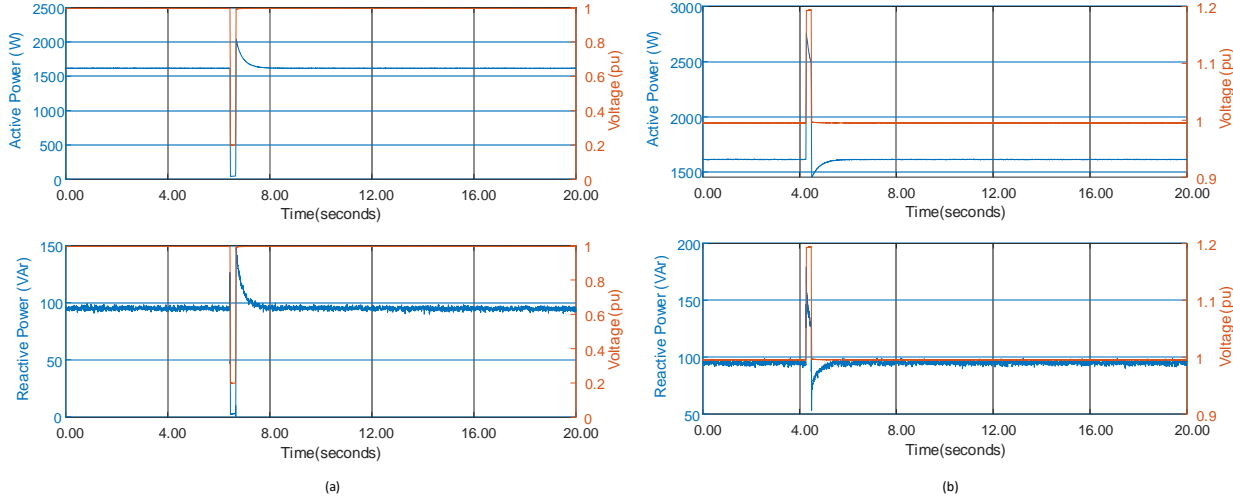


Figure 34: Response of Vacuum Cleaner (a) Sag with retained Voltage of 0.2 pu for 220ms (b) Swell with Voltage of 1.2 pu for 220ms

During the frequency tests, the vacuum cleaner exhibited no significant changes in its active power consumption, with only minor variations observed in the reactive power. Fig. 35(a) shows the response when the frequency is reduced from 50 Hz to 47 Hz at a rate of 0.4 Hz/s, revealing a reduction in reactive power from approximately 100 VAr to around 90 VAr. In Fig. 35(b), representing the step frequency change, the reactive power consumption increases from 100 VAr to about 105 VAr. For all frequency tests, the reactive power levels returned to their nominal value once the nominal frequency was restored. For phase angle jump disturbances in the applied voltage, the vacuum cleaner's current waveform experienced a phase angle jump without any overshoot at the time of the disturbance.

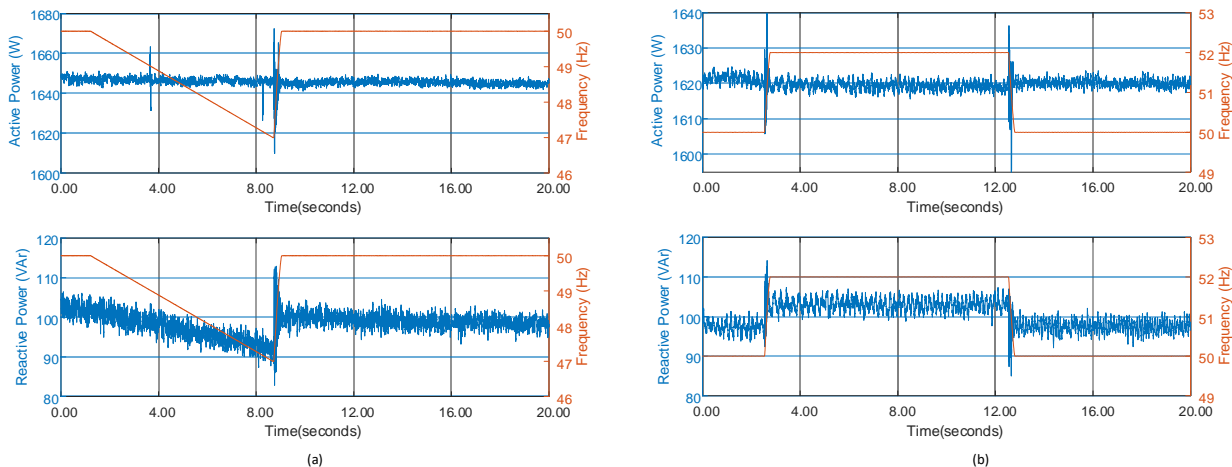


Figure 35: Frequency Response of the Vacuum Cleaner (a) Reduction in Frequency at 0.4 Hz/s (b) Step Increase in Frequency from 50 Hz to 52 Hz

### 6.4.2 Fans

This section provides a summary of the test results obtained for a pedestal stand fan. Under normal operating conditions, the fan consumed approximately 75 W of active power with a capacitive reactive power of -12 VAr.

During voltage sag and swell disturbances, the fan experienced momentary changes in both active and reactive power consumption. Fig. 36(a) illustrates the reduction in both active and reactive power levels for the fan during a sag event, where the voltage was reduced to 0.2 per unit (pu) for 220 ms. Fig. 36(b) demonstrates how the active and reactive power of the fan increased during the swell event.

In the sag test, the active power consumption of the fan dropped to 3 W from 75 W, while during the swell, the active power increased to approximately 107 W. This behaviour indicates that the fan response is similar to that of a constant impedance load, where power consumption is proportional to the square value of the applied voltage.

After the disturbances were complete, the fan returned to its normal operating conditions, albeit with a small inrush current overshoot, which is typical for such motor-based devices.

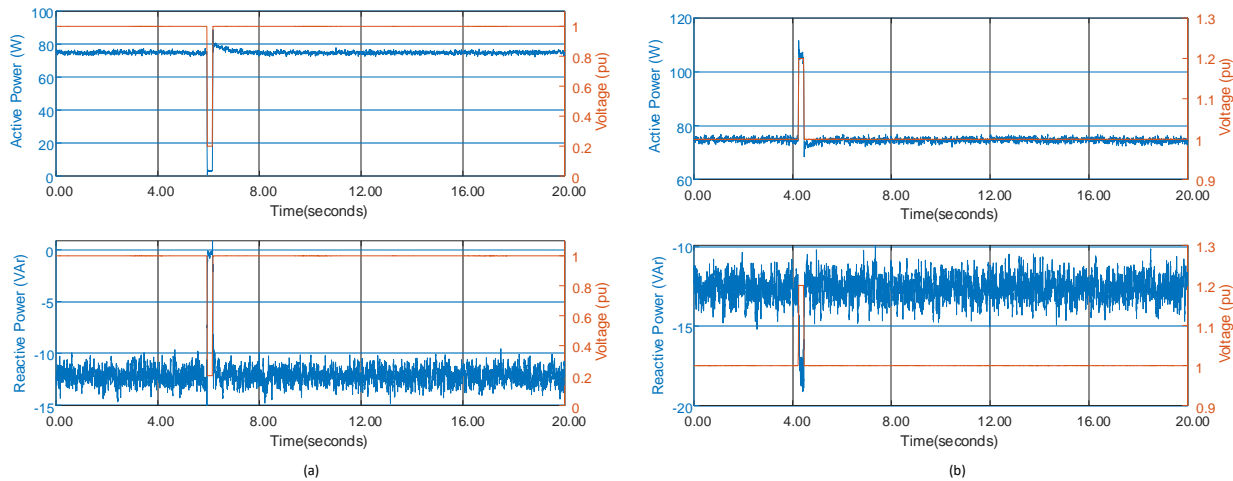


Figure 36: Response of Fan for Voltage Sag and Swell Disturbances (a) 0.2 pu Sag for 220ms (b) 1.2 pu Swell for 220ms

In terms of frequency disturbances, the active and reactive power levels of the fan exhibited a proportional change to the applied frequency of the power supply. Fig. 37(a) illustrates the variations in active power ( $P$ ) and reactive power ( $Q$ ) when the frequency was decreased from 50 Hz to 47 Hz, while Fig. 37(b) depicts the corresponding changes when the frequency was increased from 50 Hz to 52 Hz.

During the frequency decrease, the active power consumption of the fan decreased from 75 W to

72 W, while for the frequency increase, the fan's power consumption increased to approximately 78 W. These results indicate that the fan's power consumption responds in accordance with the changes in the supplied frequency. Similar behaviour was observed for the ramp frequency disturbances applied during the tests. The fan did not exhibit any significant changes in its active and reactive power consumption during the phase angle jump tests.

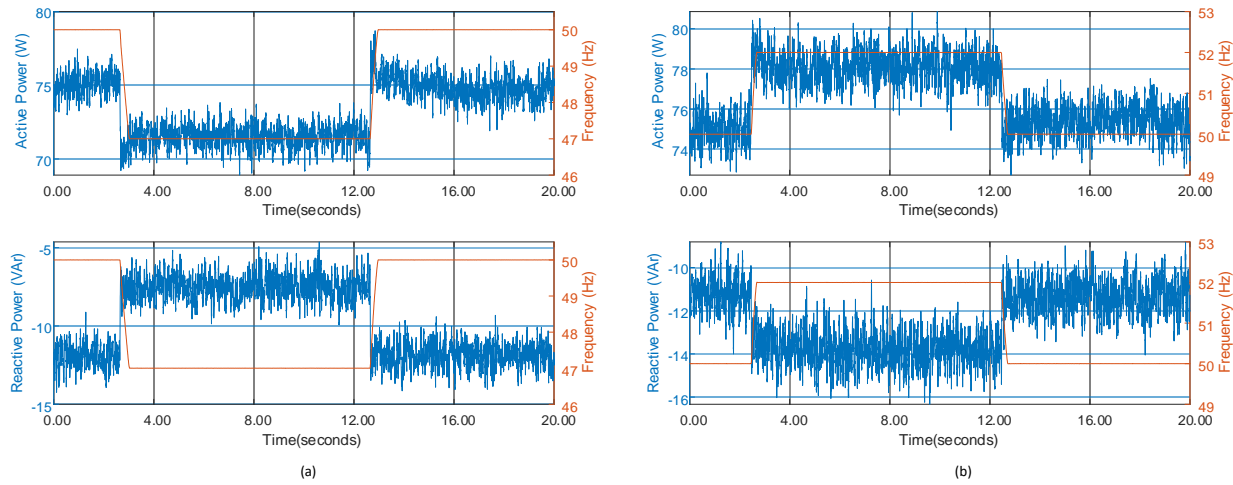


Figure 37: Frequency Response of Fan (a) Step Decrease in Frequency from 50 Hz to 47 Hz (b) Step Frequency from 50 Hz to 52 Hz

## 6.5 Static Loads

### 6.5.1 Heaters

In this section, the results of the tests conducted on two common types of heaters: Heater 1, a radiant coil-based heater, and Heater 2, an air-forced heater are presented. Under steady-state conditions, Heater 1 consumes 1200 W of active power and has a reactive power of -20 VAr, while Heater 2 consumes 800 W of active power with an inductive reactive power of +10 VAr.

Following a voltage sag event, both heaters displayed a temporary reduction in power consumption. Fig. 38(a) illustrates the active power (P) and reactive power (Q) response of Heater 1, while Fig. 38(b) demonstrates the P and Q response of Heater 2 when subjected to a voltage sag with a retained voltage of 0.2 pu for a duration of 220 ms. Once the voltage returned to its nominal value, both heaters returned to their normal power consumption levels.

During the recovery phase, a short transient overshoot in current was observed for both heaters. In the case of Heater 1, the transient overshoot may be attributed to the re-energizing of the heating coils. As for Heater 2, the overshoot could be attributed to inrush currents resulting from the fan motor.

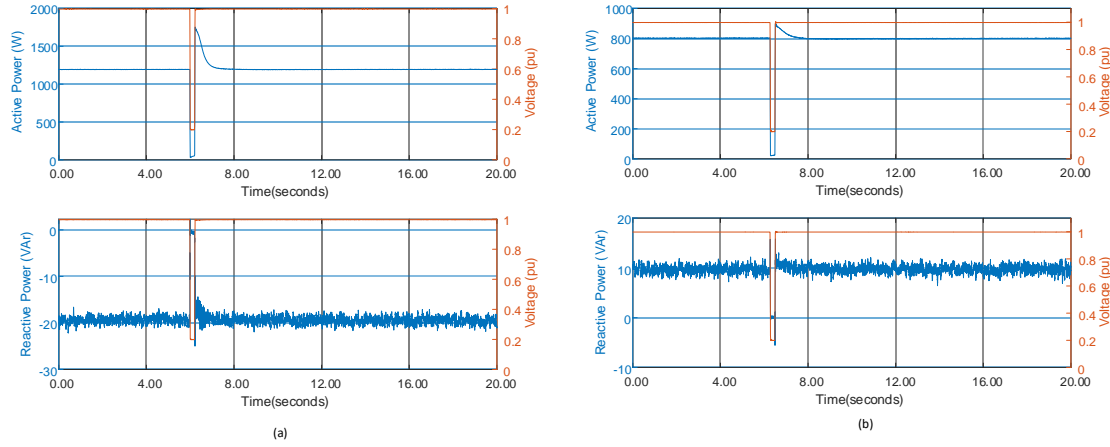


Figure 38: Heater Response to Sag of Retained Voltage Magnitude 0.2 pu for 220 ms (a) Heater 1 (b) Heater 2

The response of the heaters during voltage swell tests was similar to that observed during voltage sag tests. As the voltage increased during the swell, there was a corresponding increase in power consumption, and once the swell event concluded, the heaters returned to their normal operating conditions. This consistent behaviour was observed across all swell tests.

Regarding frequency changes, no noticeable effects were observed on the heaters. Fig. 39(a) illustrates the impact on the active power ( $P$ ) and reactive power ( $Q$ ) of Heater 1 during a gradual frequency change from 50 Hz to 47 Hz at a rate of 0.4 Hz/s. Similarly, Fig. 39(b) displays the response of Heater 2 to the same frequency disturbance. In both cases, there were no significant changes in the power consumption of the heaters.

Furthermore, the voltage phase angle tests did not appear to have any significant impact on heater operation.

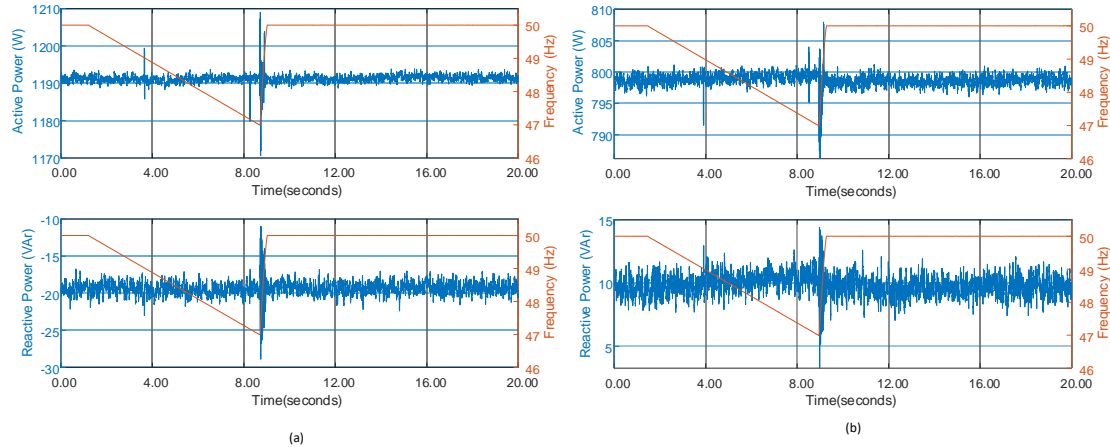


Figure 39: Impact of Frequency Disturbance (a) Heater 1 (b) Heater 2.

### 6.5.2 LED Lighting

This section presents the results of testing for a LED light bulb. Under normal operating conditions, the LED bulb consumed 10 W of active power with a capacitive reactive power of -5 VAr. During the voltage sag tests, the bulb experienced momentary cessation for all sags when the voltage dropped to 0.7 pu retained voltage or lower. However, when the voltage remained above 0.7 pu, as shown in Fig. 40(a), the LED bulb exhibited no significant changes in its active and reactive power levels.

For all voltage sags where the magnitude of the voltage fell below 0.7 pu, both the active and reactive power of the LED bulb reduced to zero during the event. An example of this is shown in Fig. 40(b) where the voltage was reduced to 0.7 pu during the sag disturbance. This behaviour was also visually observed through the flickering of the LED light during testing. These results indicate that the LED light bulb is sensitive to voltage sags, and its performance is affected when the voltage drops below a certain threshold.

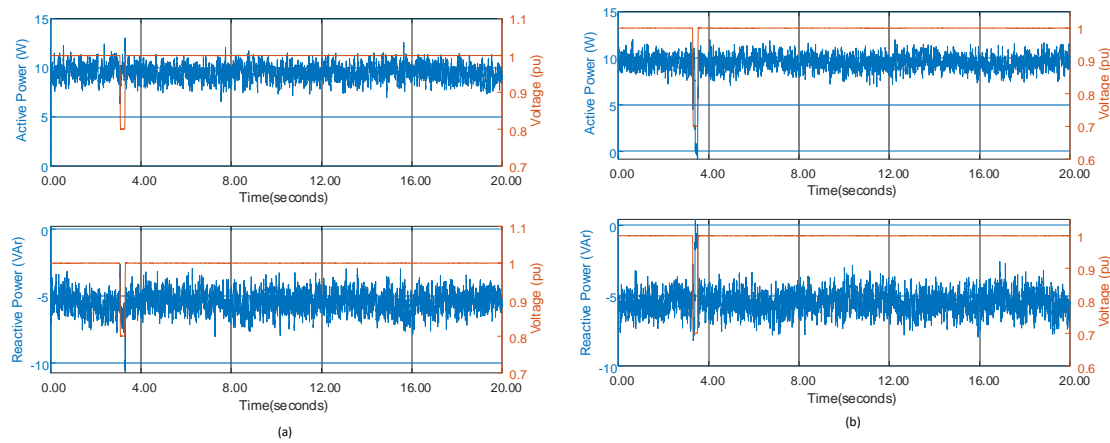


Figure 40: Response of LED Light Bulb for Voltage Sag of duration 220ms with Retained Voltage Magnitude (a) 0.8 pu (b) 0.7 pu.

Other tests conducted on the LED light bulb, including voltage swells, frequency changes, and phase angle jumps, did not result in any significant changes in both the active and reactive power levels of the device.

Fig. 41(a) presents the active and reactive power values for the LED bulb when subject to a voltage swell with a magnitude of 1.2 pu for a duration of 220 milliseconds. The graph demonstrates that the LED bulb maintained stable active and reactive power levels throughout the voltage swell event. Similarly, Fig. 41(b) illustrates the response of the LED bulb during a step frequency change from 50 Hz to 52 Hz. In this test, the LED bulb exhibited no notable variations in its active and reactive power consumption.

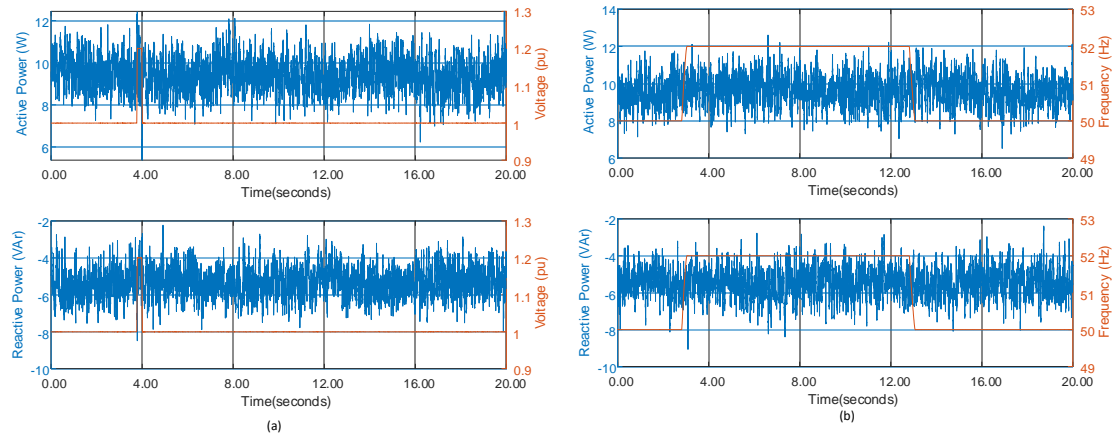


Figure 41: Response of LED Light Bulb (a) Voltage Swell of 1.2 pu for 220 ms (b) Step Frequency Increase from 50 Hz to 52 Hz

## 7 Residential Electric Vehicle Chargers

The growing popularity of electric vehicles (EVs) has raised concerns about the necessary network adaptations required to accommodate this potential substantial increase in load. The current complex load model does not include an embedded EV load model, and the authors have found only limited research on modelling of the dynamic response of EV chargers in the presence of grid faults. This report also presents the findings of tests conducted on two EV chargers, one at level 1 and the other at level 2, using an actual vehicle as the EV load. The testing of the home EV charger undertaken in this study provides valuable insights into the behaviour of EV loads in the presence of power system transients and also an indication of whether a separate EV block should be added to the AEMO Composite Load Models.

### 7.1 Level 1 EV Charger

This section summarises the results of bench testing for a home electric vehicle (EV) charger. The charger tested is a Level 1 AC charger that comes with a Type 1 EV connector. During normal operation, the device consumed 2200 W of active power with a power factor of 0.93 leading. To ensure consistency, the State of Charge (SoC) of the EV was kept below 80% for all the tests.

The EV charger was able to ride through voltage sags of all tested durations if the retained voltage was above 0.6 pu. Fig. 42(a) displays the instantaneous current response of the EV charger during a 220 ms sag with a retained voltage magnitude of 0.6 pu. The current stabilizes to its original value after an initial sag transient overshoot, indicating that the charger functions as a constant current controlled device. Once the fault is cleared, the current drawn drops briefly before returning to its nominal value. Fig. 2(b) shows the rms active and reactive power response of the EV during the same voltage sag. Both the active and reactive power decrease during the sag, while the charger continues to charge the EV once nominal voltage is restored.

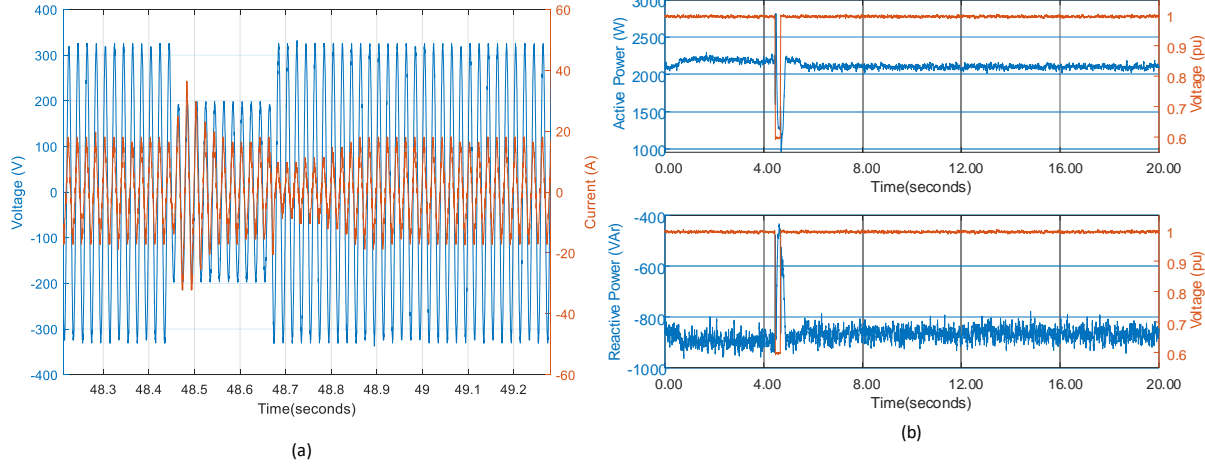


Figure 42: Response of EV Charger to Sag of 0.6 pu for 220 ms (a) Voltage- Current Response (b) PQ Response

If the retained voltage magnitude during sags was 0.5 pu or less, the EV charger disconnected from the vehicle by opening the contactor in the device. It was observed that in this case, the charger remained disconnected for a certain period before ramping up to its nominal charging power. Interestingly, two sets of reconnection time were recorded when the depth of the voltage sag was varied. Fig. 43(a) and (b) illustrate the charger's response when subjected to sags with retained voltage magnitudes of 0.4 pu and 0.3 pu, respectively.

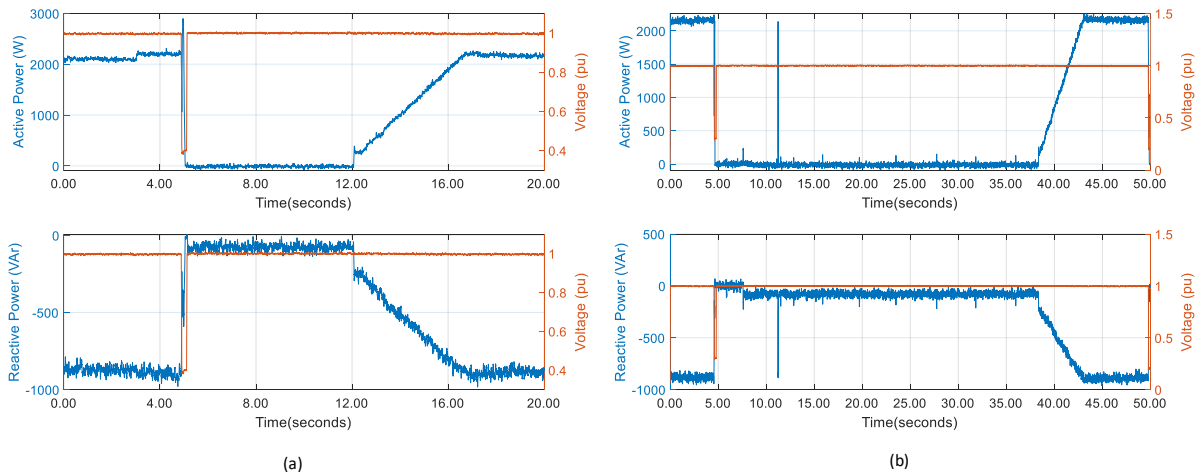


Figure 43: Demonstration of different reconnection time depending on the retained voltage during a voltage sag  
(a) 0.4 pu (b) 0.3 pu

Table 41 summarises the response and reconnection time of the tested EV charger when exposed to sags of different durations and magnitudes.

Table 41: Response of EV Charger for Voltage Sags of Different Magnitude and Duration

sag duration	Voltage amplitude during the sag (p.u.)						
	0.8	0.7	0.6	0.5	0.4	0.3	0.2
80 ms	✓	✓	✓	✓	✓	32 s	32 s
120 ms	✓	✓	✓	7 s	7 s	32 s	32 s
220 ms	✓	✓	✓	7 s	7 s	32 s	32 s

Legend:

✓: ride-through, # s: Duration of disconnection

The EV charger did not appear to be significantly impacted during the voltage swell tests. There was a temporary rise in both the active and reactive power levels of the charger. Frequency, whether in step or ramp form, did not result in any significant impact on the charger electrical performance. Fig. 44(a) and (b) depict the charger's response to a step frequency change from 50 to 52 Hz and the active and reactive power consumption during a ramp frequency change from 50 Hz to 47 Hz at a rate of -4 Hz/s, respectively. During the testing of the charger with respect to voltage phase angle jumps, no noticeable change was observed in its operation, and no disconnection occurred. The charger remained operational and did not disconnect during the testing of its response to voltage phase angle jumps. In the event of a phase angle jump disturbance in the applied voltage, the current waveform experienced a phase angle jump without any overshoot at the time of the disturbance.

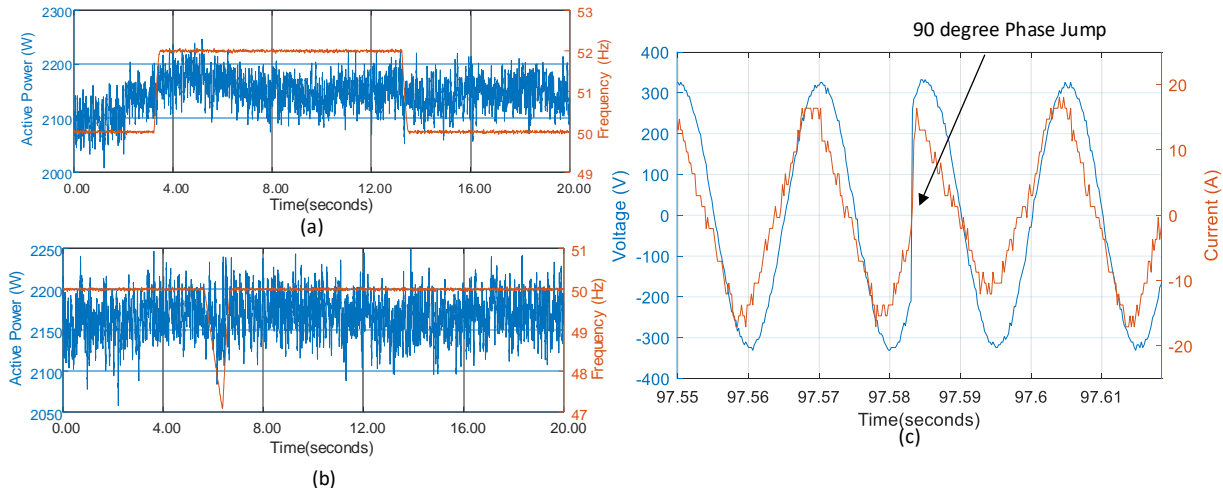


Figure 44: Impact of Frequency and Phase Angle Jump for EV Charger (a) Step Frequency Change from 50 Hz to 52 Hz (b) Ramp Frequency at -4 Hz/s (c) Phase Angle Jump

## 7.2 Level 2 EV Charger

This section presents a summary of the results obtained from the testing of a Level 2 electric vehicle (EV) charger commonly found in commercial car parks and residential homes. The charger under test has a rated power of 7.4 kW; however, the actual power drawn during testing was approximately

3.7 kW. This discrepancy is attributed to the power limitations set in the EV model tested, specifically the Nissan Leaf 2012. Under normal operating conditions, measurements showed capacitive reactive power of -500VAr, resulting in a leading power factor of 0.99. Similar to the case for the level 1 EV charger, it was ensured the EV's state of charge remained below 80% throughout all testing. Fig. 45 shows the EV charging setup used to perform these tests.

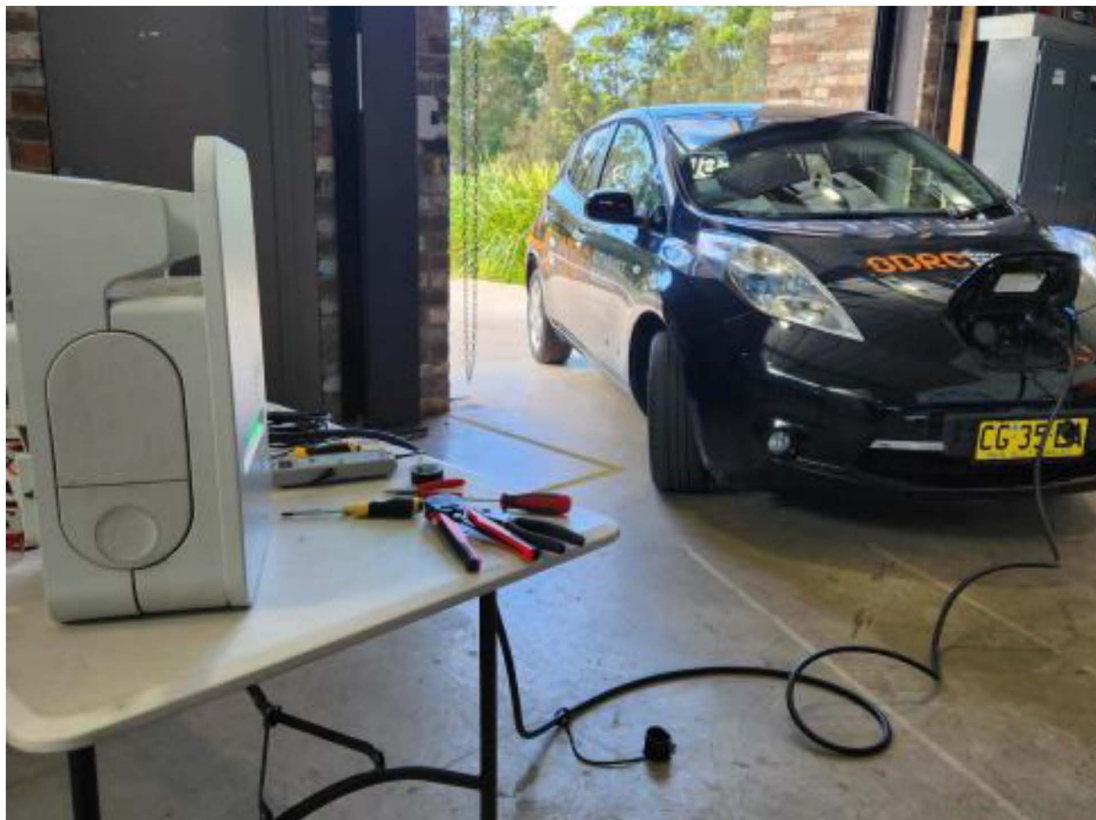


Figure 45: EV Charger Test Setup

In terms of voltage sag disturbances, the charger successfully rode through all applied sags. Fig. 46 illustrates the charger's response when subjected to a sag with a voltage depth of 0.2 per unit (pu) retained voltage for a duration of 220 milliseconds. Fig. 46(a) displays the instantaneous current and voltage waveforms during the sag, while Fig. 46(b) displays the active and reactive power responses. Both active and reactive power experience a momentary decrease during the sag, but the charger resumes charging the EV once the nominal voltage is restored.

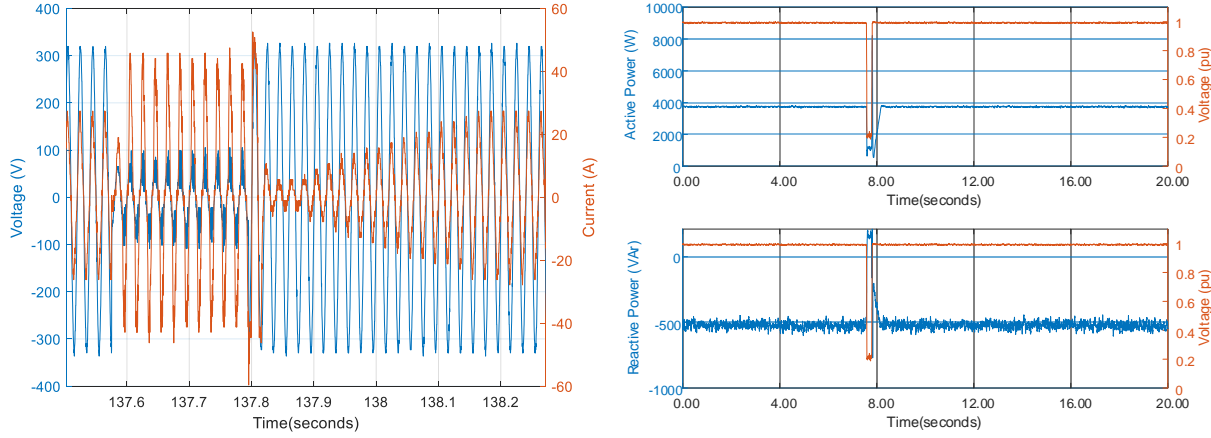


Figure 46: Response of EV Charger to a Voltage Sag of 0.2 pu Retained Voltage for 220 ms (a) Current response  
(b) P and Q response

Throughout the voltage swell tests, this particular EV charger demonstrated its ability to withstand the applied disturbances without any interruption to its normal operation. Fig. 47(a) displays the current response of the EV charger during a swell, when the voltage was momentarily increased to 1.2 per unit (pu) for a duration of 220 ms. Notably, during the swell, the charger's current draw decreased, indicating a response similar to that of a constant power load.

The response of the charger's real and reactive power during a voltage swell test is depicted in Fig. 47(b), illustrating its ability to ride through the disturbance with only minor transient oscillations. Once the voltage swells cleared, the charger promptly resumed its normal operation.

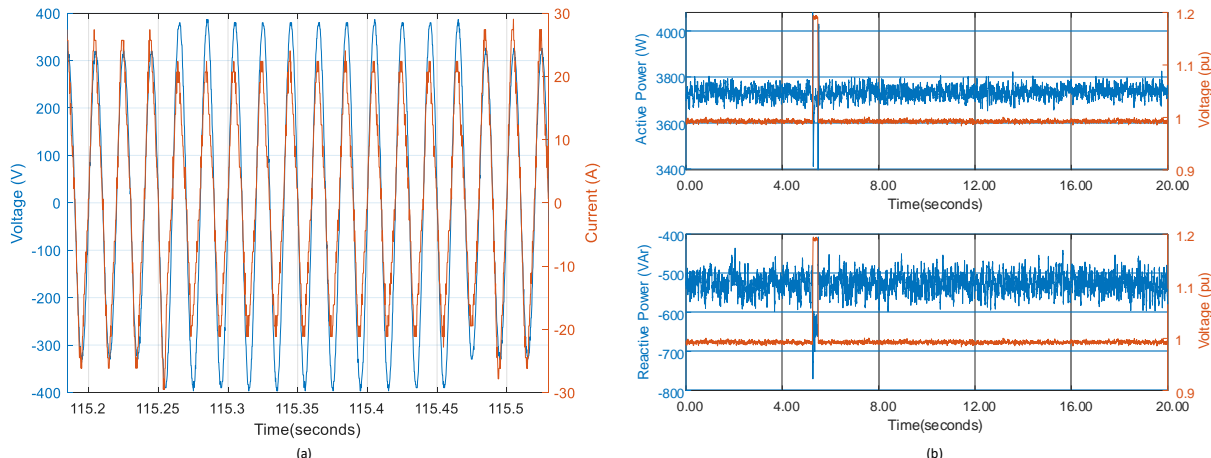


Figure 47: EV Charger Response to a Voltage Swell of Magnitude 1.2 pu for 220 ms (a) Current Response (b) P and Q Response

During the frequency disturbance tests, the EV charger response showed no significant changes in active and reactive power levels, consistent with the definition of an electronic load as per the CMPLDW. Fig. 47(a) and (b) illustrate the P and Q response of the EV charger when subjected to a step frequency change from 50 Hz to 47 Hz and 52 Hz, respectively. As observed from the plots, there is no discernible change in either the active or reactive power values. During the phase angle jump tests, the charger demonstrated consistent performance without any significant alterations in either the active and reactive power magnitudes. Moreover, the charger withstood all the tests without experiencing any disruptions.

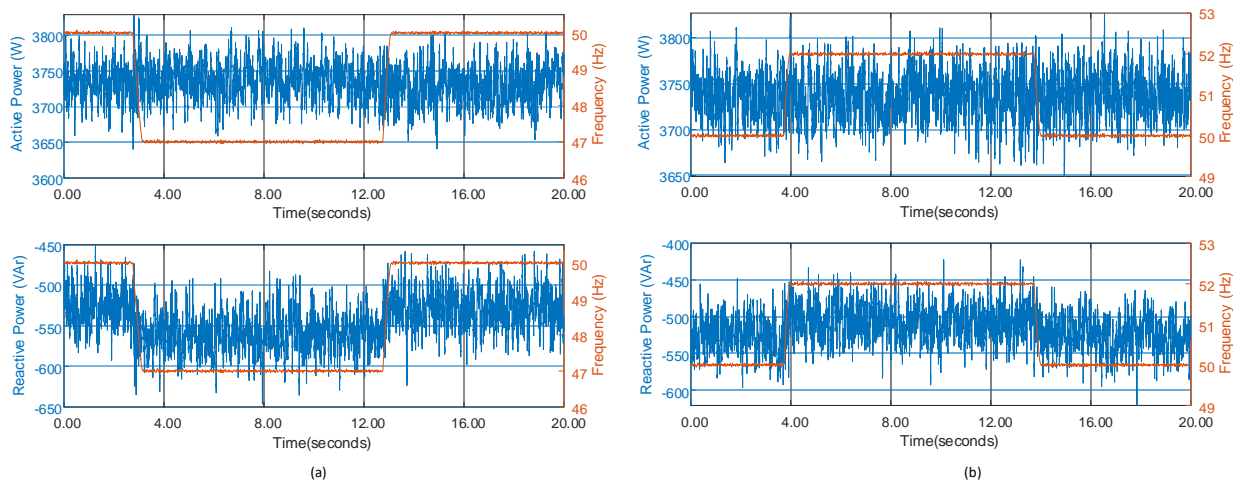


Figure 48: EV Charger Response to Step Frequency Disturbances (a) 50 Hz to 47 Hz (b) 50 Hz to 52 Hz

## 8 Load Modelling

Exhaustive international work has paved the way towards the development of more precise composite load models for power system dynamic simulations. The Western Electricity Coordinating Council (WECC) proposed a generic composite load model that includes a representation of the distribution feeder, and the aggregate behaviour of various loads and DERs connected in distribution systems. A diagram of the WECC composite load model (WECC-CMLD) is depicted in Fig. 49 and consists of several key components:

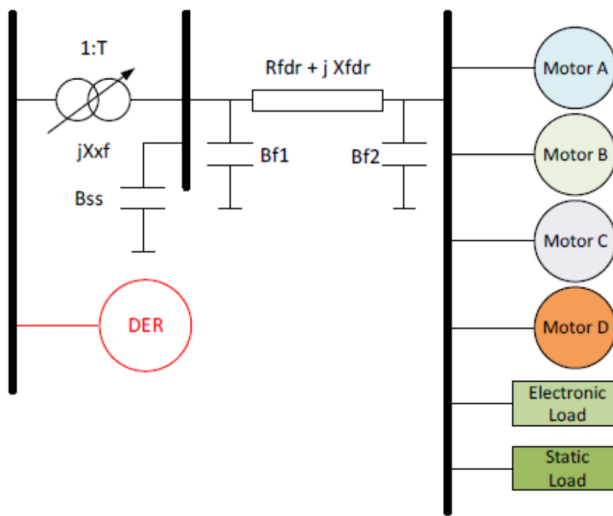


Figure 49: Diagram of the WECC Composite Load Model (WECC-CMLD).

1. A distribution transformer with an on-load tap changer, where the transformer impedance is represented by  $jX_{xf}$ .
2. A substation shunt capacitor, where  $B_{ss}$  is the susceptance in per unit (pu).
3. A single-phase equivalent model of the distribution feeders that carry power to the end-use loads ( $R_{fdr} + jX_{fdr}$ ). Shunt capacitors are implemented at both ends to account for reactive power losses in the feeder, ensuring that the net apparent power at the transmission bus matches that of the power flow case.
4. Six different classifications of loads which are connected to the load bus, including a combination of four different types of motors, an equivalent electronic load model, and the remaining loads combined into a static polynomial load model.

The six different classifications of load types in the CMPLDW model are:

- **Motor A:** Motor A refers to 3-phase induction motors that have high locked-rotor torque and low inertia (with an  $H$  value of 0.1 seconds) and are designed to drive constant torque loads. These types of motors are typically used in commercial and industrial air conditioning compressors and refrigeration systems.
- **Motor B:** Motor B is also a 3-phase induction motor, but with high inertia (with an  $H$  value

ranging from 0.25 to 1.0 seconds), and it's designed to drive loads whose torque is proportional to speed squared. These motors are commonly used in commercial ventilation fans and air-handling systems, with typical ratings ranging from 4 to 19 kW.

- **Motor C:** Motor C is a 3-phase induction motor that has low inertia (with an  $H$  value ranging from 0.1 to 0.2 seconds) and is designed to drive loads whose torque is proportional to speed squared. These motors are typically used in commercial water circulation pumps in central cooling systems, with typical ratings ranging from 4 to 19 kW.
- **Motor D:** Motor D is a specialised performance model that's specifically designed to represent single-phase (1P) compressors used for residential air-conditioning loads in the United States. These motors have a constant torque load characteristic and minimal inertia, which can make them prone to stalling. They're commonly used in 1P residential and light commercial refrigerator compressor motors in Australia, with typical ratings ranging from 2 to 4 kW.
- **Electronic Load:** A power electronic load refers to electronic devices used by consumers (such as computers and televisions), appliances (like dishwashers), office equipment, and variable frequency drives (VFDs) used in commercial and industrial settings.
- **Static Load:** A static load represents the remaining unclassified aggregate loads, including constant impedance loads like such as incandescent lighting.

One of the primary focuses of the project is to provide updates from the inverter testing to improve the aggregate model of distributed generation (DG), which is part of the WECC model. It is essential to tune the model based on the existing DGs features and characteristics analysed through testing in the system. An aggregated response can be derived from the testing to provide essential parameters for the model. The model of DER consists of two things, one creating the model and the other deriving the parameters for the model. The process of tuning the parameters for the model is as follows:

1. The default values of the parameters are checked against those relevant for the Australian grid, and the default values are used if they are suitable.
2. Some of the parameters are directly set by AS4777:2005, AS4777:2015 and AS4777:2020 depending on the fleet composition. Accordingly, these values are used in the model.
3. Some of the model parameters, which cannot be defined according to the previous two steps, can be calculated using the inverter test results described in the previous sections.
4. The parameters, which cannot be calculated using the steps mentioned above, are estimated using available technical references, relevant information, or engineering judgement.

## 8.1 Comparison with PSSE Results

UOW is currently analysing the load testing results with PSSE Single Machine Infinite Bus (SMIB) simulation of each of the individual load types in CLMD. The task will allow the individual loads to be grouped easily and demonstrate if any of the devices fall under a category that is not defined in the CMLD model. To highlight this, Fig 50 presents the active power response of the vacuum cleaner

load and a SMIB case assuming the device falls under the power electronic load category. It can be seen that the simulation case is unable to capture the inrush current of the device after the sag is cleared. This may be due to the inability of RMS models to capture transients or may also be due to the vacuum cleaner falling under a category (VSD for example) not defined in the current CMLD structure.

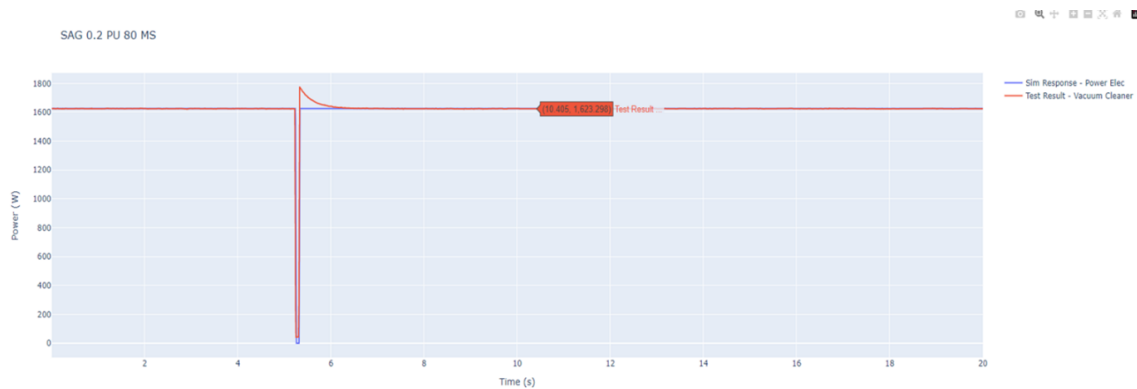


Figure 50: Comparison of bench test and SMIB simulation for vacuum cleaner under voltage sag

## References

- [1] J. Fletcher, N. Stringer, G. Konstantinou and I. MacGill. "Ensuring System Security and Modelling Fast Load DER Responses with high penetrations of IBR" [Online]. Available: <https://www.csiro.au/en/research/technology-space/energy/g-pst-research-roadmap>
- [2] GPST Consortium Inaugural Research Agenda March 2021, accessed at: [https://globalpst.org/wp-content/uploads/042921G-PST-Research-Agenda-Master-Document-FINAL\\_updated.pdf](https://globalpst.org/wp-content/uploads/042921G-PST-Research-Agenda-Master-Document-FINAL_updated.pdf)
- [3] F. Arraño-Vargas, Z. Shen,, S. Jiang, J. Fletcher, and G. Konstantinou, "Challenges and Mitigation Measures in Power Systems with High Share of Renewables—The Australian Experience". Energies 2022, 15, 429. <https://doi.org/10.3390/en15020429>
- [4] N. Stringer, "Navigating decentralisation: data driven analysis of distributed energy resources and a framework for their integration into the electricity industry," Doctor of Philosophy, Engineering, UNSW Sydney, 2020.
- [5] A. Arif, Z. Wang, J. Wang, B. Mather, H. Bashualdo and D. Zhao, "Load Modeling—A Review," in IEEE Transactions on Smart Grid, vol. 9, no. 6, pp. 5986-5999, Nov. 2018, doi: 10.1109/TSG.2017.2700436.
- [6] R. Quint et al., "Transformation of the Grid: The Impact of Distributed Energy Resources on Bulk Power Systems," in IEEE Power and Energy Magazine, vol. 17, no. 6, pp. 35-45, Nov.-Dec. 2019, doi: 10.1109/MPE.2019.2933071.
- [7] Hirsch, A., Parag, Y., & Guerrero, J. (2018). Microgrids: A review of technologies, key drivers, and outstanding issues. Renewable and sustainable Energy reviews, 90, 402-411.
- [8] A. Ahmad, H. D. Tafti, G. Konstantinou, B. Hredzak and J. E. Fletcher, "Analysis on the Behavior of Grid-Connected Single-Phase Photovoltaic Inverters Under Voltage Phase-Angle Jumps," 2021 IEEE 12th Energy Conversion Congress & Exposition - Asia (ECCE-Asia), Singapore, Singapore, 2021, pp. 291-296, doi: 10.1109/ECCE-Asia49820.2021.9479264.
- [9] Australian Energy Market Operator, "Fault at Torrens island switchyard and loss of multiple generating units on 3 March 2017," [Online], [https://www.aemo.com.au/-/media/Files/Electricity/NEM/Market\\_Notes\\_and\\_Events/Power\\_System\\_Incident\\_Reports/2017/Report-SA-on-3-March-2017.pdf](https://www.aemo.com.au/-/media/Files/Electricity/NEM/Market_Notes_and_Events/Power_System_Incident_Reports/2017/Report-SA-on-3-March-2017.pdf).
- [10] AS 4777.2:2020, AU/NZ Standard, Grid connection of energy systems via inverters part 2: Inverter requirements, Standards Australia/New Zealand Std. AS 4777.2: 2020
- [11] A. Ahmad, H. D. Tafti, G. Konstantinou, B. Hredzak and J. Fletcher, "Sensitivity Analysis of Grid-Connected Single-Phase Photovoltaic Inverters to Fast Voltage Sag Disturbance," 2022 International Conference on Emerging Trends in Electrical, Control, and Telecommunication Engineering (ETECTE), Lahore, Pakistan, 2022, pp. 1-6, doi: 10.1109/ETECTE55893.2022.10007189.
- [12] T. V. Cutsem and C. Vournas, Voltage Stability of Electric Power Systems. Norwell, MA, USA: Kluwer, 1998.
- [13] W. Mauricio and A. Semlyen, "Effect of Load characteristic on the Dynamic Stability of Power Systems," IEEE Transactions on Power Apparatus and Systems, vol. PAS-91, no. 6, pp. 2295-2304, 1972, doi: 10.1109/TPAS.1972.293385.
- [14] V. Terzija et al., "Wide-Area Monitoring, Protection, and Control of Future Electric Power Networks," Proceedings of the IEEE, vol. 99, no. 1, pp. 80-93, 2011, doi: 10.1109/JPROC.2010.2060450.
- [15] J. Y. Wen, L. Jiang, Q. H. Wu, and S. J. Cheng, "Power system load modeling by learning based on system measurements," IEEE Transactions on Power Delivery, vol. 18, no. 2, pp. 364-371, 2003, doi: 10.1109/TPWRD.2003.809730.



- [16] Australian Energy Market Operator, "PSSE models for Load and Distribution PV," Australia, March 2022.
- [17] D. Kosterev et al., "Load modeling in power system studies: WECC progress update," in 2008 IEEE Power and Energy Society General Meeting - Conversion and Delivery of Electrical Energy in the 21st Century, 20-24 July 2008 2008, pp. 1-8, doi: 10.1109/PES.2008.4596557.
- [18] J. W. Shaffer, "Air conditioner response to transmission faults," IEEE Transactions on Power Systems, vol. 12, no. 2, pp. 614-621, 1997, doi: 10.1109/59.589619.
- [19] B. R. Williams, W. R. Schmus, and D. C. Dawson, "Transmission voltage recovery delayed by stalled air conditioner compressors," IEEE Transactions on Power Systems, vol. 7, no. 3, pp. 1173-1181, 1992, doi: 10.1109/59.207331.
- [20] North American Electric Reliability Corporation, "Technical Reference Document- Dynamic Load Modeling," December 2016. [Online]. Available: <https://www.nerc.com/comm/PC/LoadModelingTaskForceDL/Dynamic%20Load%20Modeling%20Tech%20Ref%202016-11-14%20-%20FINAL.PDF>
- [21] "Inverter and Load Testing Results. <http://pvinverters.ee.unsw.edu.au/> (accessed 2023).

## Paper information

Paper number	1204
Paper title	Future-proofing Power System Planning, Operational and Stability Analysis through DER and Load Bench-Testing and Modelling
Study Committee	SC C6 – Active distribution systems and distributed energy resources
Paper Stream	2. Developing practices, functionalities and applications
Authors	Georgios Konstantinou <sup>1</sup> , Awais Ahmad <sup>1</sup> , Obaidur Rahman <sup>2</sup> , Sean Elphick <sup>2</sup> , Duane Robinson <sup>2</sup> , John Fletcher <sup>1</sup> , Patrick Graham <sup>3</sup> , Jenny Riesz <sup>3</sup>
Affiliations (optional)	<sup>1</sup> UNSW Sydney (The University of New South Wales) <sup>2</sup> University of Wollongong <sup>3</sup> Australian Energy Market Operator (AEMO)
Email address	g.konstantinou@unsw.edu.au

## Summary

Growth of distributed energy resources (DER) in Australian networks continues at an accelerated pace, with less regulated and often unobserved DER accounting for a significant proportion of generation during midday hours. Combined with the expansion of Battery Energy Storage Systems (BESS), smart loads and the introduction of Electric Vehicles (EVs) at scale, challenges for network management and system security necessitate the development of new tools and methods. Traditional model-based approaches or simulations alone do not accurately represent real-world conditions and fail to encompass all possible scenarios that distributed energy resources (DER) and smart loads, like air conditioners and heat pumps, might face. While simulations and models offer valuable insights into the performance of DER, the critical and often underserved step of informing their development and validation through laboratory bench-testing and experimental analysis is essential to ensure accuracy and reliability. Research conducted under Theme 9 of the Australian Global Power System Transformation (GPST) consortium on DER and stability for power systems with large penetrations of DER, and presented in this article, aims to address this gap with a focus on an open DER and load-testing protocol, updates to results from bench-testing of DER, BESS and smart loads and recommendation for future work. The findings have significant implications for power system operators, policymakers, and industry stakeholders globally as a better understanding of DER and smart load behaviour leads to better modelling, more effective integration and management, and enhanced stability and resilience for future power grids.

## Keywords

Distributed Energy Resources (DER), Rooftop Solar PV, EV Charging Infrastructure, Battery Energy Storage Systems (BESS), Fault-Ride Through (FRT), Over/Under Frequency Response, DER and Stability, Bench-Testing Results, Load Models

## Introduction

Distribution networks of electrical power systems across the world are undergoing a major transformation with the introduction of distributed energy resources (DERs), predominantly in the form of distributed PV (DPV) [1], the anticipated growth in battery energy storage systems (BESS), electric vehicles (EVs) and modern flexible loads. However, the different response of various DER to the same grid disturbances, creates uncertainty and introduces a new element of vulnerability to power systems. Grid operators also often lack visibility as the number of DER makes these devices difficult to monitor and manage when compared to larger-scale systems [2]. The dynamic behaviour of individual DER devices, when subjected to faults and other power system disturbances, is also not accurately reflected in common static load models used by network service providers (NSPs). The unique characteristics of each inverter together with the inherent challenges of modelling, monitoring, and managing DER, underscore the need for new tools and methods that can accurately capture the dynamic behaviours of power systems with high penetrations of DERs and flexible loads. By developing and implementing these innovative solutions, operators can better understand, predict, and control the interactions between DERs and the grid, enhancing the stability and resilience of the power system.

Understanding DER and load response under normal and grid disturbance conditions is critical, as their internal settings can significantly impact their behaviour. Some common characteristics of these devices are:

- Limited monitoring and visibility of their dynamic behaviour in real-time.
- Each device, system and manufacturer offer their own unique software and hardware features.
- Older systems may continue to operate using outdated standards as standards evolve.
- Installation of new brands and models of DER and introduction of EVs can affect prior assumptions and models.

While current standards prescribe requirements for DER response under fault conditions, there are several possible grid disturbances on which no guidelines are defined. As a result, the response of DER to the same grid disturbance can vary significantly among different manufacturers [3]. DER previously connected in the power system may not be subject to newly established standards. To ensure effective planning and grid stability, understanding these DER behaviours, particularly their responses to transmission and distribution network faults, is crucial. A growing body of literature investigates the behaviour of DER, especially PV inverters [4]-[6] and EVs [7] under various grid conditions. This behaviour is analysed through laboratory bench-testing, providing valuable insights into their performance.

Precise load modelling is essential for Network Service Providers (NSPs) to evaluate power system performance under various conditions, assess network stability issues, and devise effective control solutions. Sophisticated composite load models are now available that can capture both the dynamic and static response of loads [8]. The addition of electrical distance between the transmission network and end load also allows these models to capture delayed voltage recovery events from transmission faults [9]. Composite load models consider the diverse aspects of load behaviour, such as dynamic response, sensitivity to voltage changes, and response to frequency fluctuations [10]. These models can be constantly updated using inputs from NSPs (e.g., through load surveys) and also through data measured during power system faults and laboratory testing of appliances and equipment.

To collectively address a lack of accurate dynamic models for existing DER and loads and futureproof networks for the growth in BESS and EVs, carried out under the Topic 9 of the Australian G-PST Research Roadmap, is extensive experimental testing of DER, BESS, EVs and modern loads when subjected to various voltage, frequency and phase disturbances aiming to replicating practical network disturbances. The key aim is to obtain detailed information on the response of these systems to system disturbances, enabling better comprehension of their behaviour, inform modelling approaches and defining parameters for their inclusion to existing load models. By addressing these challenges, the study contributes valuable insights to power system operators, policymakers, and industry

stakeholders, ultimately supporting the development of more effective strategies for the integration and management of DER, BESS, EVs and modern smart loads.

## Experimental Bench Testing Setup

The testing of DER is facilitated by a comprehensive laboratory bench-testing setup, which enables the examination of a wide range of devices and scenarios, simulating different grid conditions and disturbances to better understand their real-world performance and interactions. The schematic diagram of a generic bench-testing setup, designed for distributed PV testing is shown in Fig. 1(a), and a photograph of the laboratory setup is presented in Fig. 1(b). A PV emulator connects to the PV side of the single-phase inverter to simulate a solar array and generate PV current ( $i_{pv}$ ) for the inverter. Meanwhile, a bidirectional grid emulator connects to the inverter output terminals, enabling adjustment of grid voltage ( $v_g$ ) parameters at the connection point, such as magnitude, frequency, and phase-angle at the connection point. A grid inductance ( $Z_g$ ) placed between the grid emulator and the PV inverter to represent a line inductance. A similar setup can be repurposed for the testing of BESS (where no additional DC supply is required), EVs and loads.

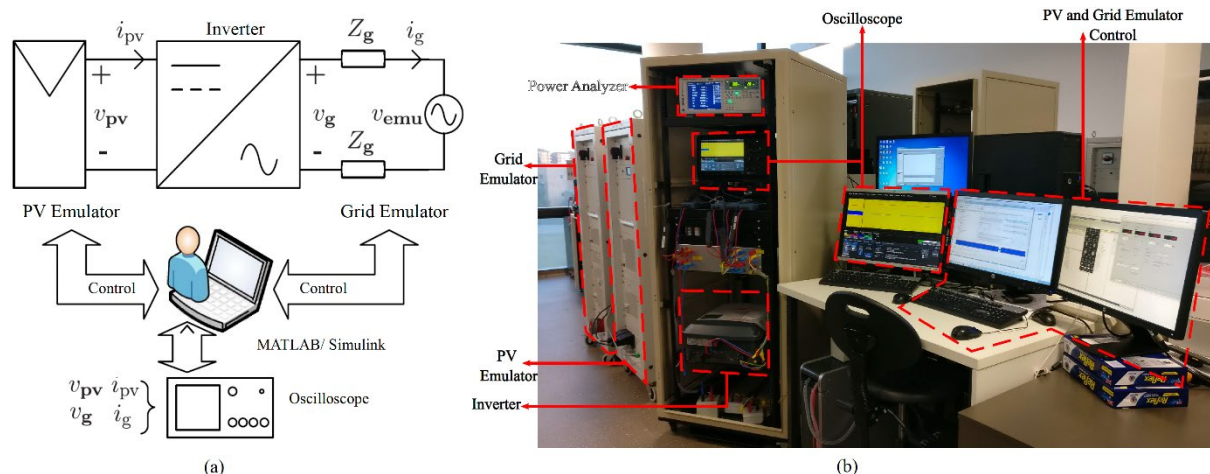


Figure 1: Inverter testing setup: (a) schematics of the bench testing setup, (b) testing setup photo showing from left to right, the bidirectional (REGATRON TC.ACS) grid emulator (50 kVA), (16 kV A Regatron TC.P) photovoltaic (PV) emulator, off the shelf inverters,  $Z_g = 0.12 + j0.16$  grid impedance and measurement equipment.

## DPV Inverter Bench Testing Results

Among all devices of interest, testing of DPV inverters is further advanced, given their prevalence in distribution networks. This section presents a detailed account of the response of various off-the-shelf DPV inverters to grid disturbances, such as ramp frequency changes, voltage phase-angle jumps (VPAJ), voltage sags and voltage swells.

### Ramp Frequency Change (RoCoF)

The value of the Rate of Change of Frequency (RoCoF) offers an indication of system strength and the size of disturbance. With greater DER penetration higher values of RoCoF are expected, and the ability of DER inverters to withstand RoCoF events means they can continue to provide power and support grid frequency, preventing or minimizing the risk of cascading failures and system outages. For example, during the September 2016 blackout in South Australia, an average RoCoF value of 6.25 Hz/s was captured, a value that is outside the normal UFLS protection schemes [11]. In a more recent event involving the separation of Queensland and South Australia [12], a maximum RoCoF of 0.65 Hz/s was recorded. Fig. 2 is an example of a desired behaviour of a DER inverter, where the inverter rides through the RoCoF event (i.e., stays connected with an output of 0 kW). On the other hand, certain inverters may disconnect following a 1 Hz/s RoCoF event at 50.2 Hz, with no injection of power to the grid (see Fig. 3 at the 4.4 s time mark).

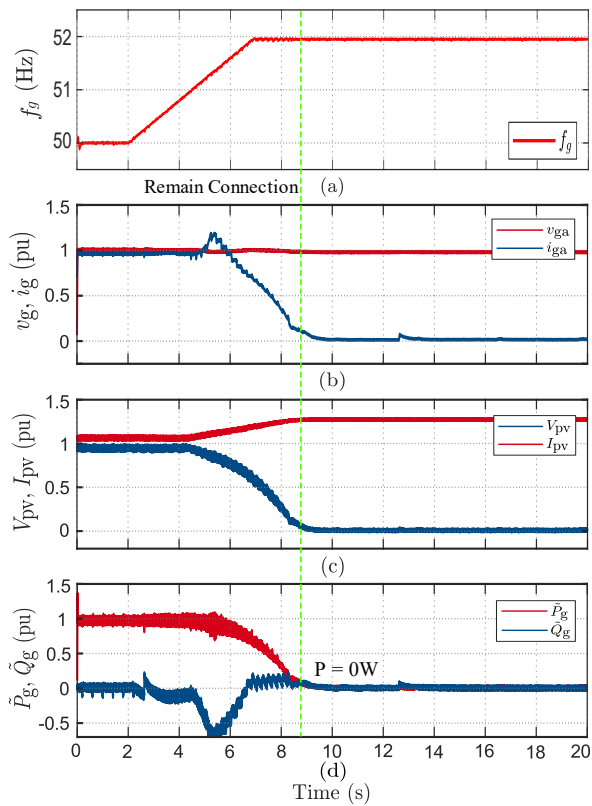


Figure 2: Ride-through for 0.4 Hz/s to 51.95 Hz.

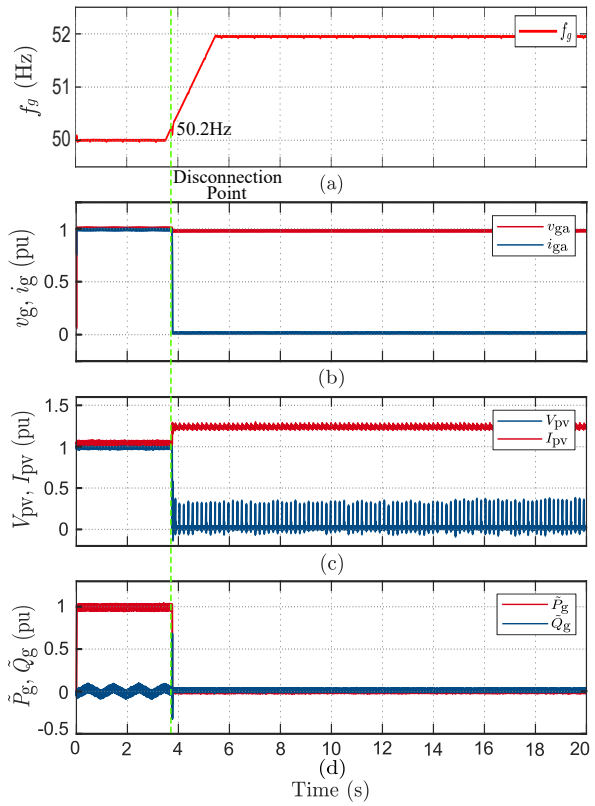


Figure 3: Disconnection for 0.4 Hz/s to 51.95 Hz.

### Voltage phase-angle jumps (VPAJ):

DER inverters may experience a VPAJ due to faults in the transmission system propagated to the distribution system through transformers, which can influence the phase between the primary and secondary voltages. Standards worldwide have introduced ride-through behaviour requirements for inverters for VPAJ disturbances. For example, a 60° VPAJ ride-through behaviour is required by IEEE Std 1547:2018 [13]. VPAJ requirements were identified and introduced in the revised version of the standard AS/NZS 4777.2:2020 [14]. A range of VPAJ tests have been undertaken to assess the percentage of inverters that display unfavourable behaviour in the event of such disturbances. Bench testing revealed three distinct behaviours of inverters in response to VPAJ disturbance: (1) ride-through, (2) power curtailment, and (3) disconnection.

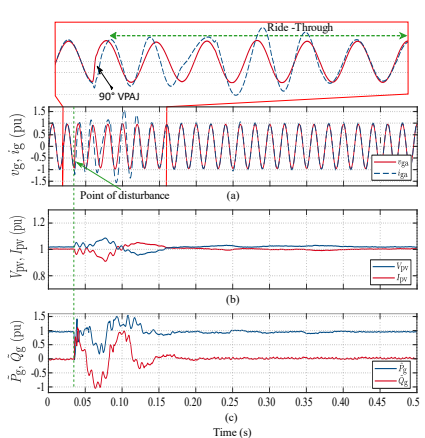


Figure 4: Inverter riding-through to VPAJ of 90°: (a) grid voltage and current; (b) PV voltage and current; (c) grid active and reactive power.

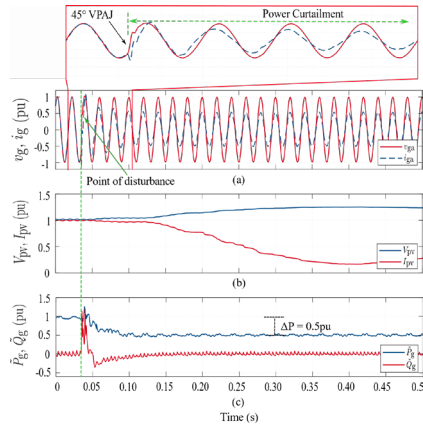


Figure 5: Inverter power curtailment to VPAJ of 45°: (a) grid voltage and current; (b) PV voltage and current; (c) grid active and reactive power.

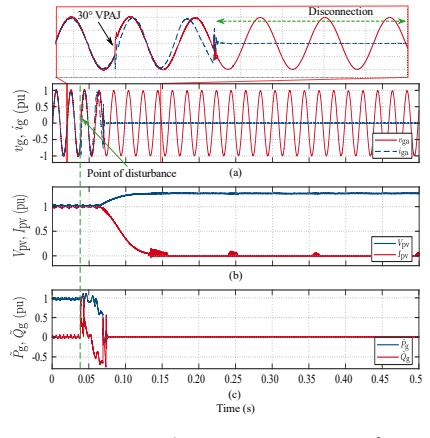


Figure 6: Inverter disconnection to VPAJ of 30°: (a) grid voltage and current; (b) PV voltage and current; (c) grid active and reactive power

Fig. 4 illustrates the ride-through behaviour of a DER inverter, (the most desirable behaviour expected under AS/NZS 4777.2:2020). This bench testing investigated the impact of a maximum VPAJ of 90° on the inverters. The inverter is expected to ride through this VPAJ without substantial disruptions in output. However, as the level of VPAJ disturbance increases, the inverter's ability to ride through it begins to deteriorate. The tests revealed that only 50% of the tested inverters could withstand VPAJ up to 45° without causing significant disturbances in the power system.

In the case of power curtailment after a fault, the inverter output power reduced from its initial value and remains below that value for a few minutes. Upon return to normal supply conditions, the inverter power output gradually returns to its pre-fault level at a rate that conforms to ramp rate requirements defined by AS/NZS 4777.2:2020. The degree of power curtailment differs among different inverters and depends on the inverter firmware. The inverter response to a 45° VPAJ is depicted in Fig. 5, where the output power is curtailed to 50% following the VPAJ disturbance. Curtailment behaviours are unfavourable, and the inverter takes several minutes to reach its maximum power output again. Other inverters (such as the one shown in Fig. 6) disconnected at only a 30° VPAJ, representing a highly undesirable response.

### Voltage Sags:

As the most common grid disturbance, comprehensive testing of the impact of voltage sags on DER inverters has been prioritised in order to identify their exact behaviour under different sag magnitudes (0.9 p.u to 0.2 p.u) and durations (80ms, 120ms and 220ms). Understanding DER response to short-duration disturbances is critical as sags less than 1 second, that correspond to typical protection times for transmission systems, are not tested under AS/NZS 4777.2:2020.

Identifying which element (i.e., depth or duration) of the voltage sag is the most critical in the misbehaviour of inverters is also an important parameter for their modelling. The results obtained from bench testing showed similar behaviours to those observed for VPAJ disturbances. While most inverters can successfully ride through minor voltage sag disturbances for short periods, they begin to exhibit undesirable behaviour when exposed to larger voltage sags. An example of such behaviour is shown in Fig. 7, where a voltage sag of 0.2 p.u and duration of 120ms caused power curtailment from the inverter. The output power of the inverter is reduced to 0.55 p.u and remains there for several minutes until returning to the pre-disturbance value. Tables 1 and 2 summarise results of two different DER inverters with very different behaviours to voltage sags.

Table 1. Summary of voltage sag results for a DER inverter curtailing at sags less than 0.4pu

sag duration	Voltage amplitude (p.u)							
	0.9	0.8	0.7	0.6	0.5	0.4	0.3	0.2
80 ms	✓	✓	✓	✓	✓	P = 0.75	P = 0.75	P = 0.65
120 ms	✓	✓	✓	✓	✓	P = 0.75	P = 0.65	P = 0.55
220 ms	✓	✓	✓	✓	✓	P = 0.75	P = 0.65	P = 0.55

Note: ✓ = ride-through; X = disconnection, P = ■ = Power curtailment

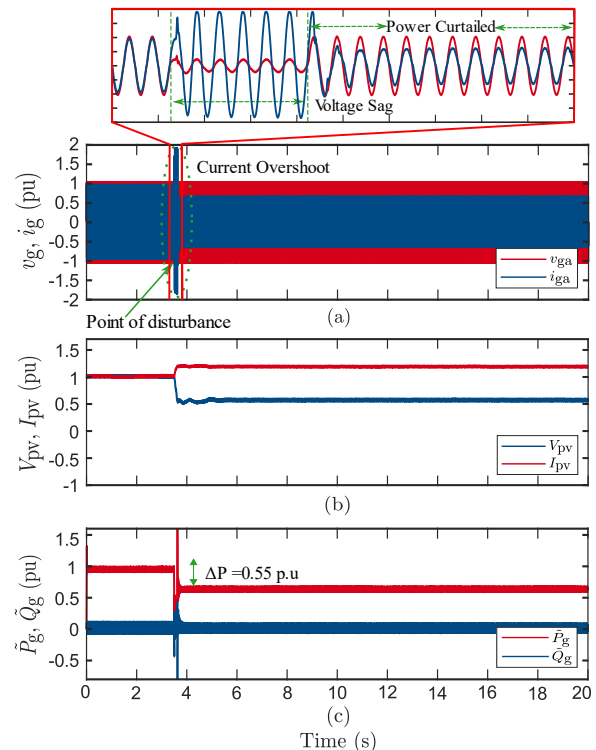


Figure 7: Inverter disconnection behaviour to VPAJ of 30°: (a) grid voltage and current; (b) PV voltage and current; (c) grid active and reactive power.

Table 2. Summary of voltage sag results for a DER inverter with disconnections under different sags

sag duration	Voltage amplitude (p.u)							
	0.9	0.8	0.7	0.6	0.5	0.4	0.3	0.2
80 ms	✓	X	X	X	X	X	X	X
120 ms	X	X	X	X	X	X	X	X
220 ms	X	X	X	X	X	X	X	X

## BESS Bench Testing Results

As testing evaluated both inverters used in standalone BESS as well as hybrid inverters (i.e., BESS and PV in a single system), the testing was separated into three modes, as shown in Table 3.

Table 3. A comparison of testing modes between hybrid and battery inverters

Mode.	Hybrid Inverters	Battery Inverters
1	PV + Battery	
2	PV	
3	Battery	Battery

The response of a standalone BESS for a frequency ramp of  $+0.4\text{Hz/s}$  to 51.95 is presented in Fig. 8. The power drawn from the supply network increases as the frequency goes above 51.1Hz; demonstrating the activation of the  $P-f$  response as required by AS/NZS 4777.2:2020 [14]. Fig. 9, on the other hand, shows the reconnection behaviour of the same BESS after the frequency disturbance. It is noteworthy that when the system reconnects to the grid, the BESS begins to absorb the same amount of power as it did prior to disconnection (similar to Fig. 8). This response raises concerns with the growth of BESS in networks, as multiple of these systems may temporarily increase the power demand upon reconnection following a frequency disturbance. This response also emphasizes the importance of conducting comprehensive laboratory evaluation of BESS and developing suitable models, going beyond just a few systems.

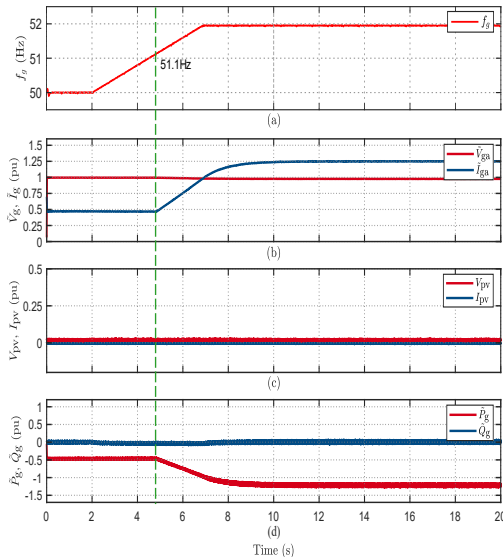


Figure 8: BESS behaviour to frequency variation of  $+0.4\text{Hz/s}$  to 51.95Hz: (a) grid frequency (b) grid voltage and current; (c) PV voltage and current; (d) grid active and reactive power.

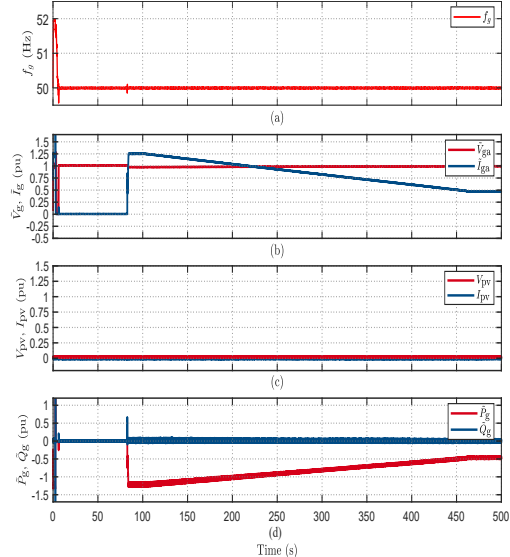


Figure 9: BESS reconnection behaviour to frequency variation from 51.95Hz to 50Hz: (a) grid frequency (b) grid voltage and current; (c) PV voltage and current; (d) grid active and reactive power.

## Load Tests

Similar tests to those performed on DER inverters have been conducted for a variety of loads, including conventional and inverter-based refrigerators, electric fans and radiant heaters, pedestal fans, inverter-based microwaves, air conditioners, desktop computer with switch mode power supplies, home electric vehicle charging units, LED lights, and equipment with direct-on-line (DOL) motors, such as vacuum cleaners and bench grinders. The different types of disturbances to which the loads were subjected the loads are divided into three categories: frequency, voltage (sags and swells), and voltage phase angle jumps. With various durations and magnitudes for each type of disturbance, a total of 52 tests per appliance have been carried out. Given the high number of tests undertaken, only a summary of the most interesting results which were observed can be presented in this paper. Emphasis has been given to the response of refrigerators, air conditioners and an EV charger.

### Refrigerators

To analyse the behaviour of refrigerators, two devices were evaluated: Refrigerator 1, a conventional unit, and Refrigerator 2, an inverter-based system; their results under a voltage sag presented in Fig. 10. For Refrigerator 1, the overshoot occurred because of the DC side capacitor charging to its nominal value, which is characterized by a short-term high magnitude current value. In contrast, Refrigerator 2 overshoot was due to motor inrush current, characterized by longer-term decaying current magnitudes. During voltage swell tests, both refrigerators withstood the voltage swells without any disconnection.

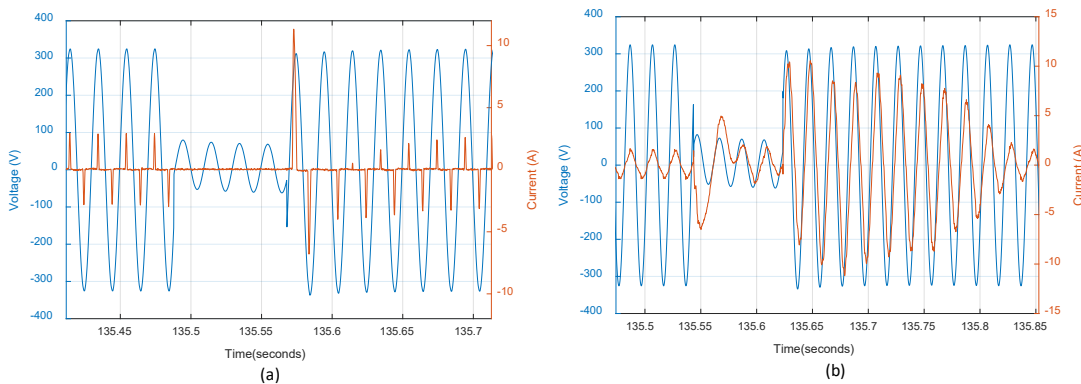


Figure 10: Impact of Voltage Sag (a) Refrigerator 1 (b) Refrigerator 2

During VPAJ tests (see Fig. 11), the conventional compressor system in Refrigerator 2 experienced a stall for a VPAJ of  $-90^\circ$ . This resulted in an increase in active power consumption from 100 W to approximately 1200 W and reactive power absorption from 45 VAr to 1000 VAr. The device remained stalled for several minutes before returning to normal operation. However, Refrigerator 2 was able to withstand all phase angle jumps with angles less than  $90^\circ$ . Conversely, the inverter-based Refrigerator 1 withstood all phase angle jumps without any noticeable issues.

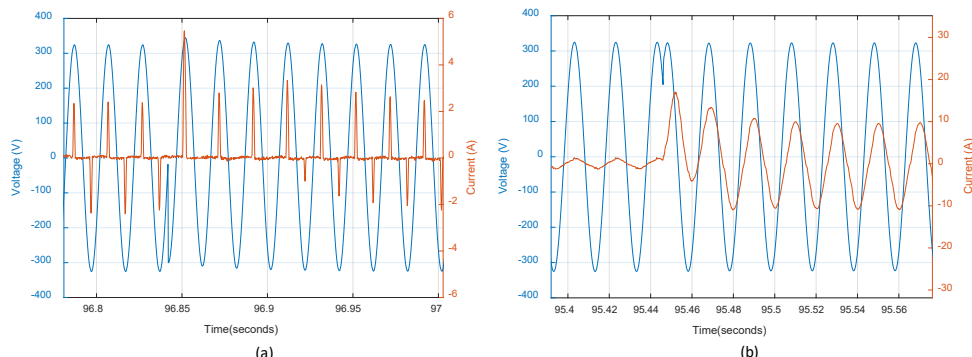


Figure 11. Impact of VPAJ (a) Refrigerator 1 (b) Refrigerator 2

## Air Conditioning Units

The air-conditioning unit tested is a portable model commonly found in Australian households. With a power consumption of approximately 1 kW and a steady-state reactive power draw of 100 VAr, the unit was set to its maximum cooling setting during testing.

For all sag and swell tests, except for the sag with a retained voltage of 0.2 pu, the air conditioning unit returned to its normal operating condition when the voltage returned to its nominal value. However, in the case of the sag with a retained voltage of 0.2 pu, the compressor motor stalled for a brief period and the cooling system turned off. The motor then resumed operation after about 30 seconds. Fig. 12 shows the stall characteristics of the air conditioning unit during a sag with a voltage reduction of 0.2 pu for 220 ms

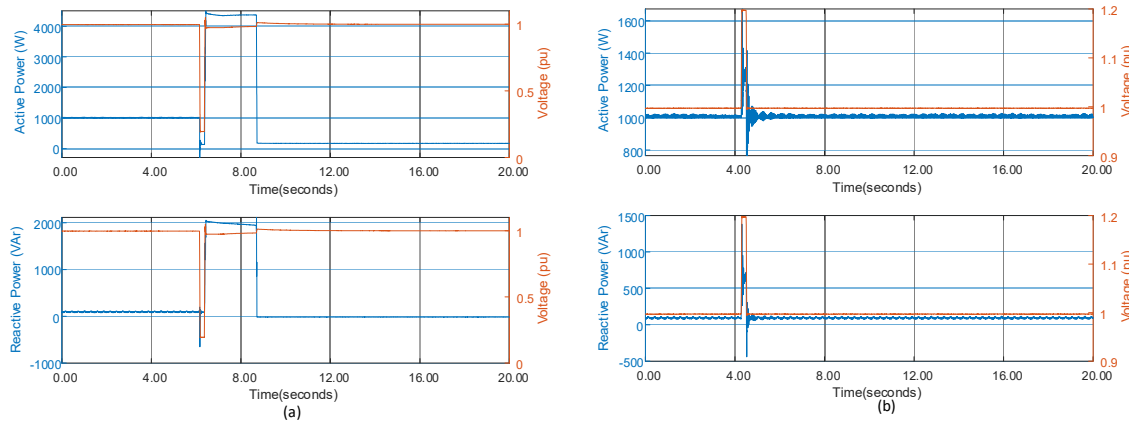


Figure 12. Response of air conditioner when subject to voltage disturbances(a) Sag (b) Swell

The air conditioner experienced brief fluctuations in active power in response to both step and ramp changes in frequency, with results shown in Fig. 13. Regarding VPAJ, the air conditioner only experienced brief changes in both active and reactive power for angle jumps below 90°. However, for a voltage phase shift of 90°, the device was able to withstand the +90°shift but failed when subjected to a phase shift of -90°.

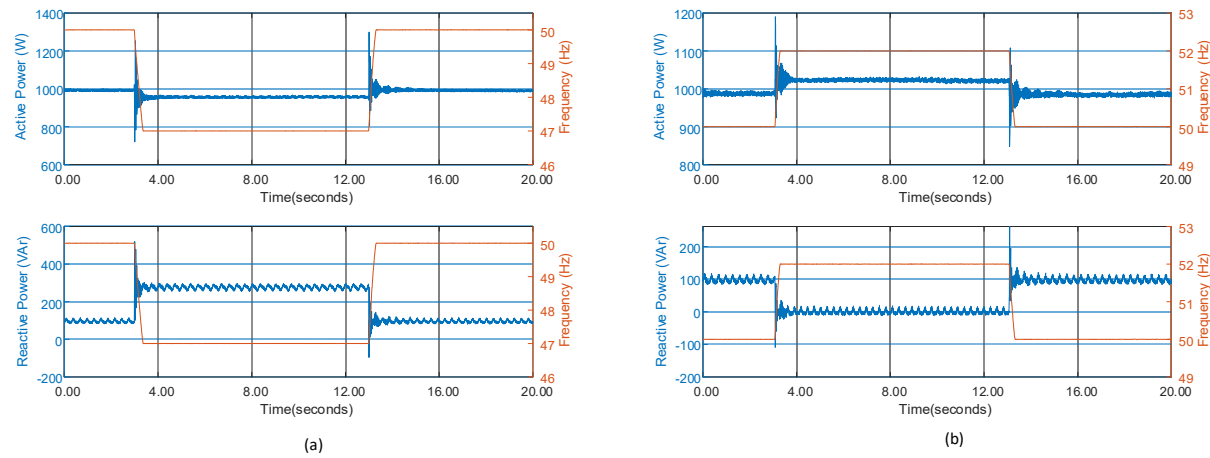


Figure 13. Frequency change response of the air conditioner (a) Step to 47 Hz (b) Step to 52 Hz

## Residential EV Charger Unit

This section summarizes the results of bench testing for a home EV charger. The EV charger is a Level 1 AC charger with a Type 1 connector. During normal operation, the device supplied 2200 W of active power with a power factor of 0.93 leading. To ensure consistency, the State of Charge (SoC) of the EV was kept below 80% for all tests. The EV charger and the EV connected to it rode-through all voltage sags above 0.6 pu. Figure 14(a) displays the instantaneous current response of the EV charger during

a 220 ms sag with a retained voltage magnitude of 0.6 pu. The current stabilizes to its original value after an initial sag transient overshoot, indicating that the charger functions as a constant current controlled device. Once the fault is cleared, the current drawn drops briefly before returning to its nominal value. Figure 14(b) shows the rms active and reactive power response of the EV during the same voltage sag with all results summarised in Table 4. Both the active and reactive power decrease during the fault, but the charger continues to charge the EV once nominal voltage is restored.

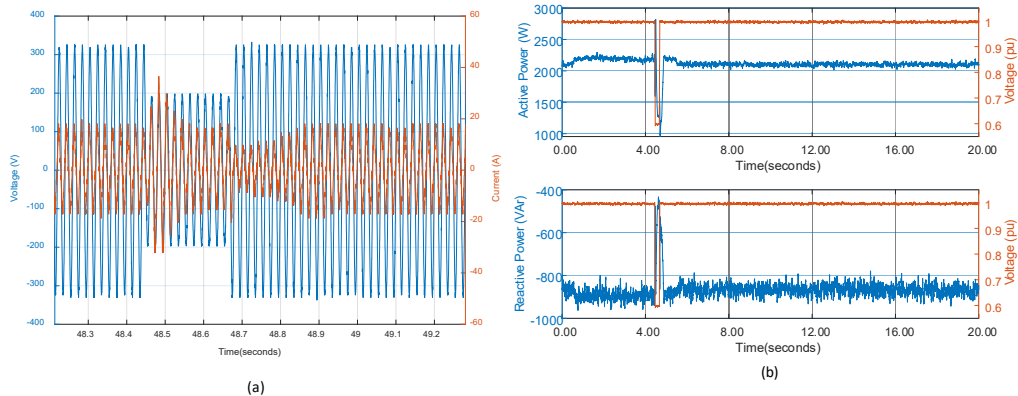


Figure 14. Response of EV Charger to sag of 0.6 pu for 220ms (a) Voltage- Current Response (b) PQ Response

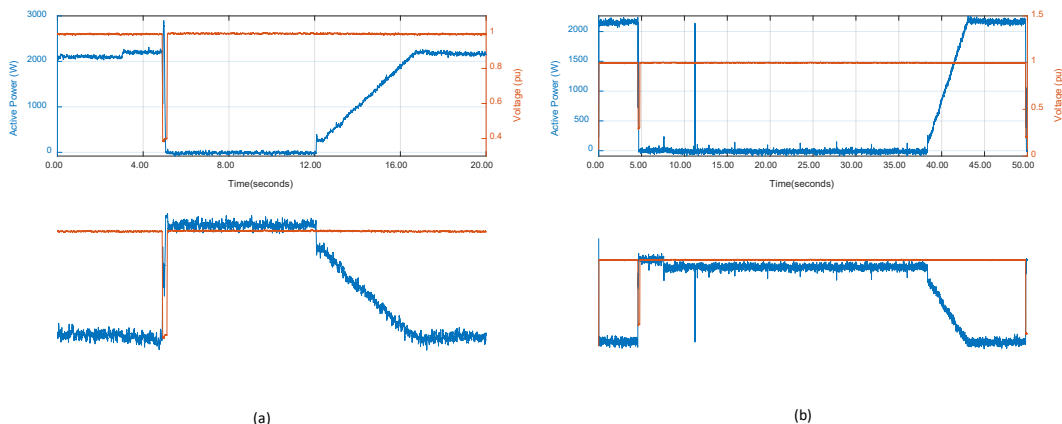


Figure 15. Different reconnection times for the EV charger following a voltage sag of (a) 0.4 pu (b) 0.3pu

*Table 4. Response of EV Charger for Voltage Sags of Different Magnitude and Duration*

sag duration	Voltage amplitude (p.u)							
	0.9	0.8	0.7	0.6	0.5	0.4	0.3	0.2
80 ms	✓	✓	✓	✓	✓	✓	32s	32s
120 ms	✓	✓	✓	✓	7s	7s	32s	32s
220 ms	✓	✓	✓	✓	7s	7s	32s	32s

Note: ✓ = ride-through; X = disconnection, P = = Disconnection

The EV charger did not appear to be significantly impacted under voltage swell tests with a temporary rise in both the active and reactive power levels of the charger. Frequency, whether in step or ramp form, did not impact the EV charger performance. Fig. 15 shows the EV charger response to a step frequency change from 50 to 52 Hz and the active and reactive power consumption during a ramp frequency change from 50 Hz to 47 Hz at a rate of -4 Hz/s, respectively. No noticeable change was observed in its regular operation, and no disconnection occurred under VPAJ, again shown in Fig. 16.

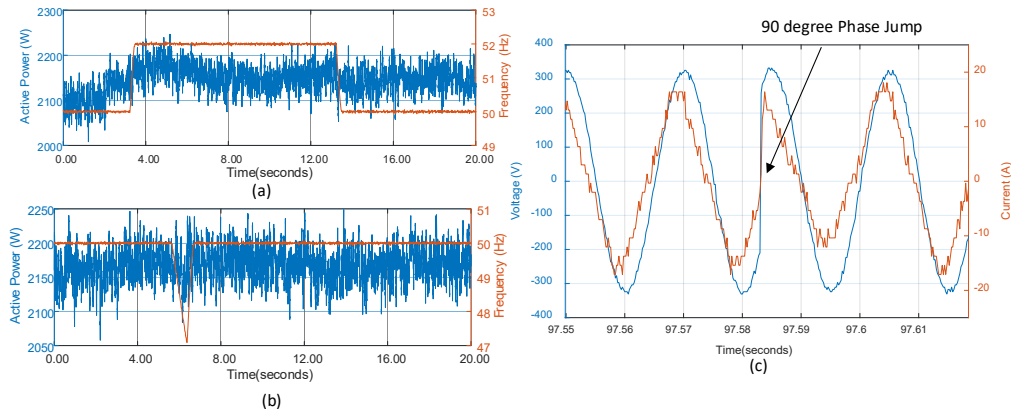


Figure 16. Impact of Frequency and Phase Angle jump for EV Charger. (a) Step Frequency Change from 50 Hz to 52 Hz, (b) Ramp Frequency at  $-4 \text{ Hz/s}$ , (c) VPAJ of  $90^\circ$ .

## Discussion – Conclusion

This paper presents a summary and emphasizes the notable findings from laboratory evaluation of the dynamic response of distributed energy resources (DER), battery energy storage systems (BESS), and loads to power system disturbances. The aim of this testing is to evaluate their performance and inform updates and revisions to load modelling, including improvements to the dynamic behaviour of the models. A diverse range of DER inverters and appliances were subjected to various tests, such as voltage sags, swells, frequency disturbances, and voltage phase angle jumps. The obtained results offer valuable insights into device behaviour and enhances the understanding of the diverse responses of these systems to power grid disturbances needed to address network stability issues. The findings in this paper can be used to develop effective control solutions tailored to the specific characteristics of each DER and load type. This comprehensive testing approach contributes a more resilient and reliable power system.

## Bibliography

- [1] The International Renewable Energy Agency (IRENA) Renewable Energy Statistics 2023.
- [2] J. V. Milanovic, K. Yamashita, S. M. Villanueva, Z. Djokic, and L. M. Korunovic, "International industry practice on power system load modelling," *IEEE Trans. Power Syst.*, vol. 28, pp. 3038-3046, 2012.
- [3] L. Callegaro, G. Konstantinou, C. A. Rojas, N. F. Avila, and J. E. Fletcher, "Testing evidence and analysis of rooftop pv inverters response to grid disturbances," *IEEE J. Phot.*, vol. 10, no. 6, pp. 1882–1891, Nov. 2020.
- [4] B. Bletterie, R. Bruendlinger, and C. Mayr, "Impact of power quality disturbances on PV inverters; performance of integrated protective functions," in 2007 IEEE EPE, pp. 1–10, 2007
- [5] H. D. Tafti, A. Ahmad, L. Callegaro, G. Konstantinou, and J. E. Fletcher, "Sensitivity of commercial rooftop photovoltaic inverters to grid voltage swell," in 2021 IEEE 12th ECCE-Asia, pp. 308–313, 2021.
- [6] Ahmad A, Tafti HD, Konstantinou G, Hredzak B, Fletcher JE. Point-on-Wave Voltage Phase-Angle Jump Sensitivity Analysis of Grid-Connected Single-Phase Inverters. *IEEE Trans. on Ind. Appl.* 2023
- [7] M. M. Haque, L. Jones, and B. C. P. Sturmberg, "Response of a bidirectional ev charger to selected grid disturbances," in 2021 IEEE Industrial Electronics and Applications Conference (IEACon), pp. 157– 162.
- [8] A. Arif, Z. Wang, J. Wang, B. Mather, H. Bashualdo, and D. Zhao, "Load Modelling—A Review," *IEEE Transactions on Smart Grid*, vol. 9, no. 6, pp. 5986-5999, 2018.
- [9] J. W. Shaffer, "Air conditioner response to transmission faults," *IEEE Transactions on Power Systems*, vol. 12, no. 2, pp. 614-621, 1997
- [10] D. Kosterev et al., "Load modelling in power system studies: WECC progress update," 2008 IEEE PES GM.
- [11] Australian Energy Market Operator (AEMO), "Black system South Australia 28 Sept. 2016," Report, Mar. 2017.
- [12] ---, "Final report Queensland and South Australia system separation on 25 August 2018," Report, Jan. 2019
- [13] IEEE Standards Coordinating Committee 21 Std. IEEE 1547.1, "IEEE standard conformance test procedures for equipment interconnecting distributed energy resources with electric power systems and associated interfaces," IEEE Std 1547-2018 (Revision of IEEE Std 1547- 2003), 2020.
- [14] AU/NZ Standard, "Grid connection of energy systems via inverters part 2: Inverter requirements," Standards Australia/New Zealand Std. AS 4777.2, 2020.